UNIVERSIDADE DE LISBOA

FACULDADE DE CIÊNCIAS

DEPARTAMENTO DE BIOLOGIA VEGETAL

Significance of mycobacterial peptidoglycan amidation in host immune recognition and antibiotic resistance

Mariana Ferreira Balula Marques

Mestrado em Biologia Molecular e Genética

Dissertação orientada por:

Prof. Drª. Maria João Catalão
Prof. Dr. Francisco Dionísio

2020

Acknowledgments

The work that I present here is the product of many hours of hard work, and it would not be possible without the assistance and guidance of several people that I would like to acknowledge.

Firstly, I would like to express my deep gratitude to my supervisor, Prof Dr Maria João Catalão, for trusting me in doing this project. Thank you for all the crucial help, understanding, encouragement, and for all of the things I had the chance to learn during the past year. Thank you for all the availability to hear and discuss my ideas, problems, and possible solutions. I am very grateful for the opportunity to work with you and I am very proud to see your group becoming more and more successful.

I would also like to show my gratitude to my internal supervisor, Prof Dr Francisco Dionísio, for accepting to supervise me on another project. Thank you for all the kindness, support, and especially, for the availability in answer all my questions and doubts during the two years of my master's degree.

To Cátia Silveiro, thank you for all the great, hard, and funny hours spent at the lab and for all the conversations and discussions. I enjoyed our teamwork very much and I am very proud of all the problems we solved together. I am sure that this project would be more difficult if it was not for you.

To Nuno Carmo, thank you for all of the things I have learned with you. Thank you for all the orientation, motivation, support, and good suggestions. Our conversations allowed me to think outside the box, from multiple perspectives, and improved my critical thinking.

To Francisco Olivença, thank you for all the support, suggestions, and great incentives during the past year. I am very grateful to you for always being available to listen, think, and help with this project, even when you were busy with your own work.

I would also like to express my gratitude to Luís Tanoeiro, an amazing college and lab partner. Especially, I would like to thank you for allowing me to use "your" vortex and for making my time at the lab even happier with our conversations and jokes.

To all the remaining lab members, colleges, and faculty technicians, Prof Dr Elsa Anes, Frederico Holtreman, Andreia Marques, Tomás Velez, Prof Dr Jorge Víctor, Ana Gouveia, Daniela Pinto, Manoj Mandal, D. São and Lucy, thank you for making me feel welcome and for all the help and availability. A very special acknowledgment to David Pires, for all the support and clarification in several matters throughout the past year and, in particular, for the great help and teaching in the last part of this thesis.

To my oldest friends, Rita Teresa, Beatriz Martinho, Márcia Grou e José Tomé, thank you for your friendship and support in everything. We have known each other since we were only 4 years old and you have accompanied me all these years, even though we have all chosen different paths. Thank you for all the happy distractions and for the time we spent together to forget about our theses for a while.

I would also like to thank my friends, Bárbara Nobre, Margarida Isidro, and Miguel Mira for all the friendship during the last 5 years. For all the things that we learned and experienced together, and in particular, for all the conversations and motivation in this very intense academic year.

A special gratitude to Miguel Alves, for believing and motivating me every day in everything. Thank you for your patience, understanding, and advice. You are always the light when I cannot see.

Finally, I must express my very gratitude to my parents, for always encouraging me to be a better person and to follow my dreams. Thank you for supporting me in everything and helping me the best way you can. This accomplishment would not be possible without you.

Abstract

Tuberculosis (TB) belongs to the top 10 causes of death in the world and it is caused by the intracellular pathogen *Mycobacterium tuberculosis* (*M. tuberculosis*). The emergence of multi- and extensive-drug resistant strains of *M. tuberculosis* remains a serious growing problem and reflects the urgent need to develop new drugs and effective treatment approaches. A typical feature of *M. tuberculosis* is its complex cell wall structure, well-known as the mycolyl-arabino-galactan-peptidoglycan (mAGP) complex and highly responsible for the resistance to many antimicrobial drugs. The mAGP complex includes a distinctive mycobacterial peptidoglycan (PG) layer that undergoes several relevant modifications, of which the amidation of D-*iso*-glutamate (D-*i*Glu) and *meso*-diaminopimelic acid residues are of special interest. Recently, these reactions were found to be catalysed in mycobacteria by the essential MurT/GatD enzymatic complex and by the AsnB enzyme, respectively. Both PG modifications have been shown to influence the bacterial antibiotic resistance, especially to β-lactams, and the host immune recognition. Therefore, to further understand the significance of PG amidation in both contexts, *murT*, *gatD*, and *asnB* knockdown mutants were constructed in the mycobacterial study model, *Mycobacterium smegmatis* (*M. smegmatis*), using the clustered regularly interspaced short palindromic repeat (CRISPR) interference (CRISPRi) system. CRISPRi is based on the anhydrotetracycline (ATc)-inducible expression of an enzymatically inactive Cas9 protein together with a small single guide RNA (sgRNA) specific to a target gene sequence. It has been proven to be a very simple, useful, and cost-effective platform to repress the expression of either essential or non-essential genes. Using this system, *murT* and *gatD* were confirmed to be essential in *M. smegmatis*, in contrast to *asnB*, and the level of *gatD* and *murT* knockdown seemed to be directly related with the associated proto-spacer adjacent motif (PAM) strength. In *murT*$^{-}$ and *gatD*$^{-}$ mutants associated with weaker PAMs, the distance of the target gene region from the beginning of the gene appeared to also influence the CRISPRi-mediated gene silencing and, consequently, the growth defects, although this was not confirmed by growth curves. By assessing the levels of knockdown in one *gatD*$^{-}$ mutant, a 8.8-fold decrease in *gatD* mRNA expression was obtained, compared to the ATc-treated wild-type (WT) strain and, in contrast to previous results, there was no evidence of a polar effect by CRISPRi. Several *gatD*$^{-}$ mutants showed increased susceptibility to β-lactams (amoxicillin, cefotaxime, and meropenem), particularly in the presence of a β-lactamase inhibitor (clavulanate). This suggested that the lack of amidation displayed by the PG precursors of these mutants could make them poorer substrates for penicillin binding proteins (PBPs) and thus, it could lead to a less efficient cross-linking and to PBPs being more susceptible to the action of these antibiotics. Moreover, it was observed a significant decrease in the bacterial intracellular survival of a *gatD* knockdown mutant within RAW 264.7 murine macrophages, compared to the ATc-treated WT strain and to the untreated mutant. The absence of a D-*i*Glu amidation in the mycobacterial PG caused a reduced resistance to β-lactams and appeared to contribute to a higher recognition of mycobacteria by host macrophages.

Keywords: Tuberculosis; Peptidoglycan amidation; Antibiotic resistance; Host immune recognition; CRISPRi.

Resumo

A tuberculose é uma das 10 principais causas de morte a nível mundial e é causada pela bactéria intracelular *Mycobacterium tuberculosis* (*M. tuberculosis*). De acordo com a Organização Mundial de Saúde, em 2019, aproximadamente 1,5 milhões de pessoas morreram com tuberculose e estima-se que, atualmente, um quarto da população mundial (cerca de 1,9 mil milhões de pessoas) esteja infetada com tuberculose latente. O aparecimento de estirpes multi e extensivamente resistentes é um problema cada vez mais grave e reflete a necessidade urgente de desenvolver novos medicamentos e estratégias que sejam eficazes no tratamento desta doença.

Uma característica típica de *M. tuberculosis* é a sua complexa parede celular, normalmente conhecida como complexo micolil-arabino-galactano-peptidoglicano (mAGP). Tal como o nome indica, o complexo mAGP é principalmente constituído por uma camada de ácidos micólicos de cadeia longa, um polissacárido de arabinogalactano altamente ramificado e uma camada de peptidoglicano (PG). Todos estes componentes contribuem para a resistência natural destas bactérias a muitos antibióticos e para a modulação da resposta imune do hospedeiro.

O PG é altamente responsável pela conservação da integridade celular e os seus processos de biossíntese e reciclagem envolvem vários enzimas essenciais para a viabilidade das micobactérias, sendo considerados, portanto, como potenciais alvos terapêuticos. O PG micobacteriano é caracterizado por diversas modificações químicas, tais como a amidação dos resíduos de D-*iso*-glutamato (D-*i*Glu) e ácido *meso*-diaminopimélico (*m*DAP). Recentemente, foi descoberto que estas reações são catalisadas pelo complexo enzimático MurT/GatD e pelo enzima AsnB, respetivamente. Foi demonstrado que a amidação do D-*i*Glu tem influência na suscetibilidade a antibióticos, especialmente a antibióticos β-lactâmicos, e no *cross-linking*, enquanto que a amidação do *m*DAP parece influenciar a modulação da hidrólise do PG. Além disso, a presença destas duas modificações tem sido associada a uma redução da ativação da proteína recetora *nucleotide-binding oligomerization domain* (NOD) 1 do hospedeiro, indicando um possível papel da amidação do PG no reconhecimento pelo sistema imune do mesmo.

Para compreender o papel da amidação do PG em micobactérias tanto na resistência a antibióticos, como no reconhecimento imune do hospedeiro, o sistema c*lustered regularly interspaced short palindromic repeat* (CRISPR) de interferência (CRISPRi) foi utilizado para construir mutantes *knockdown* dos genes *murT*, *gatD* e *asnB* (mutantes *murT*$^{-}$, *gatD*$^{-}$ e *asnB*$^{-}$, respetivamente) em *Mycobacterium smegmatis* mc^{2}155 (*M. smegmatis*), um dos modelos mais utilizados no estudo da tuberculose. O CRISPRi baseia-se na expressão indutível de uma proteína endonuclease Cas9 enzimaticamente inativa (dCas9), em conjunto com um pequeno RNA guia (sgRNA), que pode ser desenhado para ter como alvo uma sequência de DNA específica. Recentemente, este sistema foi desenvolvido e otimizado para micobactérias, sendo simples, prático e económico na inibição da expressão quer de genes essenciais, quer de genes não essenciais, sem provocar clivagem, nem efeitos *off-target*. O CRISPRi utiliza como indutor a anidrotetraciclina (ATc) e pode ser modelado por diferentes fatores, nomeadamente a concentração de ATc, o grau de complementaridade entre o sgRNA e a sequência-alvo, e o uso de um motivo de DNA de 2-5 par de bases, situado a jusante da sequência-alvo, designado de *proto-spacer adjacent motif* (PAM), com "forças" distintas.

Para avaliar os efeitos do silenciamento dos genes *gatD*, *murT* e *asnB* na viabilidade e crescimento micobacteriano, foram realizadas experiências de *spotting*. Através das mesmas, os genes *murT* e *gatD*, que pertencem a um operão com um promotor comum, foram confirmados como genes essenciais em *M. smegmatis*, ao contrário do gene *asnB*. O nível de *knockdown* dos dois primeiros genes pareceu estar diretamente relacionado com a força da PAM associada a cada mutante. Nos mutantes associados a PAMs fracas, a distância desde a região alvo ao início do gene também pareceu influenciar o silenciamento mediado pelo CRISPRi. Contudo, através da realização de curvas de crescimento dos controlos e mutantes *gatD*$^{-}$, esta última correlação não foi observada, uma vez que o perfil de

crescimento dos mutantes associados a PAMs fracas aparentou ser semelhante entre si. Apesar das diversas vantagens do CRISPRi, na ausência de indutor, o perfil de crescimento dos mutantes *gatD*$^{-}$ pareceu indicar a existência de uma expressão *leaky* da dCas9$_{Sth1}$, assim como algum nível de toxicidade causado pela sobrexpressão da mesma no controlo de *M. smegmatis* contendo um plasmídeo CRISPRi vazio não-digerido, na presença de ATc.

Os níveis de *knockdown* de um mutante *gatD*$^{-}$ foram avaliados através de qRT-PCR e obteve-se uma diminuição na expressão do *gatD* de 8,8 vezes, comparando com a estirpe *wild-type* na presença de ATc. Este resultado salienta a capacidade do CRISPRi de alcançar uma inibição considerável da expressão de genes específicos em *M. smegmatis* e, em conjunto com os resultados de caracterização fenotípica, indica que esta inibição é suficiente para causar defeitos no crescimento. Em contraste com resultados anteriormente publicados, não se observou nenhuma evidência da existência de um efeito polar provocado pelo CRISPRi, fenómeno que é bastante frequente quando se silenciam genes pertencentes a operões.

Para investigar o papel da amidação do PG na resistência a antibióticos, foram determinadas as concentrações mínimas inibitórias e bactericidas (MICs e MBCs, respetivamente) de três antibióticos β-lactâmicos de três classes diferentes (amoxicilina, cefotaxima e meropenemo), na presença e na ausência de um inibidor de β-lactamases (clavulanato), e de dois antibióticos anti-tuberculose de primeira-linha (isoniazida e etambutol) para todos controlos e mutantes *gatD*$^{-}$. Diversos mutantes *gatD*$^{-}$ mostraram uma suscetibilidade aumentada aos antibióticos β-lactâmicos testados, especialmente na presença de clavulanato. Em particular para a cefotaxima, o silenciamento do *gatD* pareceu contribuir para um maior efeito bactericida. Estes resultados sugerem que a ausência de amidação nos precursores de PG destes mutantes pode fazer com que estes sejam substratos mais pobres para as p*enicillin binding proteins* (PBPs) que catalisam as reações de *cross-linking*, levando a que estas reações sejam menos eficientes e a que as PBPs sejam mais suscetíveis à ação deste tipo de antibióticos. Assim, a inibição da amidação do resíduo de D-*i*Glu do PG através do sistema de CRISPRi e a utilização de antibióticos β-lactâmicos poderia funcionar para produzir um efeito antimicrobiano sinérgico mais eficaz.

Com o objetivo de compreender a contribuição desta modificação do PG no reconhecimento pelo sistema imune do hospedeiro, foram realizadas infeções de macrófagos de ratinho RAW 264.7 com um mutante *gatD*$^{-}$ e foi investigada a sobrevivência intracelular bacteriana. Os resultados indicaram um decréscimo no número de unidades formadoras de colónias (CFUs)/mL deste mutante, na presença de ATc, às 1, 4 e 24 h pós-infeção, comparando com a estirpe *wild-type* na presença de ATc e com o mesmo mutante na ausência de ATc. Sabendo que a amidação do resíduo de D-*i*Glu está ausente neste mutante, esta redução do *fitness* intracelular poderá ser explicada por um maior reconhecimento das micobactérias pelo macrófagos, resultando numa maior taxa de fagocitose e, consequentemente, numa menor capacidade de sobrevivência intracelular. Estes resultados sustentam a ideia de que esta modificação do PG pode ser uma estratégia das micobactérias para evitar o seu reconhecimento por parte do sistema imune inato do hospedeiro, contudo deverão ser realizadas experiências adicionais.

Os resultados apresentados nesta tese mostram o potencial da amidação do PG como possível alvo terapêutico e constituem um bom ponto de partida para uma posterior investigação desta mesma modificação em *M. tuberculosis*. Paralelamente à construção dos mutantes em *M. smegmatis*, também diversos mutantes *murT*$^{-}$, *gatD*$^{-}$ e *asnB*$^{-}$ foram construídos em *M. tuberculosis* H37Ra e todos os sgRNA desenhados foram confirmados como idênticos para *M. tuberculosis* H37Rv, o que facilitará uma aplicação futura destas experiências nestas estirpes, ou ainda, em estirpes clínicas, incluindo estirpes multi e extensivamente resistentes, em condições de biossegurança de nível 3.

Palavras-chave: Tuberculose; Amidação do peptidoglicano; Resistência a antibióticos; Reconhecimento imune do hospedeiro; CRISPRi.

Index

Acknowledgments I
Abstract II
Resumo III
Index V
Figure Index VII
Table Index X
Abbreviation List XI
1. Introduction 1
1.1 Tuberculosis 1
1.2 Phylogeny of mycobacteria 1
1.3 Mycobacterial CW structure 2
1.3.1 PG layer 3
1.3.1.1 Modifications of the mycobacterial PG 4
1.3.1.1.1 The MurT/GatD enzymatic complex 4
1.3.1.1.2 AsnB 5
1.4 Antibiotics targeting the mycobacterial CW 6
1.4.1 The β-lactam antibiotics and its potential application in TB treatment 6
1.5 Host immune response in TB 7
1.5.1 Mycobacterial PG amidation in host immune recognition 8
1.6 CRISPR 8
1.6.1 CRISPRi 9
1.7 Objectives 10
2. Materials and Methods 11
2.1 Bacterial strains, plasmids, antibiotics, and growth conditions 11
2.2 sgRNA design, plasmid cloning, and transformation 11
2.3 Spotting dilutions and growth curves 12
2.4 Evaluation of mRNA expression levels by qRT-PCR 12
2.5 Minimum inhibitory and bactericidal concentration assays 13
2.6 Infections of RAW 264.7 cells with *M. smegmatis* mc^2155 and determination of the number of CFUs of viable intracellular mycobacteria 13
3. Results and Discussion 14
3.1 Construction and characterization of *murT*, *gatD*, and *asnB* knockdown mutants in mycobacteria 14
3.1.1 Construction of *murT*, *gatD*, and *asnB* knockdown mutants in *M. smegmatis* mc^2155 and *M. tuberculosis* H37Ra using CRISPRi 14
3.1.2 Phenotypic characterization of *murT*, *gatD*, and *asnB* knockdown mutants in *M. smegmatis* mc^2155 15

3.1.3 Assessment of CRISPRi-mediated gene repression by qRT-PCR.....21
3.2 Evaluation of PG amidation role in antibiotic resistance by MIC and MBC determination for antibiotics that target the mycobacterial CW biosynthesis.....22
3.3 Determination of the PG amidation significance in host immune recognition 27
4. Conclusions and Future Perspectives.....29
5. References 30
6. Annexes.....37

Figure Index

Figure 1.1 – Schematic representation of the mycobacterial CW with focus on the amidation of the D-*i*Glu residue of the PG, catalysed by the MurT/GatD enzymatic complex. The mycobacterial CW is mainly composed by a cross-linked and modified PG layer, a highly branched AG polysaccharide and long-chain MA. ADP, adenosine diphosphate; ATP, adenosine triphosphate; AG, arabinogalactan; CM, cytoplasmatic membrane; F6P, fructose 6-phosphate; GlcNAc, *N*-acetyl-glucosamine; Gln, glutamine; Glu, glutamate; LAMs, lipoarabinomannan; MA, mycolic acids; MurNAc, *N*-acetyl-muramic acid; MurNGly, *N*-glycolylmuramic acid; OL, outer layer; PG, peptidoglycan; P_i, inorganic phosphate; PIMs, phosphatidylinositol mannosides. 3

Figure 1.2 – **Schematic representation of the mechanism of action of the CRISPRi system to achieve transcriptional repression.** bp, base pair; dCas9, deficient Cas9 protein; NT, non-template strand; PAM, proto-spacer adjacent motif; P_{con}, constitutive promoter; P_{Tet}, ATc-inducible promoter; RNAP, RNA polymerase; sgRNA, single guide RNA; T, template strand. 9

Figure 3.1 – Target sites of CRISPRi in *murT* and *gatD* in *M. smegmatis* mc^{2}155. Both genes are transcribed in the same direction and constitute an operon with a common promoter upstream *murT* with 73 bp. The two genes are overlapped by 4 bp. The CRISPRi target sites are shown in vertical black lines. Under or above the lines of the CRISPRi target sites are indicated the number of the first nucleotide of the target sequence, the corresponding sgRNA (decreasingly ordered by PAM strength) and the number of the corresponding PAM. 15

Figure 3.2 – **Spotting dilutions of *M. smegmatis* mc^{2}155 WT, ctrl PLJR962, and *murT*$^-$ mutants (PLJR962:sgRNA1 to 9) in the presence (+) and absence (–) of 100 ng/mL ATc**. The sgRNAs are decreasingly ordered by PAM strength. *M. smegmatis* WT and ctrl PLJR962 were used as controls. The ctrl PLJR962 mutant is a non-targeting control harbouring an empty vector. The first spot corresponds approximately to 0.001 $OD_{600\ nm}$ and each subsequent spot is a two-fold dilution. Each spot corresponds of plating 5µL of culture volume. These data are representative of three independent experiments. ...16

Figure 3.3 – **Spotting dilutions of *M. smegmatis* mc^{2}155 WT, ctrl PLJR962, and *gatD*$^-$ mutants (PLJR962:sgRNA1 to 7) in the presence (+) and absence (–) of 100 ng/mL ATc**. The sgRNAs are decreasingly ordered by PAM strength. *M. smegmatis* WT and ctrl PLJR962 were used as controls. The ctrl PLJR962 mutant is a non-targeting control harbouring an empty vector. The first spot corresponds approximately to 0.001 $OD_{600\ nm}$ and each subsequent spot is a two-fold dilution. Each spot corresponds of plating 5µL of culture volume. These data are representative of three independent experiments. ...17

Figure 3.4 – **Spotting dilutions of *M. smegmatis* mc^{2}155 WT, ctrl PLJR962, and *asnB*$^-$ mutants (PLJR962:sgRNA1 to 7) in the presence (+) and absence (–) of 100 ng/mL ATc**. The sgRNAs are decreasingly ordered by PAM strength. *M. smegmatis* WT and ctrl PLJR962 were used as controls. The ctrl PLJR962 mutant is a non-targeting control harbouring an empty vector. The first spot corresponds approximately to 0.001 $OD_{600\ nm}$ and each subsequent spot is a two-fold dilution. Each spot corresponds of plating 5µL of culture volume. These data are representative of three independent experiments. ...18

Figure 3.5 – **(A-G) Growth curves of *M. smegmatis* mc^{2}155 WT, ctrl PLJR962, and *gatD*$^-$ mutants (PLJR962:sgRNA1 to 7) in the presence (■) and absence (●) of ATc.** The sgRNAs are decreasingly ordered by PAM strength. *M. smegmatis* mc^{2}155 WT and ctrl PLJR962 were used as controls. The ctrl

PLJR962 mutant is a non-targeting control harbouring an empty vector. The cultures were grown from mid- to late-log phase, washed, and diluted to a theoretical $OD_{600\ nm}$ of 0.001 (t = 0 h). The 100 ng/mL ATc addition was made at 0 and 24 h. The growth profile of cultures was followed by $OD_{600\ nm}$ measurement at 0, 18, 21, 24, 42, and 45 h. The data represent the mean ± SEM of three independent experiments. 20

Figure 3.6 – **Relative *gatD, murT, MSMEG_6275,* and *MSMEG_6278* mRNA expression levels in *M. smegmatis* mc^{2}155 WT, ctrl PLJR962, and PLJR962:sgRNA2 *gatD*$^-$ mutant with (striped bars) and without (smooth bars) 100 ng/mL ATc treatment for 6 h.** *M. smegmatis* mc^{2}155 WT and ctrl PLJR962 were used as controls. The ctrl PLJR962 mutant is a non-targeting control harbouring an empty vector. The data were quantified using the $\Delta\Delta C_T$ method and normalized to the *M. smegmatis* housekeeping gene dnaK, using the *M. smegmatis* WT as calibrator sample. The bars represent the mean of three independent experiments with three biological triplicates each and the error bars correspond to the SEM. Asterisks indicate the significance of the difference in relative mRNA expression calculated using the Student t-test (* $P < 0.005$).....21

Figure 3.7 – **(A-H) Graphical representation of the medians of Minimum Inhibitory Concentrations (MICs) of eight different antibiotics for *M. smegmatis* mc^{2}155 (WT), ctrl PLJR962, and *gatD*$^-$ mutants (PLJR962:sgRNA1 to 7), in the presence (striped bars) and absence (smooth bars) of 100 ng/mL ATc.** The absence of a bar border indicated a MIC > 256 µg/mL. A bacteriostatic effect or undetermined MBCs are represented with the "■" symbol and all other cases correspond to an antibiotic bactericidal effect. *M. smegmatis* mc^{2}155 WT and ctrl PLJR962 were used as controls. The ctrl PLJR962 mutant is a non-targeting control harbouring an empty vector. The sgRNAs of mutants are decreasingly ordered by PAM strength. Each bar corresponds to the median of three independent experiments. 24

Figure 3.8 – Intracellular survival of *M. smegmatis* mc^{2}155 WT, ctrl PLJR962 and PLJR962:sgRNA2 *gatD*$^-$ mutant in the presence (striped bars) and absence (smooth bars) of ATc within RAW 264.7 cells of BALB/c mice measured by CFU/mL at 1, 4, and 24 h post-infection. *M. smegmatis* mc^{2}155 WT and ctrl PLJR962 were used as controls. The ctrl PLJR962 mutant is a non-targeting control harbouring an empty vector. Prior the macrophages infection, the bacteria were grown in the presence and absence of 100 ng/mL ATc. The bars represent the mean of two independent experiments with three biological triplicates each and the error bars correspond to the SEM. Asterisks indicate the significance of the difference in the number of CFUs/mL calculated using the Student t-test (* $P < 0.01$; ** $P < 0.05$; *** $P < 0.01$) 28

Figure 6.1 – **The CRISPRi-dCas9$_{Sth1}$ system optimized by Rock *et al.* in mycobacteria.** (A) CRISPRi backbone plasmids for *M. smegmatis* (PLJR962, left) and *M. tuberculosis* (PLJR965, right) with indication of enzymatic restriction sites. bp, base pair; dCas9, deficient Cas9 protein; KanR, kanamycin resistance cassette; L5 int, single copy L5-inegrative backbone with the integrase gene and an *attP* site; OriE, E. coli derived pBR3222 origin of replication; Sth1 dCas9, dCas9 from *S. thermophilus*. (B) Different PAM position variants for dCas9$_{Sth1}$. The 15 PAMs (PAM1-15) that were described as able to cause a >25-fold repression and that were used in this project are indicated by a blue rectangle. PAM, proto-spacer adjacent motif; SD, standard deviation; sgRNA, single guide RNA. Adapted from Rock *et al.* (2017). 37

Figure 6.2 – Growth curves of *M. smegmatis* mc^{2}155 WT, ctrl PLJR962, and *gatD*$^-$ mutants (PLJR962:sgRNA1 to 7) in the presence (■) and absence (●) of ATc. The sgRNAs are decreasingly ordered by PAM strength. *M. smegmatis* mc^{2}155 WT and ctrl PLJR962 were used as controls. The ctrl PLJR962 mutant is a non-targeting control harbouring an empty vector. The cultures were grown from mid- to late-log phase, washed and diluted to a theoretical $OD_{600\ nm}$ of 0.001 (t = 0 h). The 100 ng/mL ATc addition was made at 0 and 24 h. The growth profile of cultures was followed by $OD_{600\ nm}$ measurement at 0, 18, 21, 24, 42, and 45 h. The data represent the mean ± SEM of three independent experiments. 41

Table Index

Table 3.1 – EUCAST non-species related PK-PD breakpoints for β-lactams and critical concentrations for ethambutol and isoniazid (µg/mL). S – susceptible; R – resistant.....22

Table 6.1 – qRT-PCR primers for assessment of CRISPRi-mediated gene repression. The mRNA expression levels were evaluated and the housekeeping gene *dnaK* was used as reference. 38

Table 6.2 – ***murT*** **sgRNA oligonucleotides designed for *M. smegmatis* mc^{2}155 and *M. tuberculosis* H37Ra.** The sgRNAs were decreasingly ordered by PAM strength. 38

Table 6.3 – ***gatD*** **sgRNA oligonucleotides designed for *M. smegmatis* mc^{2}155 and *M. tuberculosis* H37Ra.** The sgRNAs were decreasingly ordered by PAM strength. 39

Table 6.4 - *asnB* sgRNA oligonucleotides designed for *M. smegmatis* mc^{2}155 and *M. tuberculosis* H37Ra. The sgRNAs were decreasingly ordered by PAM strength. 40

Table 6.5 – **Medians of MICs and MBCs of eight different antibiotics for *M. smegmatis* mc^{2}155 (WT), ctrl PLJR962, and *gatD*$^-$ mutants (PLJR962:sgRNA1 to 7) in the presence and absence of 100 ng/mL ATc.** A bacteriostatic effect or undetermined MBCs are highlighted in grey and all other cases correspond to an antibiotic bactericidal effect. Based on EUCAST non-species related PK-PD breakpoints for β-lactams and critical concentrations for ethambutol and isoniazid, the MIC values were coloured with blue (susceptible), green (intermediate), and orange (resistant). *M. smegmatis* mc^{2}155 WT and ctrl PLJR962 were used as controls. The ctrl PLJR962 mutant is a non-targeting control harbouring an empty vector. The sgRNAs of mutants are decreasingly ordered by PAM strength. The data corresponds to three independent experiments. Amoxicillin (AMX); cefotaxime (CEF); meropenem (MER); clavulanate 2.5 µg/mL (+ Clav); ethambutol (EMB); isoniazid (INH).....42

Abbreviation List

AG – Arabinogalactan
AMX – Amoxicillin
AMX-clavulanate – Amoxicillin combined with clavulanate
ATc – Anhydrotetracycline
ATP – Adenosine triphosphate
B. subtilis – *Bacillus subtilis*
BCG – Bacille Calmette-Guérin
bp – Base pair
BSL – Biosafety level
C. glutamicum – *Corynebacterium glutamicum*
CC – Competent cells
CEF – Cefotaxime
CEF-clavulanate – Cefotaxime combined with clavulanate
CFUs – Colony forming units
CRISPR – Clustered regularly interspaced short palindromic repeat
CRISPRi – CRISPR interference
crRNA – CRISPR RNA
CW – Cell wall
Cys – Cysteine
D-Ala-D-Ala – D-Alanyl-D-Alanine
DCs – Dendritic cells
D-iGln – D-*iso*-glutamine
D-iGlu – D-*iso*-glutamate
dP-P – Decaprenyl phosphate
E. coli – *Escherichia coli*
ECC – Electrocompetent cells
ELISA – Enzyme-linked immunosorbent assay
EMB – Ethambutol
Fw – Forward
GATase – Glutamine-dependent amidotransferases
GlcNAc – *N*-acetyl-glucosamine
His – Histidine
INH – Isoniazid
L-Ala – L-Alanine
LAM – Lipoarabionomannan
LB – Luria-Bertani
LDTs – L,D-transpeptidases
LMs – Lipomannans
M. smegmatis – *Mycobacterium smegmatis*
M. tuberculosis – *Mycobacterium tuberculosis*
MA – Mycolic acids
mAGP – Mycolyl-arabinogalactan-peptidoglycan
MBC – Minimum bactericidal concentration
mDAP – *Meso*-diaminopimelic acid
MDR – Multi-drug resistant
MER – Meropenem

MER-clavulanate – Meropenem combined with clavulanate
MIC – Minimum inhibitory concentration
Mϕ – Human macrophages
MOI – Multiplicity of infection
*Mtb*C – *Mycobacterium tuberculosis* complex
MurNAc – *N*-acetyl-muramic acid
MurNGly – *N*-glycolylmuramic acid
NAD – Nicotinamide adenine dinucleotide
NLR – NOD-like receptors
NOD – Nucleotide-binding oligomerization domain
NT strand – Non-template strand
NTM – Non-tuberculous mycobacteria
OADC – Oleic acid albumin dextrose catalase
OL – Outermost layer
OM – Outer membrane
PAM – Proto-spacer adjacent motif
PAMPs – Pathogen-associated molecular patterns
PBPs – Penicillin binding proteins
PBS – Phosphate buffer saline
PG – Peptidoglycan
PIMs – Phosphatidyl-*myo*-inositol mannosides
pre-crRNA – Long primary CRISPR RNA
PRRs – Pattern recognition receptors
qRT-PCR – Quantitative real-time polymerase chain reaction
R. erythroopolis – *Rhodococcus erythroopolis*
RF – Rifampicin
rpm – Rotations *per* minute
Rv – Reverse
S. pneumoniae - *Streptococcus pneumoniae*
S. pyogenes – *Streptococcus pyogenes*
S. aureus – *Staphylococcus aureus*
SEM – Standard error of the mean
sgRNA – Single guide RNA
T strand – Template strand
TB – Tuberculosis
TLR – Toll-like receptors
trans-crRNA – *trans*-acting CRISPR RNA
TSS – Transcription start site
U – Units
UDP – Uridine diphosphate
WT – Wild-type
XDR – Extensive-drug resistant

1. Introduction

1.1 Tuberculosis

Tuberculosis (TB) is an infectious disease that belongs to the top 10 causes of death in the world and is the number one cause of death from a single agent, the intracellular pathogen *Mycobacterium tuberculosis* (*M. tuberculosis*)[1]. According to the World Health Organization, in 2019, approximately 1.5 million people died and 10.0 million people fell ill with TB[1]. Currently, it is estimated that a quarter of the world's population (around 1.9 billion people) is latently infected with *M. tuberculosis* and 5 to 10% is thought to develop TB during lifetime[1,2].

TB transmission occurs mainly through the expelling of airborne droplets containing bacteria (typically by coughing), from infected to uninfected people[1–4]. The most frequent form of TB affects the lungs (pulmonary TB), but it can also affect other body locations (extrapulmonary TB) in up to a third of patients[1,2]. Active pulmonary TB is characterized by the development of symptoms like persistent cough, cough with blood, weakness, chest pains, fever, and night sweats[5].

The most common preventive strategy of TB is the Bacille Calmette-Guérin (BCG) vaccine (developed almost 100 years ago), that confers protection from severe forms of TB (TB meningitis and miliary TB) in children[1]. The current TB diagnosis comprises sputum smear microscopy, rapid molecular tests, culture-based methods that provide results in up to 12 weeks, and whole-genome sequencing methods[6,7]. The first-line anti-TB drugs used in TB treatment includes isoniazid (INH), rifampicin (RF), ethambutol (EMB), and pyrazinamide[1]. The second-line comprises injectable agents (amikacin, capreomycin, kanamycin), fluoroquinolones (levofloxacin, moxifloxacin, and gatifloxacin), ethionamide, cycloserine, linezolid, bedaquiline, and clofazimine[1,8,9].

The emergence of multi- and extensive-drug resistant (MDR and XDR, respectively) strains and the corresponding lack of efficacious treatments are major problems within TB. MDR comprise resistant strains to the first-line anti-TB drugs INH and RF, and XDR strains include MDR with additional resistance to at least one fluroquinolone and one second-line anti-TB injectable drug[1,2]. In cases of drug-susceptible TB, the treatment generally involves the use of first-line anti-TB drugs for at least 6 months, but in cases of drug-resistant TB, the treatment is usually longer (9 to 24 months), complex, expensive, and includes the combination of second-line anti-TB drugs, counselling, and monitoring[1,9–11]. With the widespread antibiotic resistance, there is urgent need of novel anti-TB strategies, which until now still strongly rely on old methods of prevention, diagnosis, and treatment[1,4,12].

Mycobacteria are extremely diverse and understanding the differences and phylogenetic relationships between *M. tuberculosis* and other related less pathogenic mycobacteria has contributed for the identification of key genomic determinants of virulence and drug resistance[13–15].

1.2 Phylogeny of mycobacteria

The *Mycobacterium* genus (phylum Actinobacteria) appears to have arisen more than 150 million years ago[16] and includes almost 200 *Mycobacterium* species that can be characterized by an aerobic or microaerophilic growth in branched filaments, with optimal growth between 25 and 50 ºC, depending on the species, by an elevated content in GC and by a great diversity at a morphological and physiological level[13,17]. For instance, depending on the degree of glycopeptidolipids glycosylation, some species, such as *Mycobacterium smegmatis* (*M. smegmatis*), can have different variants – smooth or rough[13] – or depending on pigmentation, mycobacteria can be classified into scotochromogenic, photochromogenic or nonphotochromogenic[18].

The *Mycobacterium* species are divided into the *M. tuberculosis* complex (*Mtb*C) composed by TB-causing mycobacteria (such as *M. tuberculosis*, the main causative agent of human TB, *Mycobacterium*

canettii, *Mycobacterium africanum*, and *Mycobacterium bovis*), non-tuberculous mycobacteria (NTM) and *Mycobacterium leprae.* These are also classified into fast-growers and slow-growers, depending on the formation of colonies in less or more than seven days, respectively[15,17].

The *Mtb*C and M*ycobacterium leprae* are categorized as slow-growing strictly pathogenic mycobacteria[13]. The human-adapted *Mtb*C members are obligate pathogens of humans, causing disease in order to replicate and be transmitted from host-to-host, without any environmental reservoir[3,17,19]. The genetic changes that allowed the evolution of *Mtb*C from an environmental organism to a professional pathogen are related with a biphasic evolutionary process of acquisition of new genetic elements through horizontal gene transfer and successive deletion of non-essential genetic material[15].

The NTM group includes several fast-growing and few slow-growing mycobacteria and comprises mainly environmental bacteria, present in soils or water sources[14]. NTM include strictly pathogenic, opportunistic pathogenic, and saprophyte non-pathogenic mycobacteria that can cause serious infections, particularly in immune-compromised individuals, leading to a broad spectrum of diseases, including pulmonary, skin, or disseminated diseases[20].

Due to the global burden of TB, several *Mycobacterium* species have been used by researchers to understand *M. tuberculosis* biology and pathogenicity and to improve the development of new drug targets. The *M. tuberculosis* H37Rv strain, isolated in 1905, has been extensively used, mainly due to its full virulence in animal models of TB and full anti-TB drug susceptibility[21,22]. The *M. tuberculosis* H37Ra is its avirulent counterpart, with origin in the same parental H37Rv strain, isolated from a 19-year-old male TB patient in 1935, and has also been widely used, especially due to be able to handle in a biosafety level (BSL) 2 laboratory[22,23]. In addition, several NTM species have been similarly used as study models for TB research in BSL1 and BSL2 laboratories[24]. For instance, *M. smegmatis*, isolated in 1885 from genital secretions, and, in particular, the *M. smegmatis* mc^2155 strain that has been used in genetic analysis, mainly due to its high transformation efficiency and its fast doubling time of 3 h[25].

The peculiar mycobacterial cell wall (CW) is a typical feature of mycobacteria and includes a crucial peptidoglycan (PG) layer that is responsible for the maintenance of cell integrity and shape. The processes of PG biosynthesis and recycling involve essential enzymes for *M. tuberculosis* viability and thus, are considered alternative and attractive targets for the development of new anti-TB drugs[26,27].

1.3 Mycobacterial CW structure

The CW is a key component of all bacteria and depending on its properties, bacteria can be classified into Gram-positive, Gram-negative and acid-fast[26]. The mycobacterial CW has unique features and thus, its classification is still a subject of debate[28,29]. It has properties of both Gram-positive (GC-rich DNA and a thick PG layer) and Gram-negative bacteria (presence of an inner membrane, PG layer, and an outer membrane) and is categorized as “acid fast bacilli” due to acid alcohol decolourization resistance[26,29]. The typical CW of *M. tuberculosis* accounts for its success as a pathogen, having a role in cell-shape preservation, innate resistance to several drugs, and virulence[26,29].

The main components of the mycobacterial CW are a cross-linked and typically modified PG, a highly branched arabinogalactan (AG) polysaccharide and long-chain mycolic acids (MA), all together commonly designated as the mycolyl-arabino-galactan-peptidoglycan (mAGP) complex[26]. The PG is situated outside the cytoplasmatic membrane and is covalently attached to AG, which is linked to MA[26].

Within the mAGP complex are also distributed non-covalently linked glycolipids, such as phosphatidyl-*myo*-inositol mannosides (PIMs), lipomannans (LMs), lipoarabionomannan (LAM), and mannosylated LAMs[26]. Intercalated into the MA are acyl lipids, namely trehalose monomycolate, trehalose dimycolateacyltrehalose, polyacyltrehalose, phthiocerol dimycocerosate, and sulfoglycolipid, all forming the outer membrane (OM). Moreover, there is a outermost layer that corresponds to the mycobacterial capsule, predominantly composed of polysaccharides and proteins[30].

All of the components of the mycobacterial CW are of vital importance to cell permeability, pathogenicity, and viability. As a result, its biosynthesis steps are considered useful targets for the development of anti-TB drugs, as exemplified by the well-known first-line anti-TB drugs EMB and INH that target and inhibit crucial steps in the AG and MA biosynthesis, respectively.

1.3.1 PG layer

The PG is a complex, dynamic and conserved structure with crucial functions, such as in bacterial shape, osmotic pressure withstand, cellular communication, and host immune response[26]. The PG layer is composed of β(1→4)-linked *N*-acetyl-glucosamine (GlcNAc) and *N*-acetyl-muramic acid (MurNAc) residues, forming a conserved glycan strand cross-linked by short peptide bridges[26,31–33].

The PG biosynthesis (see **Figure 1.1**) starts in the cytoplasm with the generation of uridine diphosphate (UDP)-GlcNAc in 4 steps, catalysed by the GlmS, GlmM, and GlmU enzymes[21]. The next steps include the formation of the soluble PG peptide precursor (UDP-MurNAc-pentapeptide) in sequential reactions catalysed by the Mur ligases A-F[26,30]. The UDP-GlcNAc is converted to UDP-MurNAc by MurA (UDP-GlcNAc enolpyruvyl transferase) and MurB (UDP-*N*-acetyl-enolpyruvyl-glucosamine reductase), and the pentapeptide chain is successively assembled by the adenosine triphosphate (ATP)-dependent enzymes MurC-F, that catalyse the addition of L-Alanine (L-Ala), D-*iso*-*g*lutamate (D-*i*Glu), *meso*-diaminopimelic acid (*m*DAP), and D-Alanyl-D-Alanine (D-Ala-D-Ala) residues, respectively, as well as ATP hydrolysis[26,35].

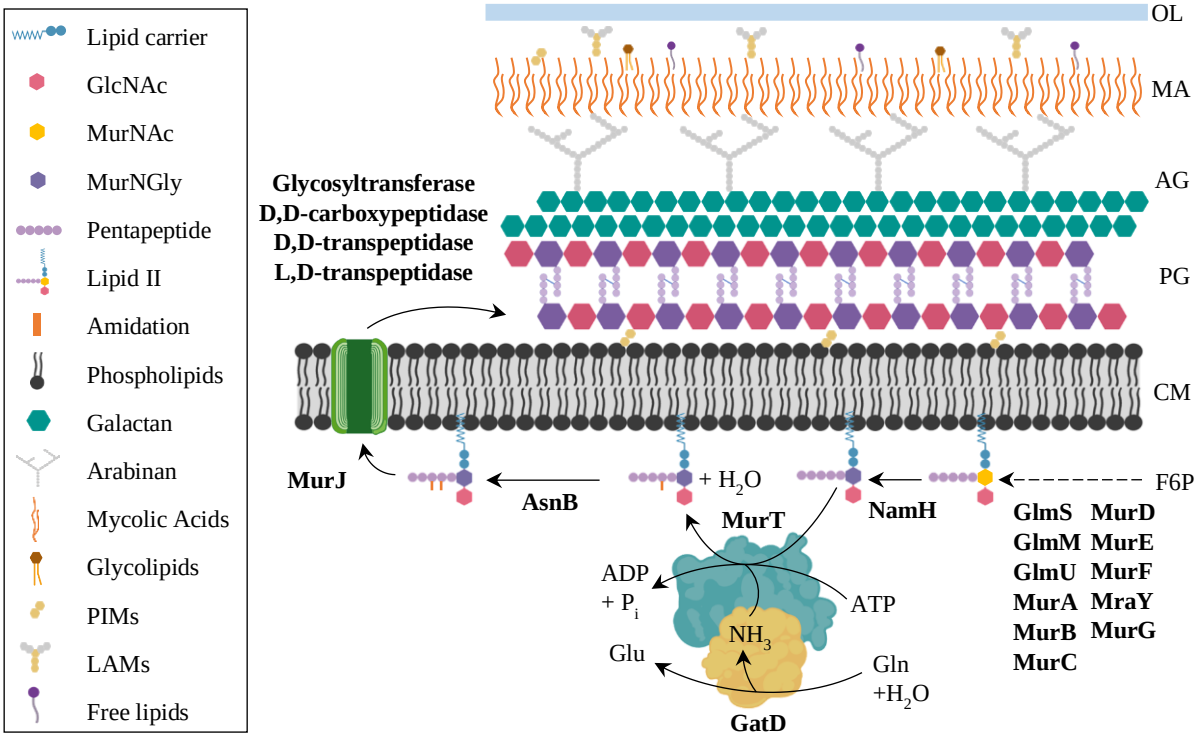

Figure 1.1 – Schematic representation of the mycobacterial CW with focus on the amidation of the D-*i*Glu residue of the PG, catalysed by the MurT/GatD enzymatic complex. The mycobacterial CW is mainly composed by a cross-linked and modified PG layer, a highly branched AG polysaccharide and long-chain MA. ADP, adenosine diphosphate; ATP, adenosine triphosphate; AG, arabinogalactan; CM, cytoplasmatic membrane; F6P, fructose 6-phosphate; GlcNAc, *N*-acetyl-glucosamine; Gln, glutamine; Glu, glutamate; LAMs, lipoarabinomannan; MA, mycolic acids; MurNAc, *N*-acetyl-muramic acid; MurNGly, *N*-glycolylmuramic acid; OL, outer layer; PG, peptidoglycan; P_i, inorganic phosphate; PIMs, phosphatidylinositol mannosides.

The following reactions are membrane-anchored steps, in which the MraY (phospho-*N*-acetylmuramoyl-pentapeptide transferase) catalyses the linkage of the PG precursor to a lipid carrier

(decaprenyl phosphate (dP-P) in *M. tuberculosis*), generating lipid I (dP-P-MurNAc-pentapeptide)[26,30]. The MurG (GlcNAc transferase) catalyses the transfer of GlcNAc from UDP-GlcNAc to lipid I, to yield lipid II (dP-P-MurNAc-pentapeptide-GlcNAc)[26]. The next reaction is the *N*-glycolylation of the MurNAc by the hydroxylase NamH, forming the *N*-glycolylmuramic acid (MurNGly)[26,36]. Besides this PG modification, MurT (a ATP-dependent Mur ligase-like protein) and GatD (glutamine transferase protein) catalyse the amidation of the lipid II D-*i*Glu residue[26,33,37] and the glutamine amidotransferase AsnB is responsible for *m*DAP amidation[26,37–39]. The transfer of the modified lipid II to the periplasm is carried out by a lipid II flippase (FtsW or MurJ)[26], which role still requires clarification[26,40–42].

The PG polymerization takes place in the periplasm, through the action of penicillin binding proteins (PBPs)[26]. In mycobacteria, class A PBPs includes the bifunctional PBP1 and PBP2 (encoded by *ponA1* and *ponA2,* respectively), with glycosyltransferase and D,D-transpeptidase activities, class B PBPs includes the D,D-transpeptidases PBPA and PBPB (encoded by *pbpA* and *pbpB,* respectively)[26,43–45], and class C PBPs are PG hydrolases with D,D-endopeptidase or D,D-carboxypeptidase activity[26]. *M. smegmatis* and other NTM have an extra gene encoding for a third class A PBP, *ponA3,* which is a paralog of *ponA2*[46]. The glycosyltransferase domain of the mycobacterial PBPs are responsible for attaching the GlcNAc moiety of lipid II monomers to the MurNGly moiety of the growing PG chain, with the concomitant release of the dP-P lipid carrier[26,43]. The D,D-transpeptidase domain catalyses the common D,D-(or 4→3) cross-links between the penultimate D-Ala and the *m*DAP residues of adjacent pentapeptide chains, with the cleavage of the last D-Ala by the action of D,D-carboxypeptidases[26,45].

A typical feature of mycobacteria is the high proportion (~80%) of L,D-(or 3→3)-cross-links, catalysed by L,D-transpeptidases (LDTs)[26]. In *M. tuberculosis* there are five LDts, LDT_{Mt1} to LDT_{Mt5}, that form L,D-cross-links between two *m*DAP adjacent residues[26]. The mycobacterial PBPs and LDts combined activities are crucial for CW synthesis during bacterial growth[47]. It is described that changes in the mycobacterial environmental or growth phase, such as in the presence of β-lactams antibiotics or in a growth stationary phase, can lead to the shift of PG D,D-cross-links into L,D-cross-links[26,48,49].

1.3.1.1 Modifications of the mycobacterial PG

During the PG biosynthesis, lipid II undergoes some unique chemical changes, such as *N*-glycolylation and amidation, that are crucial PG modifications with influence in antibiotic resistance and in host immune recognition[26,31,37,50]. Given the important role of these modifications, the corresponding PG biosynthesis steps can be interesting targets for the design of anti-TB strategies.

The *N*-glycolylation of the MurNAc by NamH is an exclusive PG modification of mycobacteria and of only five other closely related genera of bacteria[36]. A *namH* deletion seems to increase the susceptibility to β-lactams and lysozyme in *M. smegmatis*[26,36]. Also, this PG modification appears to play a key role in host immune response, since it is demonstrated that a glycolylated PG is more efficient in inducing nucleotide-binding oligomerization domain (NOD) 2-mediated host responses[50].

In mycobacteria, PG amidation occurs in the α-carboxylate of D-*i*Glu and in the *ε*-carboxylate of *m*DAP residues[31,32]. Unlike *namH,* the genes encoding for the enzymes that catalyse these reactions, *murT, gatD,* and *asnB,* are essential for *M. tuberculosis* growth[38,51,52]. D-*i*Glu amidation seems to influence the susceptibility to β-lactams and lysozyme and the PG cross-linking[26,37,53], while *m*DAP amidation appears to be involved in PG hydrolysis modulation[26,38]. Some experiments on host immune stimulation found that D-*i*Glu and *m*DAP amidation strongly reduced host NOD1 activation[37,54].

1.3.1.1.1 The MurT/GatD enzymatic complex

The amidation of the PG D-*i*Glu residue was recently described as catalysed by the MurT/GatD heterodimeric enzymatic complex in *Staphylococcus aureus* (*S. aureus*) and *Streptococcus pneumoniae*

(*S. pneumoniae*)[31,33,37]. The activity of the complex begins with the deamination of one glutamine (specific nitrogen donor) to form glutamate and ammonia by GatD, and it ends with the amidation of the α-carboxyl group of the lipid II D-*i*Glu (acceptor substrate), yielding D-*iso*-glutamine (D-*i*Gln), in an ATP and Mg^{2+}-depend reaction by MurT (see **Figure 1.1**)[31,33,37,55,56].

The corresponding genes, *murT* and *gatD*, are essential for bacterial growth and assembled in an operon with a common promoter upstream *murT* in several bacteria, including in *S. aureus*, *S. pneumoniae*, and *M. tuberculosis*[33,37,53,57,58]. In *S. aureus*, the inhibition of the operon revealed a deficit in growth rate, a decrease in the β-lactam resistance and an increased sensitivity to lysozyme[33,37]. Nevertheless, the differences in β-lactam and lysozyme resistance are also dependent on the bacterial genetic background[59]. Complementation experiments of a MurT/GatD mutant showed that this PG modification only occurs at least with the expression of *murT*, in addition to a basal level of *gatD*[37]. Moreover, the GatD protein is inactive in the absence of MurT[33,55].

In *S. pneumoniae*, a deficient amidation of the lipid II D-*i*Glu residue resulted in a reduction of PG cross-linking[53], supporting that a non-amidated lipid II is a non-preferential substrate for PG transpeptidation[31,55,56,60–62]. The presence of PG amidation causes a reduction of the CW negative net charge and polarity, contributing to a more facilitated translocation of the lipid II to the periplasm[33,37,63].

Structurally, MurT has a typical Mur ligase central substrate-binding domain with conversed motifs involved in ATP and Mg^{2+} binding[37,56]. MurT recognizes ATP and lipid II and has a ATP consensus binding site[33,37]. Among *Bacilli*, MurT showed a conserved cysteine (Cys)-rich insertion that probably binds zinc and facilitates the interface with GatD, and ammonia seems to be channelled to the MurT active site by a cavity network[31,56]. In *M. tuberculosis* and other Actinobacteria, however, this Cys-rich region is not conserved and showed higher interspecies variability[64]. The yet poorly known C-terminal domain of MurT (Pfam: DUF1727) seemed to function as the physical link with GatD and to include conserved regions important for the enzymatic activity of the complex[37,63]. The absence of the DUF1727 domain led to a decrease in β-lactam resistance and a bacterial growth rate similar to a conditional mutant lacking MurT/GatD expression[63].

GatD is similar in sequence to the catalytic domains of glutamine-dependent amidotransferases (GATases) with glutamine amide transfer activity, but lacks residues involved in dethiobiotin synthase activity and part of a ATP binding motif, that are common in these enzymes, supporting the MurT-dependent activity[31,37,56]. Among Gram-positive bacteria and also in *M. tuberculosis*, GatD active site was found to contain a catalytic triad, similarly to other GATases, with conserved Cys and histidine (His) residues, but lacking the Glu residue[33,37]. Interestingly, conserved aspartates have been proposed to substitute this Glu in *S. aureus* and *S. pneumoniae*[64].

1.3.1.1.2 AsnB

The enzyme responsible for the amidation of the lipid II *m*DAP residue was first identified in *Lactobacillus plantarum* as the product of the essential *asnB1* gene[65] and as belonging to the glutamine-dependent asparagine synthase family, catalysing the ammonia transfer from a glutamine donor to a *m*DAP acceptor on PG precursors[65–67]. Other *asnB1* homologues were later found, such as *ltsA* in *Corynebacterium glutamicum* (*C. glutamicum*) and *Rhodococcus erythroopolis* (*R. erythroopolis*), and *asnB* in *Bacillus subtilis* (*B. subtilis*), *M. smegmatis*, and *M. tuberculosis*, being *asnB* essential for *M. tuberculosis* growth[38,52,67–69]. In *M. smegmatis*, the AsnB N-terminal glutaminase domain catalyses the glutamine hydrolysis and has a Cys residue essential for GATase activity, whereas the C-terminal synthase domain catalyses the conversion of aspartate to asparagine[68,70].

In *C. glutamicum* and *R. erythroopolis*, *ltsA* mutants showed changes on cell size, susceptibility to β-lactams and lysozyme sensitivity, that could be complemented with *ltsA* homologues from *B. subtilis* and *M. smegmatis*[69,71]. Contrarily, a *M. smegmatis asnB* transposon mutant did not show sensitivity to

lysozyme, but to several hydrophobic drugs, indicating a *m*DAP amidation role in natural resistance and in CW permeability[68].

The amidation of *m*DAP residues seems to not affect the overall PG transpeptidation, but appears to be crucial for L,D-cross-linking, including in *M. tuberculosis*[26,38,52,65,67,71]. Other experiments in *B. subtilis* indicated a role of *m*DAP amidation and Mg^{2+} in PG hydrolysis control[38,67]. The *asnB* mutant of *B. subtilis* showed increased sensitivity to lysozyme and to antibiotics that target the CW synthesis (such as vancomycin, methicillin, penicillin, and cefuroxime) and exhibited a morphological phenotype similar to that presented by cells with a disrupted PG hydrolysis system[38,72,73], along with an uncontrolled PG degradation, which was reduced by high Mg^{2+} concentrations[38].

Recently, two non-essential genes (*asnB* and *asnB2*) encoding potential enzymes responsible for the *m*DAP amidation were identified in *Clostridium difficile*, and *asnB* was demonstrated as encoding for the enzyme that catalyse this modification, but only in the presence of vancomycin, in a mechanism independent of the *van*G_{Cd} cluster, that remains to be further understood[74].

1.4 Antibiotics targeting the mycobacterial CW

Since the 1990s that several drugs have been discovered and approved for administration in TB treatment regimens, many of them targeting the mycobacterial CW. The first-line anti-TB drugs EMB and INH are good examples, inhibiting the mycobacterial AG and MA biosynthesis, respectively.

EMB is a synthetic compound that inhibits the Emb arabinosyltransferases enzymes (EmbA and EmbB), both responsible for the polymerization of arabinose sugar residues that are required for the formation of D-arabinan in the mycobacterial AG biosynthesis process[30,75,76]. EMB can also inhibit the biosynthesis of glycolipids of the mycobacterial CW, such as LMs and LAMs[77,78]. More recently, EMB was postulated to target the glutamate racemase MurI, involved in PG synthesis, which racemises L-Glu to D-Glu[78,79]. EMB has been shown to compromise the cell integrity, permeability and host recognition[80]. Both in *M. smegmatis* and *M. tuberculosis*, EMB resistance have been associated with mutations in the *embCAB* operon, encoding *embA*, *embB* and *embC* genes[81]. Interestingly, *embB* mutations have been also related with altered resistance to INH and RF[82].

The INH pro-drug needs a cellular activation by the mycobacterial catalase-peroxidase KatG, resulting in an adduct with the nicotinamide adenine dinucleotide (NAD)[83]. The INH-NAD adduct inhibits the enoyl-Acyl carrier protein reductase InhA, involved in the fatty acid synthase type II pathway of the MA biosynthesis[83], and leads to the intracellular accumulation of mycolates and to a CW disintegration, rapidly killing actively growing mycobacteria[84]. The InhA I194T, KatG S315T, and f*abG1-inhA* (-15C to T) mutations are the most common causes of mycobacterial INH resistance[85–87].

Given the efficacy of these anti-TB drugs and the crucial role of the mycobacterial CW, alternative antibacterial compounds and enzymes that target this structure have been investigated, especially to deal with the increasing emergence of MDR and XDR strains. For instance, despite the natural resistance of mycobacteria to most β-lactams, these PG targeting antibiotics are widely and efficiently used against common bacterial pathogens, and in combination with β-lactamase inhibitors have been shown as bactericidal against both replicating and non-replicating forms of *M. tuberculosis*[88,89].

1.4.1 The β-lactam antibiotics and its potential application in TB treatment

β-lactams target the PG biosynthesis by inhibiting the action of PBPs and in some cases LDts[88,90]. These antibiotics mimic the D-Ala-D-Ala PG dipeptides and have a core β-lactam ring linked to diverse side groups[91], allowing the formation of a covalent adduct within the active site of PBPs[31,53]. Through the inhibition of PG cross-linking, β-lactams can lead to a bacteriostatic outcome, morphological

alterations or rapid bacteriolysis[92]. According to the side group of the core β-lactam ring, β-lactams can be classified in penicillins, cephalosporins, carbapenems, monobactams, and β-lactamase inhibitors.

Mycobacteria are naturally resistant to most β-lactams, mainly due to the: 1) expression of the class A (Amber) β-lactamase (BlaC and BlaS, in *M. tuberculosis* and *M. smegmatis*, respectively) that efficiently hydrolyses the β-lactam ring of β-lactams, preventing their interaction with PBPs[21,90,92–94]; 2) induction of drug efflux pumps; 3) alternative expression of LDts insensitive to β-lactams or low affinity PBPs; and 4) impermeable OM, rich in MA, that avoids antibiotic penetration[48,93–97]. BlaC has a broad substrate specificity, hydrolysing penicillins, cephalosporins, and some carbapenems, and is susceptible to different β-lactamase inhibitors, such as clavulanate[98]. β-lactamase inhibitors are structurally similar to β-lactams, which allow them to covalently bind and inhibit β-lactamases.

The penicillin subclass of β-lactams is known as efficient against both Gram-positive and Gram-negative bacterial infections and comprises members as penicillin, ampicillin, and amoxicillin (AMX). AMX is one of the best substrates for BlaC, but combined with clavulanate (AMX-clavulanate) has been shown success against *M. tuberculosis in vitro* and some bactericidal activity in drug-resistant TB patients[99–101]. The loss of LDt_{Mt2} showed increased susceptibility of mycobacteria to AMX-clavulanate, and more recently, by investigation of several clinical isolates and its reference strains with different drug-susceptibilities, it was observed that MDR and XDR clinical isolates were more susceptible to this combination than the reference strains, that were susceptible to first- and second-line anti-TB drugs[48,102]. AMX-clavulanate is considered an inexpensive and accessible oral drug combination[103] and thus, its potential application in TB treatment is of great interest.

The cephalosporins are divided in five groups or generations and have different antibacterial activities. Cefotaxime (CEF) is a third-generation cephalosporin and has a remarkable activity against Gram-positive bacteria. Besides inhibiting mycobacterial PBPs, CEF also seems to form covalent adducts with the mycobacterial LdT_{Mt1}, leading to its inhibition and to the elimination of the R_2 drug side chain, a reaction that appears to happen to optimize the LDt inativation[104].

The carbapenems are the third major class of β-lactams and, in addition to a high affinity to class A PBPs, this class has been described as able to bind and inhibit several LDts, in particular LDt_{Mt1} and LDt_{Mt2}, potentially leading to mycobacterial killing[48,95,105,106]. This is supported by carbapenems having an opposite chirality of the α-carbon, comparing to other β-lactams[107]. Carbapenems seem to be poorer substrates for BlaC, being hydrolysed at a lower rate than other β-lactams, and even lead to its inhibition[88,108]. Particularly, meropenem (MER) combined with clavulanate (MER-clavulanate) has shown a bactericidal activity against drug-susceptible, XDR strains and nonreplicative forms of *M. tuberculosis*[88,109–111].

All of these evidences support the further investigation and the repurposing of β-lactams, especially combined with β-lactamase inhibitors, to be alternative therapeutics against MDR and XDR TB.

1.5 Host immune response in TB

After inhalation of *M. tuberculosis* into the respiratory tract, the first line of host defence includes the airway epithelial cells and several phagocytic cells, such as human macrophages (Mϕ), neutrophils, and dendritic cells (DCs)[112], that recognize bacteria through pattern recognition receptors (PRRs). In the lungs, these cells eliminate bacteria by phagocytosis or, more likely, become infected and accumulated in the lungs, harbouring mycobacteria in phagosomes in continuous replication[113]. Particularly in Mϕ, mycobacteria can modulate the trafficking and maturation of the phagosome, evading killing mechanisms and host cell apoptosis, promoting a longer survival and replication[112,114].

Eventually, mycobacteria can lead to host cells death by necrosis or apoptosis and new phagocytes are recruited by cytokine signalling, such as TNF[5]. Several infected phagocytic cells are able to present mycobacterial antigens to activate $CD4^+$ T cells, also contributing to the recruitment of more phagocytes

to form a granuloma, the hallmark of TB[115]. This organized structure includes populations of Mϕ, DCs, and monocytes, and can benefit the host by containing and arresting bacterial growth, but also benefit the pathogen by providing several intracellular niches for bacterial expansion[112,113].

The majority of people infected with TB is able to remain in an asymptomatic latent stage the whole life, with *M. tuberculosis* in a dormant state inside the granuloma[112]. Only 5 to 10% of infected individuals is thought to later develop an active stage of TB, which is accompanied by clinical symptoms and mainly caused by deficiencies in $CD4^+$ T cells[116], therapeutic neutralization of TNF[117], imbalance between regulatory and effector T cells and altered antigen expression[112]. In active TB, the immune system is unable to control the bacterial infection and the bacterial populations destroy the granuloma luminal surface Mϕ, causing adjacent lung tissue necrosis and caseous cavities, that highly contribute to mycobacterial expelling and to host-to-host transmission via the airborne route[5,112,113,118].

1.5.1 Mycobacterial PG amidation in host immune recognition

The host immune system recognizes *M. tuberculosis* via several PRRs, such as toll-like receptors (TLRs), C-type lectin receptors, and NOD-like receptors (NLRs)[112], expressed on innate immune cells to identify conserved bacterial elements, the pathogen-associated molecular patterns (PAMPs)[54,119]. PRRs recognize PAMPs and activate signalling cascades, inducing the expression of pro-inflammatory cytokines, phagocytosis, and other host defence mechanisms[119].

Among TLRs, TLR2 senses mycobacterial lipoproteins, such as PIMs and LMs, TLR4 recognizes mycobacterial glycolipoproteins, and TLR9 senses mycobacterial DNA[120,121]. The resulting response includes the induction of pro-inflammatory cytokines, such as TNF-α, IL-1β, and IL-6 by Mϕ and DCs[112,119]. Among NLR, NOD1 and NOD2 sense mycobacterial CW elements, namely glycolipids and PG motifs[122]. NOD1 can be activated by γ-D-Glu-*m*DAP PG motifs and NOD2 senses PG MurNAc-L-Ala-D-*i*Glu fragments[123]. These PRRs induce pro-inflammatory and antimicrobial responses, such as the recruitment of innate and adaptative immune cells, activation of transcription factors, including NF-kB, and induction of pro-inflammatory cytokines and chemokines[54,124,125].

Interestingly, the specific recognition of D-*i*Glu and *m*DAP amidated residues has been shown to influence the NOD1-mediated host immune response[54] by causing an impaired recognition and activation of NOD1[37,54,126–128]. Amidated *m*DAP residues appear to interact with residues far from the NOD1-leucine-rich repeat, allowing an evasion of the recognition of PG motifs by NOD1[126,129]. Contrarily, the NOD2-mediated responses seem to not be altered by D-*i*Glu or *m*DAP amidation[37,127].

Inducing the action of certain molecules, such as defensins and lysozyme, constitute one of the host's innate mechanisms against pathogens. In particular, the susceptibility to plectasin, a fungal defensin which acts by specifically binding to the bacterial lipid II, was observed to be increased in cases of a *murT*/*gatD* depletion[33,130]. Furthermore, this depletion also increases the bacterial sensitivity to lysozyme, an innate immune system muramidase that hydrolyses PG β-(1→4) bonds[33,37].

Therefore, the PG amidation seems to somehow modulate the host immune recognition and must be further explored within this context.

1.6 CRISPR

Currently, there is an increasing demand for new and more efficient genetic tools that can be used in drug target characterization[131,132]. In the context of TB, this is urgent, especially to deal with drug-resistant cases of TB[131,132]. Recently, the use of the clustered regularly interspaced short palindromic repeat (CRISPR) system together with its associated proteins (CRISPR-Cas) emerged as a very effective and alternative genetic tool for targeted gene regulation[133–135]. The CRISPR-Cas is an adaptative RNA-mediated response mechanism present in most bacteria and archaea to cleave foreign nucleic acid[131,136].

In the CRISPR locus, *cas* genes are encoded by putative operons and are adjacent to sequences coding the CRISPR system, characterized by a set of palindromic repeats sequences[136]. The Cas heterogeneous family of proteins has typical domains of nucleases, helicases, polymerases, and polynucleotide-binding proteins[136,137]. Typically, different organisms can have distinct types of the CRISPR-Cas system, but all consist in 3 separated steps: adaptation, expression, and interference[131,136].

The best-characterized system is the *Streptococcus pyogenes* (*S. pyogenes*) type IIA system, which action begins with a Cas1 and Cas2-mediated recognition and integration of spacer precursors (proto-spacers) into the host chromosomal CRISPR locus, between short DNA repeats, forming spacers[136,138]. The recognition of proto-spacers from the invading nucleic acids is achieved by a prior identification of unique proto-spacer adjacent motif (PAMs)[131,134,136]. The second step includes the transcription of the CRISPR locus containing the spacers, forming a long primary CRISPR RNA (pre-crRNA), that is processed into short crRNAs by a *trans*-acting RNA (*trans*-crRNA), who has complementarity with pre-crRNA repeat fragments and guides the RNase III and the endonuclease Cas9 protein to catalyse pre-crRNA cleavage in a repeat or spacer fragment, respectively[136,139]. The last step is interference, where, the mature crRNAs guide the Cas9 protein to the foreign nucleic acid sequences, complementary to crRNA spacers and adjacent to the respective PAM, leading to cleavage within the proto-spacer[131,139,140].

Recently, it was found that this type II CRISPR-Cas system from *S. pyogenes* can be simplified by a Cas9 protein and a designed small single guide RNA (sgRNA)[141]. This sgRNA has 3 different domains: 20 base pair (bp) complementary to the target gene sequence adjacent to a PAM and containing a "seed sequence", a 42 bp hairpin that mimics the fusion of the two RNAs (crRNA and *trans*-crRNA) and that holds the Cas9 protein, and a 40 bp transcription terminator from *S. pyogenes*[135,141]. The specific double stranded cleavage in the target sequence by Cas9 is dictated by the sgRNA-DNA base pairing and by the crucial presence of the PAM sequence in the target DNA, next to the hybridization site[131,133,139,141].

1.6.1 CRISPRi

More recently, an altered CRISPR system (**Figure 1.2**), the CRISPR interference (CRISPRi) system, was developed by transferring the original CRISPR-Cas9 system from *S. pyogenes* to *E. coli*, and by using a catalytically inactive modified version of this Cas9 protein ($dCas9_{Spy}$)[135]. The $dCas9_{Spy}$ contains two point mutations (D10A and H840A) in the nuclease domains, causing a deficient endonuclease activity[135,141] and thus, when co-expressed with a designed sgRNA that is complementary to a target sequence located next to an appropriate PAM sequence, causes a specific gene silencing[132,135].

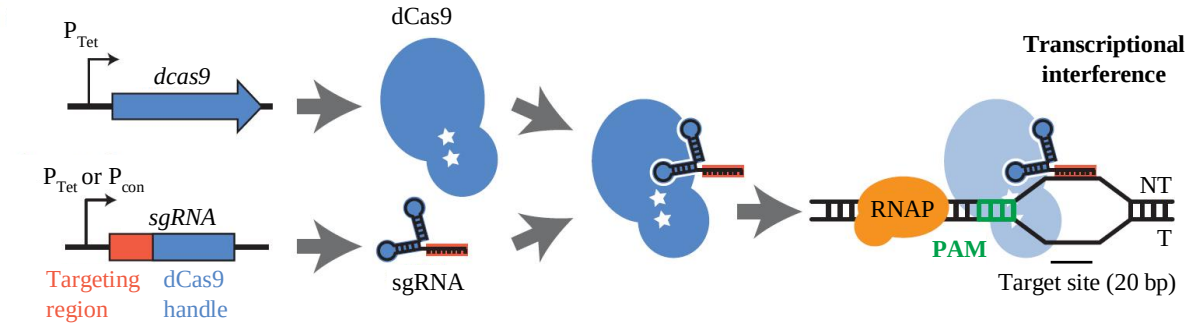

Figure 1.2 – **Schematic representation of the mechanism of action of the CRISPRi system to achieve transcriptional repression.** bp, base pair; dCas9, deficient Cas9 protein; NT, non-template strand; PAM, proto-spacer adjacent motif; P_{con}, constitutive promoter; P_{Tet}, ATc-inducible promoter; RNAP, RNA polymerase; sgRNA, single guide RNA; T, template strand.

The characterization of CRISPRi in both *Escherichia coli* (*E. coli*) and *B. subtilis* indicated that when the sgRNA-$dCas9_{Spy}$ complex binds the DNA target, it leads to a transcription repression due to a

physical collision with the RNA polymerase, that prevents promoter targeting and transcription initiation or transcription elongation[135,142,143]. The targeting of the non-template (NT) strand seems to lead to a more effective gene silencing (up to 300-fold repression) than targeting the template (T) strand of the target gene[135], which can suggest that the RNA polymerase is able to overcome the sgRNA-dCas9 obstruction and continue the transcription process in the T strand orientation[135]. Regarding the gene promoter silencing efficiency, it appears to be independent of which DNA strand is targeted[135]. Additionally, this system did not show significant off-target effects and seems to lead to a highly specific gene targeting and interference, dictated by a PAM presence, the sgRNA length and sgRNA-DNA degree of complementary[135].

Interestingly, less remarkable results were obtained in the first attempts of implementation of CRISPRi-dCas9$_{Spy}$ system in mycobacteria[131,144]. The induction of this system in mycobacteria resulted in some degree of dCas9$_{Spy}$ toxicity and poor level of gene repression (around 3- to 4-fold)[131,132,144]. However, these limitations seemed to be overcome by the use of an alternative deficient Cas9 protein derived from CRISPR1 locus of *Streptococcus thermophilus* (dCas9$_{Sth1}$)[145].

Rock and co-workers developed a similar but more efficacious CRISPRi system, using a single plasmid system (**Figure 6.1A** in **Annexes**) containing: 1) a codon-optimized dCas9$_{Sth1}$[145] under the control of an anhydrotetracycline (ATc)-inducible promoter; 2) a sgRNA under the control of a constitutive or ATc-inducible promoter; 3) a Tet repressor; 4) a single-copy L5-integrative backbone that contains the integrase gene and an *attP* site; 5) an *E. coli* derived pBR3222 origin of replication**;** 6) a kanamycin resistance cassette[132]. Remarkably, 24 permissive PAM position variants for dCas9$_{Sth1}$ were identified, increasing the number of possible target sites and allowing different efficiencies of gene silencing[132]. Each one out of the 24 PAMs showed a different fold-repression ("PAM strength") and PAM1-15 were able to cause a >25-fold repression (**Figure 6.1B** in **Annexes**)[132]. Using this system, two or more mismatches in sgRNA-DNA base-pairing were demonstrated as sufficient for inefficient gene silencing, indicating that off-target effects are extremely rare[132,135]. The targeting of essential genes caused an inhibition of growth and a robust gene knockdown for all genes and PAM variants tested[132] and, unlike previous results[135], no relation was found between fold-repression and the distance of the designed sgRNA from the transcription start site (TSS)[132]. However, in line with previous data[135,142], this system has the primary disadvantage of being polar – when targeting operonic genes, levels of downstream and upstream gene silencing were obtained, in addition to the targeted gene[132].

The CRISPRi- dCas9$_{Sth1}$ system represents a very efficient, specific, and programmable method for gene regulation and investigation, that can be applicable to different organisms, including slow and fast-growing mycobacteria, enhancing the discovery of new drug targets[131,132,135,142,144]. The simple requirement of cloning a ~20 bp targeting region into the sgRNA scaffold within the CRISPRi plasmid backbone makes this system very simple and inexpensive, allows the target of a high number of regions and the control of the expression of multiple genes simultaneously[135]. Furthermore, it has been demonstrated as suitable to essential genes manipulation, since is inducible and can be tuneable by different factors, such as the concentration of the CRISPRi inducer (ATc), the degree of sgRNA-DNA target complementarity and the use of targeted PAM sequences with distinct strengths[132,135,143].

1.7 Objectives

Regarding the current emergence of MDR and XDR strains of *M. tuberculosis*, there is an urgent need of research for more effective anti-TB drugs and strategies, in which the complex mycobacterial CW comprises a promising target. The PG biosynthesis process includes multiple key enzymes for bacterial survival and for the success in host immune evasion. Recently, the typical amidation of the mycobacterial PG D-*i*Glu and *m*DAP residues was found to be catalysed by the essential MurT/GatD enzymatic complex and by the AsnB enzyme, respectively[33,37,65]. Both PG modifications have been

shown to influence the bacterial antibiotic resistance, especially to β-lactams, and the host immune recognition. Therefore, the main goal of this project is to understand their significance in both contexts, using CRISPRi. For this purpose, the detailed aims are:

A. Construction of *murT*, *gatD*, and *asnB* knockdown mutants in *M. smegmatis* mc^{2}155 and *M. tuberculosis* H37Ra using CRISPRi, followed by phenotypic characterization of the knockdown mutants, through growth curves and spotting dilutions assays, and confirmation of gene repression by quantitative real-time polymerase chain reaction (qRT-PCR).

B. Characterization of the role of the PG D-*i*Glu amidation in: 1) antibiotic resistance, by determination of the minimum inhibitory and minimum bactericidal concentrations (MICs and MBCs, respectively) to three β-lactams (AMX, CEF, and MER), with and without the presence of a β-lactamase inhibitor (clavulanate) and to two first-line anti-TB drugs (INH and EMB); and 2) in host immune recognition, by performing RAW 264.7 murine macrophages infections with *gatD* knockdown mutants and by analysis of the bacterial intracellular survival by counting colony forming units (CFUs).

2. Materials and Methods

2.1 Bacterial strains, plasmids, antibiotics, and growth conditions

The bacterial strains used were *E. coli* JM109, *M. smegmatis* mc^{2}155, and *M. tuberculosis* H37Ra. *E. coli* JM109 was cultured in Luria-Bertani (LB) medium (Merck) supplemented with 25 µg/mL kanamycin (Sigma-Aldrich) when appropriate. Mycobacteria were handled in BSL2 conditions and were cultured in liquid Difco™ Middlebrook 7H9 (BD) broth supplemented with 0.05% (v/v) tyloxapol (Sigma-Aldrich) and 0.5% (v/v) D-(+)-glucose (Sigma-Aldrich) for *M. smegmatis* or 10% (v/v) oleic acid albumin dextrose catalase (OADC) for *M. tuberculosis*. Mycobacteria were cultured in solid Difco™ Middlebrook 7H10 medium supplemented with 10% OADC for *M. tuberculosis*. Both media were supplemented with 25 µg/mL kanamycin when appropriate. All bacterial cultures were grown at 37°C, with shaking at 160 rotations *per* minute (rpm) in liquid conditions.

For mycobacterial gene silencing, the CRISPRi backbone single-plasmids used were PLJR962 (Addgene #115162) for *M. smegmatis* and PLJR965 (Addgene #115163) for *M. tuberculosis* H37Ra[132] (**Figure 6.1**A in **Annexes**). To induce CRISPRi, the medium was supplemented with 100 ng/mL ATc (Sigma-Aldrich).

In all experiments, mycobacterial cultures were grown from mid- to late-log phase in 5 mL of 7H9 medium supplemented with 0.5% glucose, 0.05% tyloxapol, and 25 µg/mL kanamycin, if appropriate. The cultures were then washed by centrifugation at 3000×g for 5 minutes, the pellet was resuspended in an equal volume of 7H9 medium, ultra-sound bath (Bardelin sonorex RK-52) for 5 minutes to remove bacterial clumps, and centrifugation at 500×g for 1 minute to eliminate the larger cell aggregates.

Antibiotic stocks were prepared to the following final concentrations: 25 mg/mL kanamycin, 100 µg/mL ATc, 1.28 mg/mL AMX, CEF, MER, and EMB (Sigma-Aldrich), 1 mg/mL INH (Sigma-Aldrich), 10 mg/mL clavulanate (Sigma-Aldrich), and 50 mg/mL gentamycin (Sigma-Aldrich).

2.2 sgRNA design, plasmid cloning, and transformation

In this work, the i*n silico* design of the sgRNAs was adapted from Rock *et al.*[132,146]. Using SnapGene™ software (version 1.1.3), the 15 "strongest" PAM sequences (PAM1-15) (**Figure 6.1B** in **Annexes**) were searched in the T strand of each target gene sequence and in the T or NT strand of each promoter sequence[132,135,146].

To define the sgRNA targeting sequence, the ~20 nucleotides upstream the PAM sequence were selected. These sequences were extended until the last nucleotide is an "A" or a "G", since it leads to a

more efficient transcription initiation in mycobacteria[132]. The sequence in the T strand ("forward" (Fw) primer) corresponds to the transcribed sequence of the sgRNA and the sequence in the NT strand ("reverse" (Rv) primer) is the reverse complement. Since the backbone plasmids would be digested with the BsmBI enzyme (NEB), the 5'-GGGA-3' and 5'-AAAC-3' BsmBI restriction sequences were added in the Fw and Rv primers, respectively, to restore the sgRNA promoter and the dCas9 handle[132].

The CRISPRi backbones were amplified in *E. coli* chemically competent cells (CC) by double heat-shock transformation. Afterwards, both plasmids were digested at the BsmBI site and purified using the QIAquick PCR Purification Kit (Qiagen). The DNA was quantified using NanoDrop® ND-1000 Spectrophotometer and stored at -20ºC. All pairs of sgRNAs oligos were synthesized (Eurofins Genomics), annealed, and then ligated into the digested CRISPRi backbones (PLJR962 or PLJR965, see **Figure 6.1A** in **Annexes**). Each ligated plasmid was transformed into *E. coli* CC by double heat-shock transformation and the plasmid DNA from the recombinant clones was extracted using the Miniprep kit (NZYTech) and quantified by NanoDrop. The sequence of the recombinant plasmids was confirmed by Sanger sequencing (Eurofins Genomics). Lastly, mycobacterial electrocompetent cells (ECC) were transformed with the corresponding recombinant CRISPRi plasmids by eletroporation[147]. Both mycobacterial species were also transformed with a non-targeting non-digested CRISPRi plasmid as control (ctrl PLJR962 or PLJR965). One colony from each transformation was grown in 7H9 supplemented with 25 µg/mL kanamycin and -80ºC stocks were made.

2.3 Spotting dilutions and growth curves

To perform spotting dilutions, mycobacterial cultures were grown and washed as described before. The $OD_{600\ nm}$ of each supernatant was measured and diluted to a theoretical $OD_{600\ nm}$ of 0.001 in a final volume of 1 mL. A volume of 200 µL of each resulting bacterial suspension was added to a well of a 96-well plate (Sarstedt) and five serial two-fold dilutions were made. Spotting dilutions were performed by plating 5 µL of each dilution in 7H10 agar square plates with and without ATc. The plates were incubated at 37ºC for 48 h. Three independent spotting dilutions experiments were done.

To perform growth curves, mycobacterial cultures were grown and washed as described before. The $OD_{600\ nm}$ of each supernatant was measured and diluted to a theoretical $OD_{600\ nm}$ of 0.001 in a final volume of 40 mL. Each culture was divided into equal volumes and incubated for 45 h with and without ATc, respectively, at 37ºC with shaking at 160 rpm. Several $OD_{600\ nm}$ measurements were made, namely at 18, 21, 24, 42, and 45 h after incubation and an additional supplementation of ATc was made in the corresponding cultures after 24 h of incubation. Three independent growth curves experiments were performed and both mean and standard error of the mean (SEM) were calculated.

2.4 Evaluation of mRNA expression levels by qRT-PCR

To collect cultures for total RNA extraction, mycobacteria were grown and washed as described above. The $OD_{600\ nm}$ of each supernatant was measured and diluted to a theoretical $OD_{600\ nm}$ of 0.001 in a final volume of 160 mL. Each culture was divided into equal volumes and incubated 18 h at 37ºC with shaking at 160 rpm. After 18 h of incubation (t = 0 h), 100 ng/mL ATc was added to one culture of each bacteria and all cultures were allowed to grow 6 h. A corresponding volume of $1x10^9$ cells were collected from each culture at 0, 3, and 6 h after incubation. Three samples were harvested in each time point.

Mycobacterial cells were lysed using zirconium beads in a bead-beater (BeadBug 6; Benchmark) and the total RNA was extracted using the NZY Total RNA Isolation kit (NZYTech), RNAprotect Bacteria Reagent (Quiagen) and β-mercaptoethanol (Merck). The extracted RNA was treated with TURBO™ DNase (2 U/mL) (Invitrogen) and quantified by NanoDrop. The absence of DNA was

confirmed by PCR, using the NZYTaq II 2x Green Master Mix kit (NZYTech), followed by 1.5% electrophoresis agarose gel.

To synthesize cDNA, the NZY First-Strand cDNA Synthesis kit (NZYTech) was used, using 200 ng of purified RNA as template. The mRNA expression levels were assessed by qRT-PCR using the SYBR Green PCR Master Mix (NZYTech) and the primers of **Table 6.1** in **Annexes**. All primers used were verified to have a 90-110% efficiency. The data were quantified using the $\Delta\Delta C_T$ method and normalized to the housekeeping gene *dnaK*. Three independent experiments were done with three biological triplicates and the mean and SEM were calculated. For statistical analysis, the Student t-test was used.

2.5 Minimum inhibitory and bactericidal concentration assays

To investigate the role of PG D-*i*Glu amidation in antibiotic resistance, MIC assays were performed using three β-lactams (AMX, CEF, and MER), tested alone or in the presence of clavulanate, and two first-line anti-TB drugs (EMB and INH). MIC assays were performed as described elsewhere[148,149]. Firstly, two solutions of each β-lactam were prepared to a concentration of 512 µg/mL and 5 µg/mL clavulanate was added to one of them. EMB and INH were prepared to a concentration of 128 µg/mL. A volume of 200 µL of each antibiotic was added to the first well of a 96-well plate column and 100 µL of 7H9 medium supplemented with 0.5% glucose, 0.05% tyloxapol, and 5 µg/mL clavulanate, when appropriate, was added to each remaining well of the plate. Nine two-fold serial dilutions of each antibiotic were made, and the last two plate rows were used as positive (without antibiotics) and negative controls (without bacteria).

Mycobacterial cultures were grown and washed as described before. The $OD_{600\ nm}$ of each supernatant was measured and diluted to an $OD_{600\ nm}$ of 0.002 in a final volume of 30 mL. Each culture was divided into equal volumes and 100 ng/mL ATc was added to one of them. Afterwards, 100 µL of each bacterial suspension was added *per* well in the corresponding 96-well plate, except in the last row (negative control). All plates were incubated at 37ºC for 48 h.

MBC assays was performed as described previously with additional alterations[149,150]. For each bacteria and antibiotic, a 50 µL sample of the MIC, 2-fold MIC and 4-fold MIC was transferred to a new 96-well plate and then, 5 µL of each well was platted into 7H10 square agar plates, with and without 100 ng/mL ATc. The plates were incubated at 37ºC for 48 h.

MICs and MBCs were determined as the lowest concentration of antibiotic for which there is no visible mycobacterial growth. Antibiotics were considered bactericidal when MBCs were up to 4-fold higher than MICs. When MBCs were more than 4-fold higher than MICs, antibiotics were considered bacteriostatic. Both types of assays were performed three times for each control and mutant and medians and MBC/MIC ratios were calculated.

2.6 Infections of RAW 264.7 cells with *M. smegmatis* mc^{2}155 and determination of the number of CFUs of viable intracellular mycobacteria

RAW 264.7 cells were cultured in DMEM/High Glucose (HyClone) medium, supplemented with 10% fetal bovine serum (Gibco), 1% sodium pyruvate (Gibco), 1% HEPES (Gibco), and 1% glutamine (Gibco). RAW 264.7 cells have origin in a Abelson leukemia virus transformed cell line derived from BALB/c mice and are monocytes/macrophages-like cells with phagocytosis capacity, being widely used as a human macrophage model[151]. These cells were seeded onto 48-well tissue culture plates (Sarstedt) at a density of 3×10^4 cells per well and incubated for 48 h at 37ºC with 5% CO_2.

Mycobacterial cultures were grown until exponential phase in 7H9 medium with 25 µg/mL kanamycin, if appropriate and then, each culture was diluted 1:100 twice, separately, with and without 100 ng/mL ATc, respectively, and allowed to grow overnight. All cultures were centrifuged at 3000×g

for 5 minutes, washed in phosphate-buffered saline (PBS) (HyClone) and subjected to 5 minutes of ultrasonic bath, in order to dismantle bacterial clumps. Then, a centrifugation of 500×g for 1 minute was performed and mycobacteria were resuspended in cell culture medium without antibiotics. Bacterial cultures were normalized to a final $OD_{600\ nm}$ of 0.05, corresponding to 0.5×10^7 bacteria/mL.

The infection protocol was performed as previously described[152]. Cells were infected with a multiplicity of infection (MOI) of 5 for 1, 4, and 24 h at 37°C with 5% CO_2. After 1 h of bacterial internalization by macrophages, at 37ºC and 5% CO_2, cells were washed with PBS and medium with or without ATc, supplemented with 5 µg/mL gentamycin (Sigma-Aldrich) (to kill extracellular bacteria), was added. Two independent experiments with biological triplicates were performed.

For CFUs counting, at 1, 4, and 24 h post-infection, cells were washed with PBS and were disrupted with 0.05% IGEPAL (Sigma-Aldrich), a non-ionic and non-denaturing detergent that is able to disrupt eukaryotic cells without compromising mycobacterial viability. Three serial dilutions were made from the lysate in a 96-well plate and 5 µL of each dilution was platted in 7H10 agar medium. After 48 h of incubation at 37ºC with 5% CO_2, CFUs were counted. The mean and SEM were calculated and for statistical analysis, the Student t-test was used.

3. Results and Discussion

3.1 Construction and characterization of *murT, gatD,* and *asnB* knockdown mutants in mycobacteria

3.1.1 Construction of *murT, gatD,* and *asnB* knockdown mutants in *M. smegmatis* mc^{2}155 and *M. tuberculosis* H37Ra using CRISPRi

Given the demonstrated success of the CRISPRi-dCas9$_{Sth1}$ system in mycobacterial gene repression, including in essential genes[132], the first aim of this project was the construction of *murT*, *gatD*, and *asnB* knockdown mutants in *M. smegmatis* mc^{2}155 and *M. tuberculosis* H37Ra, using the referred system in order to further study the role of PG amidation in antibiotic resistance and host immune evasion.

The genes of interest were identified in *M. smegmatis* mc^{2}155 (*MSMEG_6276*, *MSMEG_6277*, and *MSMEG_4269*) and in *M. tuberculosis* H37Ra (*MRA_3749*, *MRA_3750*, and *MRA_2217*). *MurT*, *gatD,* and *asnB* genes encode for the enzymes responsible for the mycobacterial PG amidation and have similar size sequences in both species, around 1200, 700, and 2000 bp, respectively.

The first step of the construction of knockdown mutants was the design of diverse sgRNAs targeting different PAMs and different sites of *murT*, *gatD*, and *asnB* genes (**Table 6.2**, **Table 6.3**, and **Table 6.4** in **Annexes**), following the procedures adopted by Rock *et al.*[132]. In total, for *M. smegmatis* mc^{2}155, nine, seven (**Figure 3.1**), and seventeen sgRNAs, and, for *M. tuberculosis* H37Ra, seven, eight, and twenty-four sgRNAs were designed for *murT*, *gatD*, and *asnB*, respectively. From the seventeen *M. smegmatis asnB* sgRNAs, seven were selected for synthesis, following a criterion of selecting different PAMs and, when possible, the same PAM for different gene sites, in order to access the effect of both factors in gene knockdown. Additionally, only one *M. tuberculosis* H37Ra *asnB* sgRNA was synthesized, targeting the promoter region. All sgRNAs base pairing regions were confirmed as non-complementary to any other sequence in the corresponding genome and all *M. tuberculosis* H37Ra sgRNAs were confirmed as identical for *M. tuberculosis* H37Rv, allowing a future application of these experiments in *M. tuberculosis* H37Rv or in MDR and XDR strains, in BSL3 conditions.

The sgRNAs were cloned into PLJR962 or PLJR965 CRISPRi backbones (**Figure 6.1A** in **Annexes**) and *E. coli* CC were transformed with the cloned plasmids. The plasmid DNA was extracted, quantified (**Supplementary Table 1**) and its sequence was confirmed by sequencing (**Supplementary Table 2**).

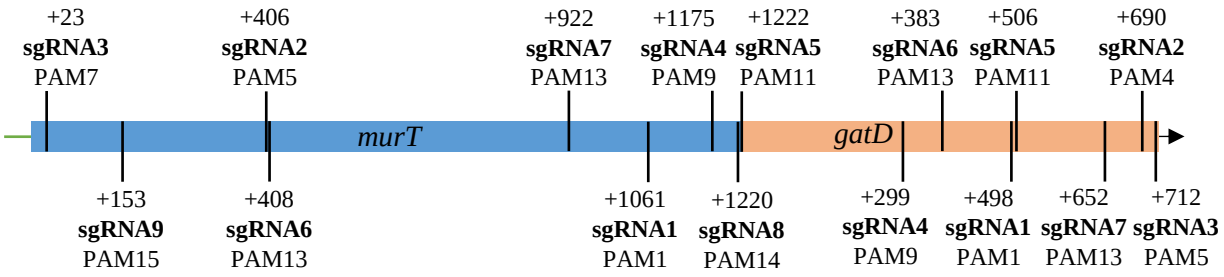

Figure 3.1 – Target sites of CRISPRi in *murT* and *gatD* in *M. smegmatis* mc²155. Both genes are transcribed in the same direction and constitute an operon with a common promoter upstream *murT* with 73 bp. The two genes are overlapped by 4 bp. The CRISPRi target sites are shown in vertical black lines. Under or above the lines of the CRISPRi target sites are indicated the number of the first nucleotide of the target sequence, the corresponding sgRNA (decreasingly ordered by PAM strength) and the number of the corresponding PAM.

Lastly, *M. smegmatis* mc²155 and *M. tuberculosis* H37Ra ECC were transformed with the corresponding plasmids by electroporation to obtain mycobacteria harbouring the CRISPRi system. The mycobacterial species were also transformed with a non-targeting non-digested PLJR962 or PLJR965 plasmid (ctrl PLJR962 or ctrl PLJR965), to serve as control. To induce the CRISPRi system, mycobacteria were grown in the presence of 100 ng/mL ATc.

As mentioned above, the initial aim of this work was to investigate the role of PG amidation in both mycobacterial species. However, due to the long replication time of *M. tuberculosis* H37Ra (~24 h) and due to the short duration of this project, the following experiments were only performed in *M. smegmatis* mc²155. Since *M. tuberculosis* H37Ra mutants were already constructed, in the future, these experiments will be easily performed in this specie.

3.1.2 Phenotypic characterization of *murT*, *gatD*, and *asnB* knockdown mutants in *M. smegmatis* mc²155

In order to investigate the effects of CRISPRi-mediated *murT*, *gatD*, and *asnB* silencing on mycobacterial growth and viability, spotting dilutions were performed. The first gene to be investigated was *murT* and the results of spotting dilutions of *M. smegmatis* WT, ctrl PLJR962, and *murT*⁻ mutants (PLJR962:sgRNA1 to 9), in the presence and absence of 100 ng/mL ATc, are shown in **Figure 3.2**. In the absence of ATc, it was observed a normal and similar growth of all controls and *murT*⁻ mutants. The growth of controls was identical in both conditions, confirming a non-toxic effect of 100 ng/mL ATc. In the presence ATc, all *murT*⁻ mutants exhibited growth defects, which is in agreement with the predicted essentiality of *murT* in mycobacteria[31,33,37].

The CRISPRi system used in this work is ATc-inducible and the resulting gene repression is described as determined by diverse factors, namely the sgRNA-DNA target complementarity and the PAM strength[132]. For essential genes, a stronger PAM is predicted to cause higher gene fold-repression and thus, higher inhibition of growth[132]. The CRISPRi-mediated *murT* repression led to an inhibition of growth with all sgRNAs, but by comparing the magnitude of growth inhibition with the PAM strength, PLJR962:sgRNA8 showed a surprising phenotype. This mutant, grown in the presence of ATc, showed less growth defects than another mutant associated with a weaker PAM (PLJR962:sgRNA9).

The target site of sgRNA8 is in the final region of *murT* (around 1220 bp) and is associated with the 14th PAM, out of the 15 PAMs used and decreasingly ordered by strength (see **Figure 3.1** and **Figure 6.1B** in **Annexes**). According to Rock *et al.*[132], there is no influence of the sgRNA targeting site distance from the TSS on the gene fold-repression, opposing earlier results that revealed evidences of this relation[135]. However, a justification for these results could be that the CRISPRi-mediated gene silencing is not only determined by PAM strength, but also by the gene region that is targeted, when weaker PAMs

are used. The sgRNA targeting site of PLJR962:sgRNA9 is in the beginning of *murT* (around 153 bp) and that could contribute to a more efficient gene silencing and therefore, to stronger growth defects.

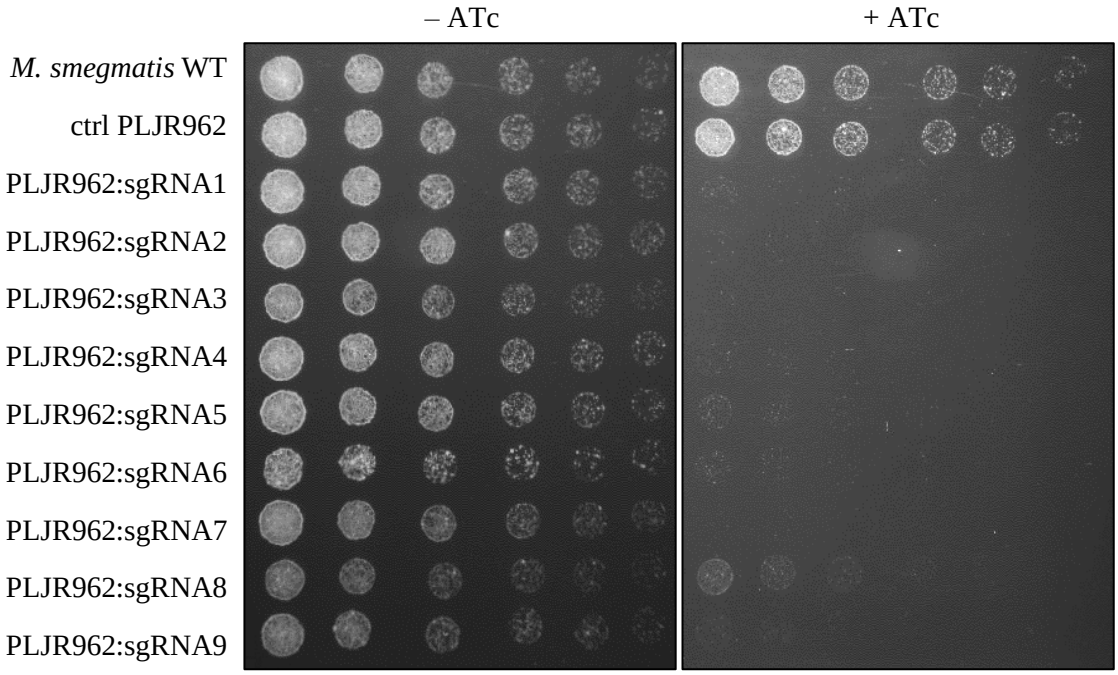

Figure 3.2 – **Spotting dilutions of *M. smegmatis* mc²155 WT, ctrl PLJR962, and *murT*⁻ mutants (PLJR962:sgRNA1 to 9) in the presence (+) and absence (–) of 100 ng/mL ATc**. The sgRNAs are decreasingly ordered by PAM strength. *M. smegmatis* WT and ctrl PLJR962 were used as controls. The ctrl PLJR962 mutant is a non-targeting control harbouring an empty vector. The first spot corresponds approximately to 0.001 $OD_{600\,nm}$ and each subsequent spot is a two-fold dilution. Each spot corresponds of plating 5µL of culture volume. These data are representative of three independent experiments.

MurT has two main domains, a Mur ligase homologous central domain and a C-terminal domain (known as DUF1727)[33,37,63]. The MurT central domain comprises five conserved regions involved in ATP and Mg^{2+} binding[37]. The sgRNA2, 3, 6, and 9 target sequence regions that encode for the MurT central domain. Amino acid sequence alignment of MurT from *S. aureus* and *M. smegmatis* (**Supplementary Figure 1**) show that these sequence regions include sites near the motifs of ATP and Mg^{2+} binding. The reaction catalysed by MurT is ATP- and Mg^{2+}- dependent[37] and the inhibition of transcription elongation by the CRISPRi system can result in incomplete transcripts and non-functional proteins, deficient in these vital regions, contributing to the lethal phenotype displayed by these mutants.

The DUF1727 domain highly contributes to the physical interaction of the MurT/GatD enzymatic complex and has four conserved amino acid regions (I, II, III and IV), found in several species, including in *M. tuberculosis*[63]. In *S. aureus*, L313 and Y418 residues and the DNAAD motif are involved in recognition and channel of the ammonia group produced by GatD, and D355 is involved in glutaminase activity regulation, due to an interaction with Y17 of GatD[63]. The sgRNA1, 4, 5, 7, and 8 target sequence sites that encode for the DUF1727 domain, and more specifically, sites that include these four conserved regions. The growth defects of the corresponding mutants could be explained by the final formation of a non-functional protein that lacks these regions and that is not able to interact with GatD, not catalysing the PG amidation reaction. Regarding PLJR962:sgRNA8, its sgRNA targets the final gene nucleotides and may still allow the RNA polymerase to transcribe almost the entire sequence before being prevented to continue by a dCas9 blockage, likely still allowing the coding of a semi-functional protein.

Afterwards, the phenotypic effects of CRISPRi-mediated *gatD* repression were also evaluated. The results of the spotting dilutions of *M. smegmatis* WT, ctrl PLJR962, and *gatD*⁻ mutants (PLJR962:sgRNA1 to 7) are shown in **Figure 3.3**. In the absence of ATc, it was observed a normal and similar growth of all mycobacterial controls and mutants. The growth of controls was identical in both

conditions, confirming a non-toxic effect of 100 ng/mL ATc. In the presence of ATc, almost all *gatD*$^{-}$ mutants showed growth defects, confirming the predicted essentiality of *gatD* in mycobacteria[31,33,37]. Together with the results of **Figure 3.2**, this is in accordance with previous data that showed that neither MurT, nor GatD alone were sufficient to catalyse the essential reaction of PG D-*i*Glu amidation[33].

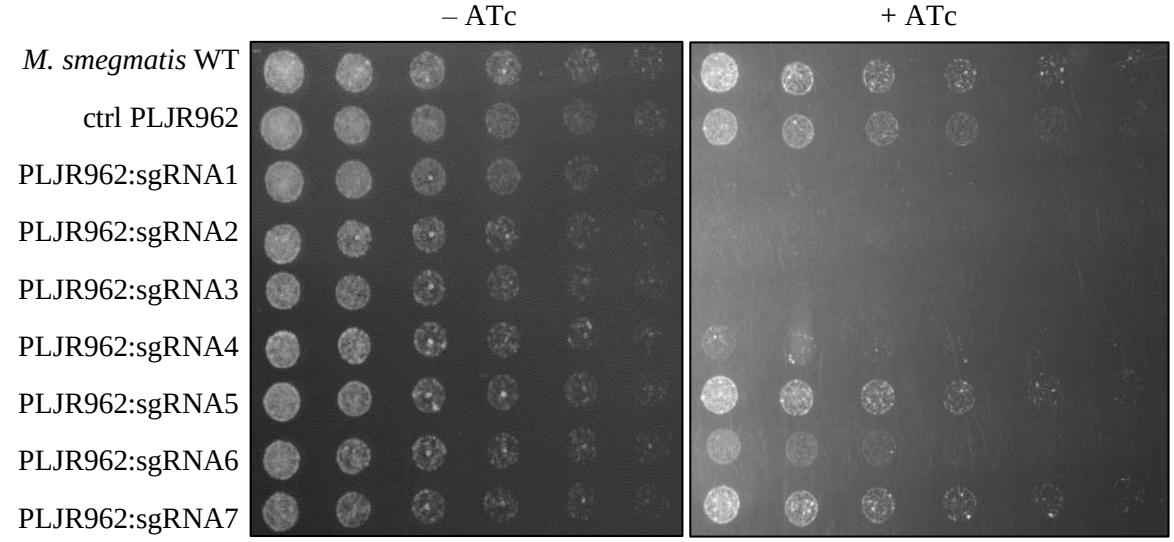

Figure 3.3 – **Spotting dilutions of *M. smegmatis* mc^{2}155 WT, ctrl PLJR962, and *gatD*$^{-}$ mutants (PLJR962:sgRNA1 to 7) in the presence (+) and absence (–) of 100 ng/mL ATc**. The sgRNAs are decreasingly ordered by PAM strength. *M. smegmatis* WT and ctrl PLJR962 were used as controls. The ctrl PLJR962 mutant is a non-targeting control harbouring an empty vector. The first spot corresponds approximately to 0.001 $OD_{600\,nm}$ and each subsequent spot is a two-fold dilution. Each spot corresponds of plating 5µL of culture volume. These data are representative of three independent experiments.

In **Figure 3.3**, by comparing all mutants in the presence of ATc, the magnitude of growth inhibition seemed to be in agreement with the associated PAM strength, except for PLJR962:sgRNA6. This mutant is associated with PAM13 (see **Figure 6.1B** in **Annexes**) and was expected to show less or, at least, identical growth defects than PLJR962:sgRNA5, which is associated with PAM11. Moreover, both PLJR962:sgRNA6 and 7 are associated with PAM13, and so, it was expected that these growth phenotypes were similar. Contrarily, PLJR962:sgRNA6 exhibited more growth defects than both PLJR962:sgRNA5 and 7. As stated above, one explanation could be the fact that sgRNA6 targets a site more at the beginning of *gatD* (around 380 bp) than sgRNA5 (around 506 bp) and 7 (around 650 bp), resulting in a more robust gene silencing and growth inhibition.

Both *murT* and *gatD* silencing results indicated that CRISPRi can mediate robust gene knockdown irrespective of the distance from the TSS, as previously reported by Rock *et al.*[132]. For instance, *gatD* PLJR962:sgRNA2 and 3, that are associated with strong PAMs, target the very final nucleotides of *gatD* and still resulted in severe growth defects. However, this correlation seemed to not be verified when concerning weaker PAMs. In that case, the target site appears to influence the level of gene repression.

Interestingly, with sgRNAs associated with weaker PAMs, the *gatD* silencing (**Figure 3.3**) showed less impaired growth than the *murT* silencing (**Figure 3.2**). For instance, *murT* PLJR962:sgRNA8, associated with a weaker PAM (PAM14) than *gatD* PLJR962:sgRNA7 (PAM13), showed a more lethal phenotype, although the target is in the end of the gene. This is in agreement with complementation experiments of a *murT*/*gatD* conditional mutant, in which, compared to the WT strain, the growth rate was lower when the conditional mutant was complemented with *gatD* than when complemented with *murT*, especially on solid medium[37].

GatD shares sequence similarities with the glutaminase amide transfer domain of class I-type GATases and has conserved residues of Cys and His, essential for the glutaminase activity, similarly to the catalytic triad found in the active site of GATases[33,37]. By amino acid sequence alignment of GatD from *S. aureus* and *M. smegmatis* (**Supplementary Figure 2**), the target sites of sgRNA1, 4, 5 and 6

were found near the sequence that encodes for these conserved residues. Since the absence of the referred residues can have implications on the enzymatic complex assemble and activity[56], the CRISPRi-mediated interference in this gene region, especially with stronger PAMs (like in PLJR962:sgRNA1 and 4), and the consequent formation of incomplete transcripts, could result in a deficient activity of the overall enzymatic complex and could explain the growth inhibition phenotypes observed in **Figure 3.3**.

As with *murT* and *gatD* silencing, the consequences of CRISPRi-mediated *asnB* silencing on mycobacterial viability were also investigated. The results of the spotting dilutions of *M. smegmatis* WT, ctrl PLJR962, and *asnB*$^-$ mutants (PLJR962:sgRNA1 to 7) are shown in **Figure 3.4**. In the absence of ATc, it was observed a normal and similar growth of all mycobacterial controls and mutants. The growth of controls was identical in both conditions, confirming a non-toxic effect of 100 ng/mL ATc.

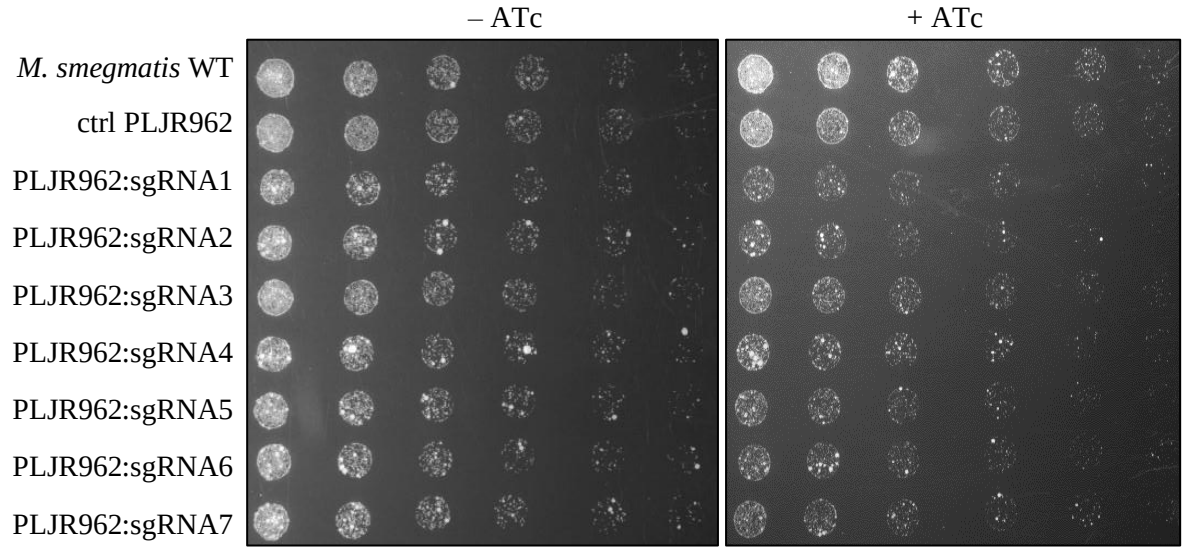

Figure 3.4 – **Spotting dilutions of *M. smegmatis* mc^{2}155 WT, ctrl PLJR962, and *asnB*$^-$ mutants (PLJR962:sgRNA1 to 7) in the presence (+) and absence (–) of 100 ng/mL ATc**. The sgRNAs are decreasingly ordered by PAM strength. *M. smegmatis* WT and ctrl PLJR962 were used as controls. The ctrl PLJR962 mutant is a non-targeting control harbouring an empty vector. The first spot corresponds approximately to 0.001 $OD_{600\ nm}$ and each subsequent spot is a two-fold dilution. Each spot corresponds of plating 5µL of culture volume. These data are representative of three independent experiments.

Figure 3.4 shows that in the presence of ATc, all *asnB*$^-$ mutants presented an identical growth phenotype among each other and only a minor growth inhibition, comparing to controls, suggesting that *asnB* is not essential in *M. smegmatis*. This supports a previous report, in which a *M. smegmatis asnB* mutant only showed a growth delay, compared to the WT strain[68]. As in *C. glutamicum*, $asnB_{Msmeg}$ seemed to not be essential in *M. smegmatis*, but since it has been shown that it has a role in natural resistance to antibiotics and in L,D-transpeptidation efficiency, it can still be required for an optimal CW integrity and growth, explaining the slight impaired growth showed in **Figure 3.4**.

The $asnB_{Msmeg}$ is the *M. tuberculosis* $asnB_{Mtb}$ orthologue and both share 80% of sequence identity. In contrast to $asnB_{Msmeg}$, the $asnB_{Mtb}$ gene was shown to be essential for bacterial growth and survival[52]. Interestingly, in *M. smegmatis* there are two *asnB* identified genes ($asnB_{Msmeg}$ (*MSMEG_4269*) and $asnB2_{Msmeg}$ (*MSMEG_2594*)), both poorly studied and described as asparagine synthases (glutamine-hydrolysing). As well as in *M. smegmatis*, in *C. difficile* there are two *asnB* genes ($asnB_{Cdf}$ and $asnB2_{Cdf}$), that appear to not be required for bacterial growth[74]. The $asnB_{Cdf}$ gene was reported as the responsible for *m*DAP amidation, but, surprisingly, when $asnB2_{Cdf}$ was overexpressed in $asnB_{Cdf}$ mutants, low levels of amidation were detected in PG precursors, and it was suggested that $AsnB2_{Cdf}$ could contribute to the PG amidation to some extent. Hereupon, the presence of two *asnB* genes in *M. smegmatis* could contribute to the non-essentiality of $asnB_{Msmeg}$, and both proteins may catalyse the PG amidation in a way that, when $asnB_{Msmeg}$ is inhibited, the bacteria can survive with the $AsnB2_{Msmeg}$ activity, even if the reaction is catalysed with less efficiency and different subtract specificity[74].

Through *in silico* analysis, using the pfam database (http://pfam.xfam.org), both $AsnB_{Msmeg}$ and $AsnB2_{Msmeg}$ have a GATase7 domain at the N-terminal position and an asparagine synthetase domain at the C-terminal position. By using the BLASTp tool, the proteins showed approximately 33% of identity (**Supplementary Figure 3**) and, according to the mycobrowser data repository (https://mycobrowser.epfl.ch/) $AsnB2_{Msmeg}$ has a transcription orientation opposite to $asnB_{Msmeg}$ and a 3 bp overlap with the upstream gene (*MSMEG_2593* encoding for a Gcn5-related *N*-acetyltransferase-family protein), both being predicted to be part of an operon (**Supplementary Figure 4**).

In order to further address the effects of CRISPRi-mediated gene silencing on mycobacterial growth over time, growth curves of *M. smegmatis* WT, ctrl PLJR962, and *gatD*$^{-}$ mutants (PLJR962:sgRNA1 to 7), grown in the presence and absence of 100 ng/mL of ATc, were performed. The obtained growth curves are shown in **Figure 3.5** and in **Figure 6.2** (**Annexes**). The *gatD*$^{-}$ mutants were selected over the *murT*$^{-}$ mutants, since effects of polarity would be less likely and the results of spotting dilutions of *gatD* silencing had shown a growth inhibition in a magnitude related to PAM strength.

Without ATc, it was observed a similar growth of both controls, but several mutants, especially PLJR962:sgRNA1, 2, and 4, exhibited a decreased growth rate when compared to *M. smegmatis* WT (**Figure 3.5**), contrary to what was obtained in spotting dilutions (**Figure 3.3**). Even using the optimized ATc-regulated promoter provided by Rock and colleges[132], some leaky expression of $dCas9_{Sth1}$ from the ATc-regulated promoter could have occurred and could explain these growth differences in the absence of ATc. Moreover, some differences in $OD_{600\,nm}$ after 42 h can also be explained by a bacterial stationary growth stage and by very high $OD_{600\,nm}$ values that make the measurements not as real as until 24 h.

Based on **Figure 3.5**, the growth of *M. smegmatis* WT was identical in both –ATc and +ATc conditions, indicating a non-toxic effect of 100 ng/mL ATc. However, the ctrl PLJR962 with ATc, showed a decreased growth, comparing to WT and to untreated ctrl PLJR962. It could be associated with a level of toxicity caused by $dCas9_{Sth1}$ overexpression, although this effect had only been reported for $dCas9_{Spy}$ by Rock et. *al.*[132]. The sequence of ctrl sgRNA was confirmed as not complementary to any sequence in *M. smegmatis* and a CRISPRi off-target silencing is reported as requiring a near-perfect sgRNA sequence complementarity, a suitably spaced PAM, and targeting of the promoter or the NT strand[132]. The combination of all factors is rare and thus, an off-target effect is extremely improbable.

All *M. smegmatis gatD*$^{-}$ mutants in the presence of ATc exhibited a reduced growth rate when compared to WT + ATc, supporting the predicted essentiality of *gatD* in *M. smegmatis* and the fact that its inhibition can lead to a decreased growth rate and effects in cellular division[31,37,59]. Comparing to ctrl PLJR962 + ATc, PLJR962:sgRNA1, 2, 3, 4, and 6 + ATc were the mutants with more evident growth differences, as also obtained in spotting dilutions (**Figure 3.3**).

The magnitude of growth inhibition seemed to be related with the associated PAM strength. For instance, PLJR962:sgRNA1, 2, and 3 are associated with the strongest PAMs and showed the most notorious growth inhibition phenotypes. Interestingly, already after 18 h of incubation, the cultures of these mutants showed growth inhibition and visible clumps. Likewise, the remaining mutants, associated with weaker PAMs, exhibited less growth defects.

Either from 0 to 24 h (**Supplementary Figure 5**) or to 45 h (**Figure 3.5**), in the presence of ATc, the growth profile of PLJR962:sgRNA4, 5, 6, and 7 was very similar between each other, in contrast to what was previously obtained in spotting dilutions in **Figure 3.3**. In solid medium, the growth variations between these mutants were more evident, in a magnitude related with the PAM strength and, in some cases, with the target site of the sgRNA. Curiously, in experiments with a *murT*/*gatD* conditional mutant, the defective growth was also more obvious when mutants were grown on solid medium[37].

After 24 h, the growth defects of PLJR962:sgRNA4, 5, 6, and 7 seemed to be less notorious and more similar to the ctrl PJR962 than up to 24 h. Despite a second addition of ATc at 24 h, this could be explained by a decline in $dCas9_{Sth1}$ expression, as reported by Singh *et al.*[144]. This decline may be caused by a generalized decrease in gene expression as bacteria enter the stationary phase of growth.

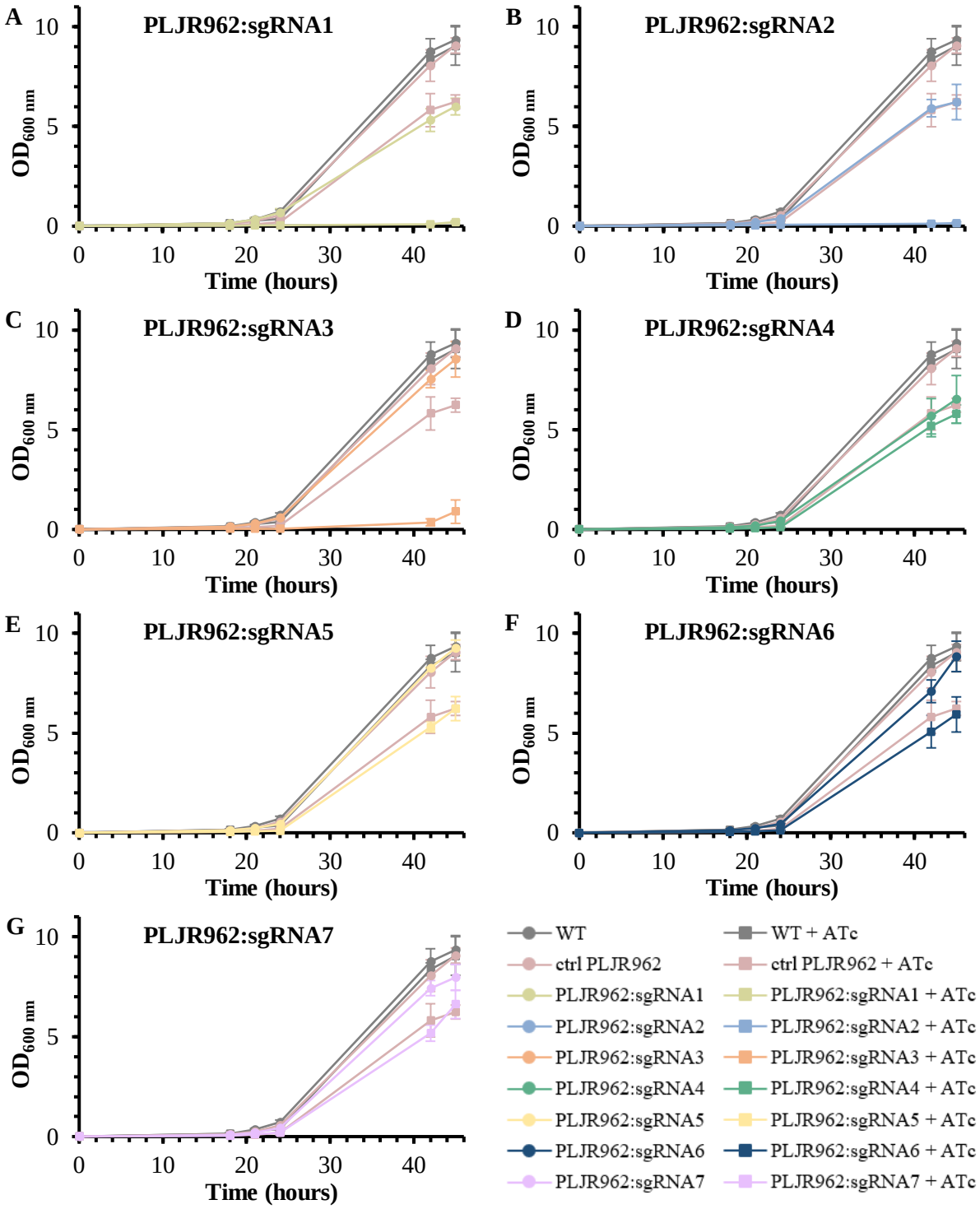

Figure 3.5 – (A-G) Growth curves of *M. smegmatis* mc²155 WT, ctrl PLJR962, and *gatD*⁻ mutants (PLJR962:sgRNA1 to 7) in the presence (■) and absence (●) of ATc. The sgRNAs are decreasingly ordered by PAM strength. *M. smegmatis* mc²155 WT and ctrl PLJR962 were used as controls. The ctrl PLJR962 mutant is a non-targeting control harbouring an empty vector. The cultures were grown from mid- to late-log phase, washed, and diluted to a theoretical $OD_{600\ nm}$ of 0.001 (t = 0 h). The 100 ng/mL ATc addition was made at 0 and 24 h. The growth profile of cultures was followed by $OD_{600\ nm}$ measurement at 0, 18, 21, 24, 42, and 45 h. The data represent the mean ± SEM of three independent experiments.

Both results of spotting dilutions and growth curves support the essentiality of *murT* and *gatD* in *M. smegmatis* and show that the targeted gene knockdown by the CRISPRi system was successfully accomplished.

3.1.3 Assessment of CRISPRi-mediated gene repression by qRT-PCR

In addition to constructing the *gatD*$^{-}$, *murT*$^{-}$, and *asnB*$^{-}$ mutants and performing the phenotypical characterization, it was crucial to confirm the achievement of a gene-specific knockdown level.

The CRISPRi-mediated *gatD* repression was investigated by qRT-PCR in *M. smegmatis* WT, ctrl PLJR962, and in one *gatD*$^{-}$ mutant (**Figure 3.6**), in the presence and absence of ATc. Since polarity effects had been reported using this system[132], in addition to assessing the *gatD* mRNA expression levels, the expression levels of *murT* and both immediately upstream (*MSMEG_6275*) and downstream (*MSMEG_6278*) genes of the *murT*/*gatD* operon were also investigated. The selected *gatD*$^{-}$ mutant was PLJR962:sgRNA2, as it is related with one of the strongest PAMs and it had shown growth defects in prior results (**Figure 3.3** and **Figure 3.5B**), being expected to show a strong level of *gatD* knockdown.

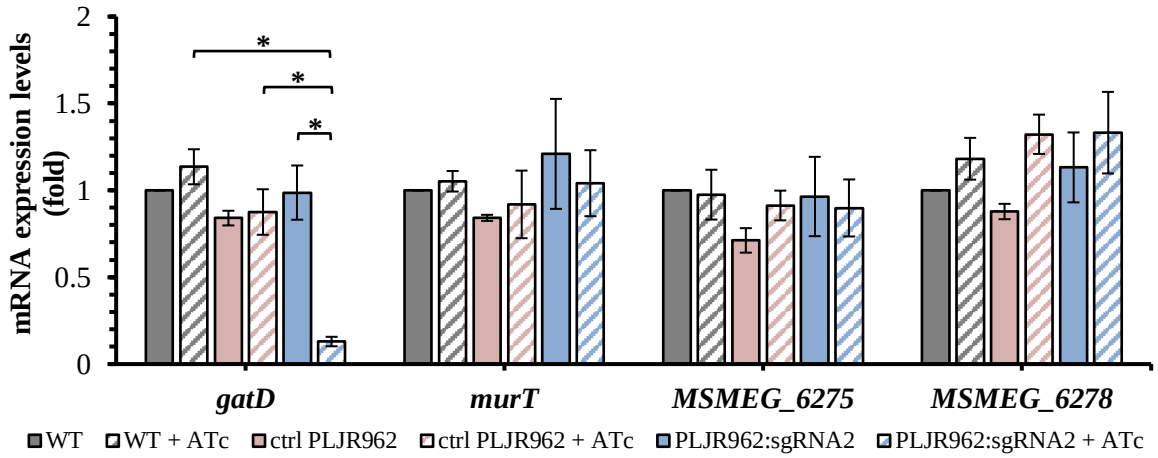

Figure 3.6 – **Relative *gatD, murT, MSMEG_6275,* and *MSMEG_6278* mRNA expression levels in *M. smegmatis* mc^{2}155 WT, ctrl PLJR962, and PLJR962:sgRNA2 *gatD*$^{-}$ mutant with (striped bars) and without (smooth bars) 100 ng/mL ATc treatment for 6 h.** *M. smegmatis* mc^{2}155 WT and ctrl PLJR962 were used as controls. The ctrl PLJR962 mutant is a non-targeting control harbouring an empty vector. The data were quantified using the $\Delta\Delta C_T$ method and normalized to the *M. smegmatis* housekeeping gene *dnaK*, using the *M. smegmatis* WT as calibrator sample. The bars represent the mean of three independent experiments with three biological triplicates each and the error bars correspond to the SEM. Asterisks indicate the significance of the difference in relative mRNA expression calculated using the Student t-test (* $P < 0.005$).

The CRISPRi system reaches maximal gene knockdown between one and two cell divisions after the addition of ATc[132]. As so, bacterial cultures for total RNA extraction were collected 6 h after ATc addition and it should be noted that after the 6 h, the PLJR962:sgRNA2 had still an $OD_{600\ nm}$ similar to the WT strain (data not shown), contrary to what happened in phenotypical characterization (**Supplementary Figure 5B**). This is caused by the fact that in this experiment the $OD_{600\ nm}$ of cultures at the time of ATc addition was approximately 0.1, being much higher when comparing to the 0.001 $OD_{600\ nm}$ at the time of ATc addition in growth characterization experiments. The mRNA expression levels were quantified using the $\Delta\Delta C_T$ method and normalized to the *M. smegmatis* housekeeping gene *dnaK*, which encodes for a member of the HSP70 chaperone family of proteins, with crucial functions in protein folding and response to stress. The *M. smegmatis* WT was used as calibrator sample.

Figure 3.6 shows that no significant differences were obtained in *gatD*, *murT*, *MSMEG_6275* or *MSMEG_6578* mRNA expression levels between WT and ctrl PLJR962, in the absence and presence of ATc. Without ATc, comparing to the WT strain, PLJR962:sgRNA2 did not show any significant difference in the mRNA expression of the genes under investigation, not supporting earlier evidences (**Figure 3.5**) of a leaky expression of the $dCas9_{Sth1}$ from the ATc-regulated promoter. Interestingly, in the presence of ATc, PLJR962:sgRNA2 showed a significant 8.8-, 6.7-, and 7.6-fold decrease in *gatD* mRNA expression, comparing to WT + ATc, ctrl PLJR962 + ATc, and PLJR962:sgRNA2 in the absence of ATc, respectively.

According to Rock *et al.*, either upstream or downstream polarity effects could result from the CRISPRi system[132]. Based on **Figure 3.6**, no significant changes in *murT*, *MSMEG_6275* or *MSMEG_6278* mRNA expression levels were found between *M. smegmatis* WT and PLJR962:sgRNA2 in the presence of ATc, indicating an absence of a polar effect by CRISPRi. The fact that sgRNA2 targeting site is in the end of the *gatD* gene (see **Figure 3.1**), and that *gatD* is the last operon gene, could explain the absence of an upstream polarity. The evidence that *MSMEG_6278* has a transcription orientation opposite to the *murT*/*gatD* operon (**Supplementary Figure 4C**) could explain the absence of a downstream polarity.

Although the obtained 8.8-fold decrease in gene mRNA expression was below the 145.2 fold-repression that was reported for the same associated PAM (PAM4) (see **Figure 6.1B**)[132], these data show the ability of CRISPRi to achieve considerable inhibition of specific gene expression in *M. smegmatis*, and together with the previous phenotype characterization experiments, show that this inhibition is enough to cause a defect in bacterial growth.

3.2 Evaluation of PG amidation role in antibiotic resistance by MIC and MBC determination for antibiotics that target the mycobacterial CW biosynthesis

Since previous experiments have demonstrated a role of PG amidation in antibiotic resistance, especially for β-lactams, the effect of CRISPRi-mediated *gatD* silencing on mycobacterial antibiotic susceptibility was evaluated by determining the MIC and MBC of three different β-lactams of different classes (AMX, CEF, and MER), in the presence and absence of a β-lactamase inhibitor (clavulanate), and two first-line anti-TB drugs (EMB and INH). The MIC and MBC assays were performed for *M. smegmatis* WT, ctrl PLJR962, and *gatD*$^{-}$ mutants, in the presence or absence of 100 ng/mL ATc.

The MICs and MBCs were determined by direct observation and were considered as the lowest concentration of antibiotic for which no bacterial growth was visually detected in liquid and solid medium, respectively. Antibiotics were considered bactericidal when the MBCs were up to 4-fold higher than the MICs. When the MBCs were more than 4-fold higher than the MICs, antibiotics were considered bacteriostatic. The medians (**Table 6.5** in **Annexes**) and MBC/MIC ratios (**Supplementary Table 3**) were calculated. The median was chosen over mean and standard deviation, since the concentrations tested were pre-defined discrete values and the median is not as skewed by outliers as the mean might be. Since β-lactams are not used in TB treatment, EUCAST does not have a determined reference methodology to test breakpoints of mycobacterial susceptibility to this class of antibiotics. As so, non-species related PK-PD breakpoints were used to classify mycobacteria as susceptible or resistant to the β-lactams tested and, together with the previously reported critical concentrations of ethambutol and isoniazid for *M. tuberculosis* in 7H10 medium[153], are represented in **Table 3.1**.

Table 3.1 – EUCAST non-species related PK-PD breakpoints for β-lactams and critical concentrations for ethambutol and isoniazid (µg/mL). S – susceptible; R – resistant.

Breakpoints/Critical concentrations (µg/mL)		
	S ≤	R ≥
Amoxicillin	2	8
Amoxicillin + Clavulanate	2	8
Cefotaxime	1	2
Meropenem	2	8
Ethambutol	5	
Isoniazid	0.2	

The medians of MICs and MBCs are summarized in **Table 6.5** (**Annexes**) and for an easier analysis the medians of MICs were graphically represented in **Figure 3.7**. Bacteriostatic effects or undetermined MBCs are highlighted in grey in **Table 6.5** (**Annexes**) and with a "■" symbol in **Figure 3.7**, all other cases correspond to bactericidal effects. These assays with mycobacteria have an increased variability, due to lack of synchrony in the culture, i.e. the presence of bacteria in different growth stages. Moreover, since the concentration values were annotated by direct visualization of plates, human-associated experimental errors may occur and thus, changes of 2-fold were not considered.

AMX-clavulanate has been shown to have bactericidal activity in *M. tuberculosis in vitro* and in drug-resistant TB patients[98,100,101], being its potential application in TB treatment of great interest. According to Li *et al.*[154], the MIC of AMX in *M. smegmatis* mc^2155 is 64 µg/mL, similarly to what was obtained for *M. smegmatis* controls and *gatD*$^-$ mutants in the absence of ATc (**Figure 3.7A**). Likewise, in the presence of ATc, the MICs of AMX for *M. smegmatis* controls and *gatD*$^-$ mutants only ranged between 32 and 128 µg/mL, indicating that controls were not affected by ATc and that the *gatD* silencing did not influence the mycobacterial AMX susceptibility. This is likely due to the presence of a class A β-lactamase, BlaS, for which AMX is a very good substrate[94,155]. BlaS catalyses the hydrolysis of AMX β-lactam ring, prevents its interaction with PBPs[98] and is found as functioning with penicillins at the diffusion-limited rate[98]. Based on the EUCAST breakpoints, all *M. smegmatis* controls and *gatD*$^-$ mutants are classified as resistant to AMX.

The obtained MICs for AMX-clavulanate (**Figure 3.7B**), in –ATc conditions, for both *M. smegmatis* controls was 8 µg/mL and for *gatD*$^-$ mutants was 4 – 8 µg/mL. Comparing to AMX alone (**Figure 3.7A**), the values decreased up to 32-fold. Similarly, the MIC of AMX-clavulanate in patients with TB was reported to be 4 – 8 µg/mL[100], and the MIC of AMX was found to be reduced by the presence of clavulanate up to 16-fold and at least 32-fold in *M. smegmatis* and *M. tuberculosis*, respectively[94,100]. The same 16 – 32-fold differences were obtained when *blaS* and *blaC* were deleted, compared to the WT strain[94], indicating that the addition of clavulanate had a similar effect as the deletion of the major mycobacterial β-lactamase in other experiments. Actually, clavulanate targets and inhibits the action of the BlaS enzyme that is deleted in the referred mutant. The presence of ATc did not change the MIC of AMX-clavulanate for *M. smegmatis* controls, but the *gatD*$^-$ mutant PLJR962:sgRNA1 + ATc exhibited a 4-fold decrease (**Table 6.5** in **Annexes**). This mutant is associated with the strongest PAM, suggesting a possible role of PG D-*i*Glu amidation in AMX resistance. In fact, according to EUCAST breakpoints, in +ATc conditions, PLJR962:sgRNA1 is classified as susceptible to AMX-clavulanate, PLJR962:sgRNA2, 4, and 6 as having intermediate susceptibility and the remaining as resistant. Accordingly, previous results showed that the inhibition of PG D-*i*Glu amidation caused a reduced resistance to oxacillin and methicillin, also members of the penicillin class of β-lactams[33,37].

Besides inhibiting PBPs, CEF has been shown to cause inhibition of some mycobacterial LDTs which are responsible for almost 80% of the mycobacterial cross-linking[104]. In *M. smegmatis*, the MIC of CEF is reported as 64 – 128 µg/mL[156–158]. In this work, without ATc, the MIC of CEF for *M. smegmatis* controls and *gatD*$^-$ mutants was ≥256 µg/mL (**Figure 3.7C**). The presence of ATc did not change the MIC of CEF for WT, in contrast to ctrl PLJR962, that exhibited a non-significant >2-fold decrease. In the presence of ATc, all *gatD*$^-$ mutants with the exception of PLJR962:sgRNA5 had decreased MICs of CEF, compared to *M. smegmatis* controls. PLJR962:sgRNA1, 2, 3, and 6 showed >8 – >16-fold differences and PLJR962:sgRNA4 and 7 showed a >4-fold change, indicating that the lack of D-*i*Glu amidation has an effect on the CEF resistance.

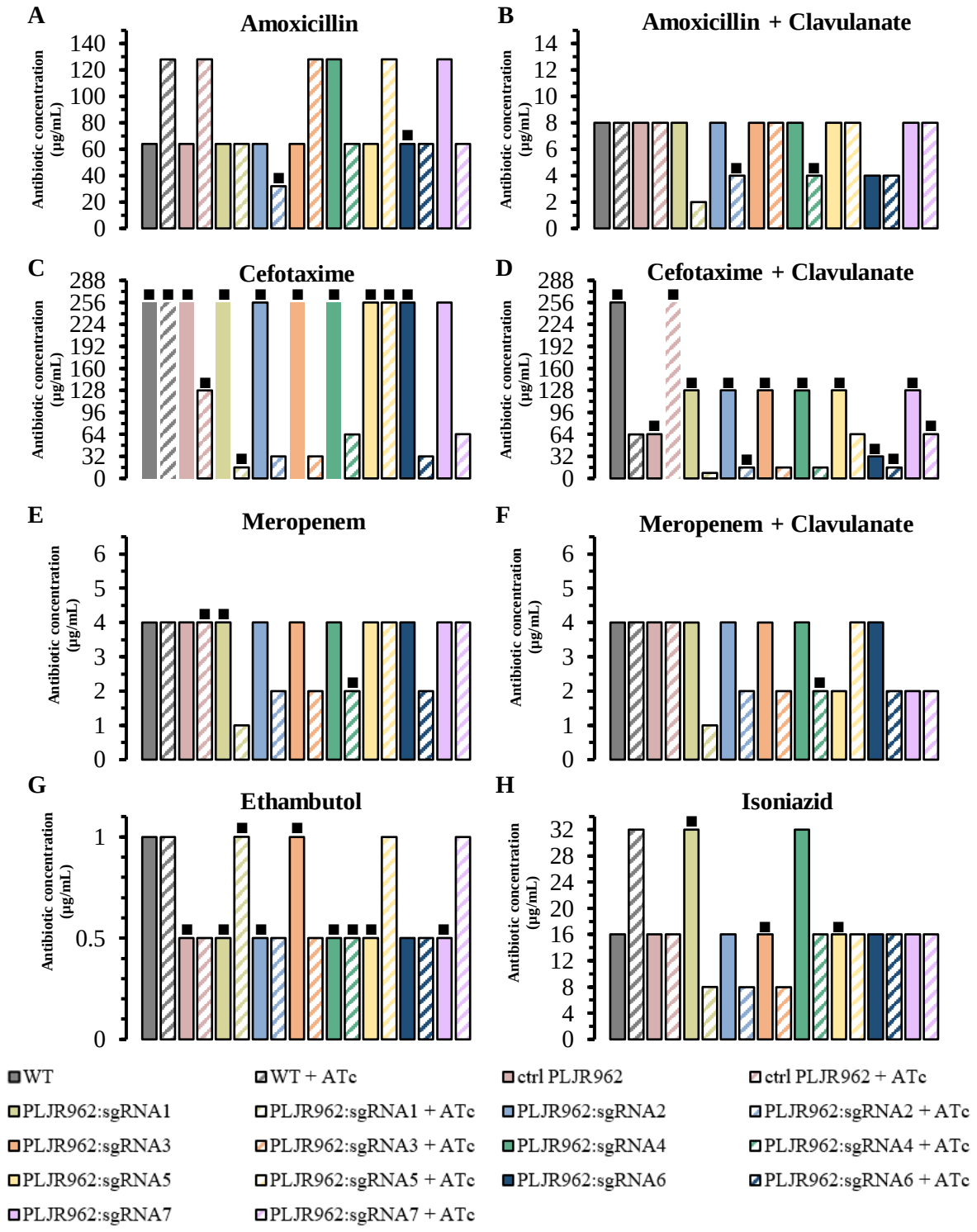

Figure 3.7 – **(A-H) Graphical representation of the medians of Minimum Inhibitory Concentrations (MICs) of eight different antibiotics for *M. smegmatis* mc^{2}155 (WT), ctrl PLJR962, and *gatD*$^-$ mutants (PLJR962:sgRNA1 to 7), in the presence (striped bars) and absence (smooth bars) of 100 ng/mL ATc.** The absence of a bar border indicated a MIC > 256 µg/mL. A bacteriostatic effect or undetermined MBCs are represented with the "■" symbol and all other cases correspond to an antibiotic bactericidal effect. *M. smegmatis* mc^{2}155 WT and ctrl PLJR962 were used as controls. The ctrl PLJR962 mutant is a non-targeting control harbouring an empty vector. The sgRNAs of mutants are decreasingly ordered by PAM strength. Each bar corresponds to the median of three independent experiments.

In –ATc conditions, the MIC of CEF combined with clavulanate (CEF-clavulanate) (**Figure 3.7D**) for WT and ctrl PLJR962 was 256 and 64 µg/mL, respectively and 128 µg/mL for all *gatD*$^{-}$ mutants, except for PLJR962:sgRNA6 (32 µg/mL). Unexpectedly, these values slightly varied between themselves, most likely due to human-associated errors. The MICs of CEF-clavulanate were lower than those obtained without clavulanate, but in accordance with the obtained by Viswanathan *et al.*[156] and Nguyen *et al.*[157] without this β-lactamase inhibitor. In the presence of ATc, the MIC of CEF-clavulanate for WT and ctrl PLJR962 was 64 and >256 µg/mL, respectively, which was also surprising and the *gatD*$^{-}$ mutants PLJR962:sgRNA1, 2, 3, 4, and 6 showed 4 – 8-fold changes from the controls. These mutants are associated with the strongest *gatD* silencing, contributing to the evidence that the PG D-*i*Glu amidation has a role in β-lactams resistance. Based on the EUCAST breakpoints, all *M. smegmatis* controls and *gatD*$^{-}$ mutants in all conditions are classified as resistant to CEF and CEF-clavulanate.

Comparing to AMX and AMX-clavulanate results, the MICs of CEF were higher and only slightly decreased in the presence of clavulanate. Despite BlaS being reported as a penicillinase and using penicillins as preferred substrates, this enzyme is an extended spectrum β-lactamase, hydrolysing penicillins, cephalosporins, including third-generation cephalosporines, and carbapenems[98]. Furthermore, in *M. smegmatis* there is a minor β-lactamase, BlaE, that has homology with class C β-lactamases and appears to have a cephalosporinase activity[159,160], explaining the need of a higher concentration of CEF for bacterial growth inhibition. Besides that, the poor effect of clavulanate here could be due to the fact that CEF can also inactivate LDTs[104].

MER has been shown to inhibit several mycobacterial LDTs, in addition to PBPs[48,94,95,105]. MER-clavulanate exhibited activity against XDR clinical isolates and *M. tuberculosis in vivo*[49,88,109–111]. According to Li *et al.* and Viswanathan *et al.*, in *M. smegmatis*, the MIC of MER is 8 and 4 µg/mL, respectively[154,156]. In the absence of ATc, the MIC of MER was 4 µg/mL for all *M. smegmatis* controls and *gatD*$^{-}$ mutants (**Figure 3.7E**). In +ATc conditions, no changes were found in the MICs of *M. smegmatis* controls and only PLJR962:sgRNA1 exhibited a 4-fold change comparing to WT and ctrl PLJR962. Based on the EUCAST breakpoints, all controls and mutants in all conditions have intermediate susceptibility, except for PLJR962:sgRNA1, 2, 3, 4, 6 + ATc that are susceptible to MER.

Based on Veziris *et al.* and Hugonnet *et al.* results, in *M. tuberculosis* H37Rv, the addition of 2.5 µg/mL of clavulanate resulted in an 8-fold decrease in the MIC of MER[88,110]. However, here, with clavulanate (**Figure 3.7F**), no significant changes were observed, either in + ATc or –ATc conditions, compared to **Figure 3.7E** results. As for AMX, the effect of clavulanate seemed to be the same as the effect caused by the deletion of the major *M. smegmatis* β-lactamase in the work of Li *et al.* – the ΔblaS mutant showed only up to 2-fold decrease in the MIC of MER, compared to the WT strain[154]. According to EUCAST breakpoints, PLJR962:sgRNA5 and 7 in the absence of ATc and PLJR962:sgRNA1, 2, 3, 4, 6, and 7 + ATc are classified as susceptible and the remaining as resistant to MER-clavulanate.

Comparing to AMX-clavulanate, CEF-clavulanate and MER-clavulanate combinations showed a lower efficient synergistic effect against all mycobacteria tested. This effect may be caused by differences in catalytic efficiencies of the mycobacterial β-lactamase in the presence of different classes of β-lactams[161]. In fact, cephalosporins and carbapenems were reported to have 10- to 100-fold lower catalytic efficiency for *M. tuberculosis* β-lactamase than the penicillin class[161].

Contrary to AMX and CEF results and to what was previously reported[88], the MICs of MER did not change in the presence of clavulanate, and the antibiotic concentration values needed to achieve a visual inhibition of growth are lower, not exceeding 4 µg/mL. This may be due to MER efficiently inhibits cross-linking, since: 1) carbapenems, including MER, are potent inhibitors of class A β-lactamases, such as BlaS[98], and are hydrolysed at a lower rate than other β-lactams[88,108]; 2) carbapenems have high affinity to class A PBPs; 3) MER is described as able to bind covalently and to inhibit LDTs[48,94,95,105]. All of these evidences support the previous activity of MER against XDR clinical isolates[49,88,109,111,162].

As mentioned above, the CRISPRi system used is ATc-inducible and the resulting gene silencing is influenced by different factors, namely the sgRNA-DNA target complementarity and the strength of the PAM[132]. This was confirmed in the phenotypical characterization results, where stronger PAMs resulted in higher bacterial growth defects, and surprisingly, it was observed that the effects of *gatD* silencing were also determined by the gene region that is targeted, when weaker PAMs are used. Likewise, the *M. smegmatis gatD*$^{-}$ mutant PLJR962:sgRNA1, that is associated with the strongest PAM, was the mutant that showed the greatest susceptibility to β-lactams. Besides that, in general, the MICs differences for *gatD*$^{-}$ mutants seem to be of the same magnitude as the growth defects observed in spotting dilutions and growth curves. There was an overall decrease in susceptibility from the mutant harbouring PLJR962:sgRNA1 to 7, but for the majority of antibiotics, PLJR962:sgRNA6 had a greater susceptibility than PLJR962:sgRNA5, which has a stronger associated PAM, indicating that the antibiotic resistance was also influenced by the target site of CRISPRi, when concerning weaker PAMs.

Mycobacteria are intrinsically resistant to β-lactams, but recently it has been shown that these antibiotics in combination with β-lactamase inhibitors have activity against *M. tuberculosis*[88,99–101,109,110], indicating a new potential application in TB treatment. Here, we present the effect of three different classes of β-lactams, in combination with clavulanate, against *M. smegmatis* WT and *M. smegmatis* lacking the D-*i*Glu PG amidation, an essential PG modification for mycobacterial growth. The observed susceptibility of some mutants to AMX, CEF, and MER is in agreement with previous data that showed that the inhibition of D-*i*Glu amidation caused reduced resistance to β-lactams, suggesting a role of PG amidation in β-lactams resistance[37]. The susceptibility to β-lactams of *gatD*$^{-}$ mutants could be explained by the lack of amidation displayed by PG precursors in these mutants that, consequently, are poorer substrates for PBPs, leading to cross-linking being less efficient and to PBPs being more susceptible to the action of these antibiotics. Hence, the inhibition of D-*i*Glu amidation and the use of β-lactams can work to produce an effective synergistic antimicrobial effect.

In addition to β-lactams, the effect of the inhibition of mycobacterial PG D-*i*Glu amidation was also evaluated for INH and EMB susceptibility, since these antibiotics comprise two crucial first-line anti-TB drugs that also target the mycobacterial CW. The MICs of EMB (**Figure 3.7G)** for *M. smegmatis* controls and *gatD*$^{-}$ mutants, in both –ATc and +ATc conditions, were found to be 0.5 or 1 µg/mL, in accordance to previous experiments performed in identical conditions[163–165]. These results suggest that the interference in the PG amidation did not result in an altered susceptibility to EMB. According to Li *et al.*[154] and Viswanathan *et al.*[156], the MIC of INH for *M. smegmatis* is 8 µg/mL. In –ATc conditions, the MICs of INH for *M. smegmatis* controls and *gatD*$^{-}$ mutants were 16 – 32 µg/mL (**Figure 3.7H**). In the presence of ATc, both *M. smegmatis* controls and *gatD*$^{-}$ mutants showed MICs within the range values obtained without ATc, except PLJR962:sgRNA1, 2, and 3, that displayed a MIC of 8 µg/mL. These differences are only of a 2-fold magnitude and thus, the lack of PG amidation also seemed to not affect the susceptibility of *M. smegmatis* to INH. The unaltered susceptibility to EMB and INH could be explained by the fact that the CRISPRi-mediated *gatD* silencing leads to a deficiency in the PG composition and may not result in substantial effects in outmost CW layers, like AG and MA, where EMB and INH act. According to the critical concentrations indicated in **Table 3.1**, all *M. smegmatis* controls and *gatD*$^{-}$ mutants are considered susceptible to EMB and resistant to INH.

After MICs determination, MBC assays were also performed. By analysing **Figure 3.7A and B**, AMX as well as AMX-clavulanate, were found to be bactericidal in most cases, in agreement to what was reported by Solapure *et al.*[161]. In the absence of ATc, CEF and CEF-clavulanate (**Figure 3.7C and D**) were found to be bacteriostatic for almost all *M. smegmatis* controls and *gatD*$^{-}$ mutants, which was not in agreement with Solapure *et al.*[161]. Particularly for CEF results, this can be caused by the fact that a large number of mutants have a non-defined value of MIC (>256 µg/mL), making it impossible to determine the associated MBC. Interestingly, the bacteriostatic effect of CEF was highly reduced in the case of *gatD*$^{-}$ mutants in the presence of ATc. MER and MER-clavulanate (**Figure 3.7E and F**)

were bactericidal in the majority of *M. smegmatis* controls and *gatD*$^{-}$ mutants, not in agreement with prior results[161]. When this effect was not observed, the MBCs were undetermined and >2-fold higher than MICs. Especially for CEF, the *gatD* silencing seemed to contribute to a more bactericidal effect, suggesting a role of PG D-*i*Glu amidation in the mycobacterial resistance to this type of antibiotics.

In the absence of ATc, EMB was bacteriostatic for most *M. smegmatis* controls and *gatD*$^{-}$ mutants, as previously described[80,166], and bactericidal in the presence of ATc. Thus, the role of PG amidation on EMB resistance should be further investigated. Since the AG is the CW layer adjacent to PG and is the target of EMB, changes in PG composition could influence the integrity of AG. INH was bactericidal for the great majority of *M. smegmatis* controls and *gatD*$^{-}$ mutants in both conditions, in agreement with reported results[161,166]. These data support the absence of D-*i*Glu PG amidation effect in INH resistance.

Based on **Table 6.5** (**Annexes**), it is possible to conclude that rarely the addition of ATc influences the MBCs of *M. smegmatis* controls. Regarding *gatD*$^{-}$ mutants, it was somehow expected that in +ATc conditions, the bactericidal effect was more frequently, since the PG is weakened and the cross-linking is less efficient, leading the antibiotic to likely have a bactericidal effect with a lower concentration, compared to –ATc conditions. The results did not show a direct connection between the strength of *gatD* silencing and the bactericidal effect of the antibiotics tested. However, it is possible to say that for PLJR962:sgRNA3 + ATc a bactericidal effect was achieved for all antibiotics tested and that, overall, in the presence of ATc, antibiotics were bactericidal more frequently in *gatD*$^{-}$ mutants, than in the absence of ATc, supporting a potential role of the PG D-*i*Glu amidation, especially in β-lactams resistance.

3.3 Determination of the PG amidation significance in host immune recognition

The mycobacterial PG is sensed by the human innate system via NOD1 and NOD2 and the modulation of host immune response by NOD1 has been shown to be influenced by the specific recognition of PG amidated residues[54]. In order to investigate the role of PG D-*i*Glu amidation in host immune response, infections of RAW 264.7 cells with *M. smegmatis* mc^{2}155 WT, ctrl PLJR962, and one *gatD*$^{-}$ mutant (PLJR962:sgRNA2) were performed. The *gatD*$^{-}$ mutant PLJR962:sgRNA2 was selected, since its level of targeted gene knockdown was confirmed by qRT-PCR and it is associated with a strong PAM and to severe growth defects.

The effect of *gatD* silencing by CRISPRi on the intracellular survival of *M. smegmatis* in macrophages was evaluated and it is represented as the number of CFUs/mL observed at 1, 4, and 24 h post-infection in **Figure 3.8**. In all time points, the number of CFUs/mL of *M. smegmatis* controls and *gatD*$^{-}$ mutant in the absence of ATc was similar to each other and, in the case of controls the presence of ATc did not lead to significative changes. These results support the absence of a leaky expression in PLJR962:sgRNA2 and a non-toxic effect of ATc either for bacteria or cells. The overall number of CFUs/mL of *M. smegmatis* controls and PLJR962:sgRNA2 decreased from 1 to 4 h and from 4 to 24 h post-infection, in agreement with previous results[167]. At 1 h post-infection, there was already a significant decrease in the number of CFUs/mL of *M. smegmatis* PLJR962:sgRNA2 in the presence of ATc, comparing to WT (44-fold) and ctrl PLJR962 (49-fold) in the presence of ATc and to PLJR962:sgRNA2 without ATc (42-fold). Similarly, at 4 and 24 h post-infection, these significative differences were also observed between *M. smegmatis* PLJR962:sgRNA2 + ATc and WT + ATc, ctrl PLJR962 + ATc and PLJR962:sgRNA2 in the absence of ATc, obtaining a 319-, 260-, and 263-fold decrease and a 258-, 214-, and 224-fold decrease, respectively.

The presence of a PG amidated D-*i*Glu residue have been shown to contribute to mycobacterial evasion of the host innate immune system, by an impaired recognition and activation of NOD1[37,54,126,128]. Thus, the differences obtained here could be explained by a higher recognition of mycobacteria by

macrophages due to CRISPRi-mediated absence of PG amidation, resulting in a higher phagocytosis rate and, consequently, in a reduced capacity of intracellular survival inside the macrophages.

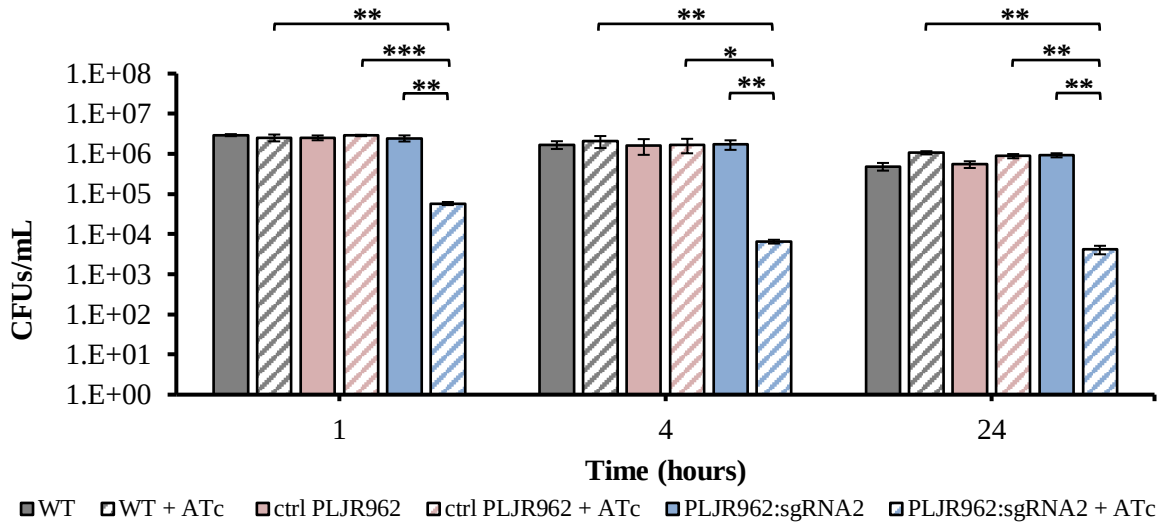

Figure 3.8 – Intracellular survival of *M. smegmatis* mc²155 WT, ctrl PLJR962 and PLJR962:sgRNA2 *gatD*⁻ mutant in the presence (striped bars) and absence (smooth bars) of ATc within RAW 264.7 cells of BALB/c mice measured by CFU/mL at 1, 4, and 24 h post-infection. *M. smegmatis* mc²155 WT and ctrl PLJR962 were used as controls. The ctrl PLJR962 mutant is a non-targeting control harbouring an empty vector. Prior the macrophages infection, the bacteria were grown in the presence and absence of 100 ng/mL ATc. The bars represent the mean of two independent experiments with three biological triplicates each and the error bars correspond to the SEM. Asterisks indicate the significance of the difference in the number of CFUs/mL calculated using the Student t-test (* $P < 0.01$; ** $P < 0.05$; *** $P < 0.01$)

To make sure that ATc had reached bacteria and had time to act before the infection of macrophages, bacteria were treated with ATc 24 h before the experiment. As in the collection of cultures for total RNA extraction (section 3.1.3), the inducer was added to an $OD_{600\ nm}$ much higher than in growth characterization experiments, and the final $OD_{600\ nm}$ of PLJR962:sgRNA2 in the presence of ATc was similar to the WT strain (data not shown), before macrophages infections. However, in the case of the *gatD*⁻ mutant, the presence of ATc can lead to growth defects, as was previously observed in spotting dilutions (**Figure 3.3**) or in growth curves (**Figure 3.5**), and this can also contribute to the PLJR962:sgRNA2 + ATc reduced number of CFUs/mL, comparing to the WT strain. As so, in the future, it would be interesting to treat bacteria less than 24 h before infection, still ensuring that ATc have time to act, but not enough to cause a severe growth defect, and a lower concentration of ATc or other *gatD*⁻ mutants associated with weaker PAMs could be used.

Together, these results indicate that PG amidation affect intracellular survival and pathogenesis of mycobacteria and support previous evidences that PG D-*i*Glu amidation could be a mycobacterial strategy to avoid recognition by the innate immune system. More experiments are required for the investigation of this PG modification role in host immune recognition, namely in the induction of host pro-inflammatory responses.

4. Conclusions and Future Perspectives

The main objective of this thesis was to study the role of the mycobacterial PG amidation in antibiotic resistance and in host immune recognition. For this purpose, the CRISPRi system was used to silence *murT*, *gatD*, and *asnB* genes, which encode for the enzymes that catalyse the mycobacterial PG amidation.

The CRISPRi platform optimized by Rock *et al.* is very simple, useful, and effective in silencing essential mycobacterial genes. Through this system, different ~20 bp gene regions could be targeted and it only required the cloning of the designed sequences into the sgRNA scaffold. Moreover, off-target effects are extremely rare and the CRISPRi-mediated knockdown is inducible and tunable by several factors, such as the concentration of inducer and the PAM strength. This is very advantageous to investigate essential genes, which are considered potential drug targets.

Using this system, the mycobacterial essentiality of the PG amidation genes was investigated, and it was proven to be useful in determining the degree of knockdown required to inhibit growth. The *murT* and *gatD* genes, which are assembled in an operon, were found to be essential in *M. smegmatis*, in contrast to *asnB*. Through spotting dilutions, it was found that the level of *gatD* and *murT* knockdown appeared to be directly related with the associated PAM strength. However, when weaker PAMs were used, the distance of the target gene region from the beginning of the gene, seemed to also influence the CRISPRi-mediated gene silencing, and, consequently, the growth defects, in opposition to the results of Rock and colleges, but supporting other previous experiements[132,135]. By performing growth curves of *M. smegmatis* controls and *gatD*$^{-}$ mutants, the referred correlation was not evident. The growth profile of mutants associated with weaker PAMs was very different from mutants related with strong PAMs, but very similar between each other. Despite the mentioned advantages of CRISPRi system, through growth curves, some leaky expression of dCas9$_{Sth1}$ from the ATc-regulated promoter seemed to have occurred in the *gatD*$^{-}$ mutants, in the absence of ATc, in addition to a level of toxicity caused by dCas9$_{Sth1}$ overexpression in ctrl PLR962, in the presence of ATc.

The level of knockdown in the PLJR962:sgRNA2 + ATc *gatD*$^{-}$ mutant was assessed by qRT-PCR and a significant 8.8-fold decrease in *gatD* mRNA expression was obtained, compared to the corresponding WT strain in the presence of ATc. This result supports the ability of CRISPRi to achieve considerable inhibition of specific gene expression in *M. smegmatis*, and together with phenotype characterization experiments, it indicates that the inhibition is enough to cause a defect in growth. Neither the previous evidence of a leaky expression was confirmed by qRT-PCR, nor the occurrence of a polarity effect by CRISPRi, which was previously reported as a limitation by Rock *et al.*. Nevertheless, both events should be further investigated, in particular, the existence of a downstream polarity in *murT*$^{-}$ mutants or an upstream polarity in *gatD*$^{-}$ mutants with sgRNAs targeting the beginning of the gene.

β-lactams are not usually included in TB treatments, mainly because mycobacteria are naturally resistant to them, but with the current emergence of MDR and XDR strains of *M. tuberculosis*, there is an urgent need of alternative anti-TB strategies. β-lactams combined with clavulanate have been shown activity against *M. tuberculosis*[27,161]. Additionally, amidation of PG have been shown to influence the bacterial antibiotic resistance, especially to β-lactams[33,37]. Therefore, the role of D-*i*Glu amidation, that is catalysed by the MurT/GatD enzymatic complex, was investigated within this context. Several *gatD*$^{-}$ mutants showed increased susceptibility to the β-lactams tested (AMX, CEF, and MER), particularly in the presence of clavulanate. Particularly for CEF, the *gatD* silencing seemed to contribute to a more bactericidal effect. The lack of amidation displayed by the PG precursors of these mutants make them poorer substrates for PBPs[53], which could lead to a less efficient cross-linking and to PBPs being more susceptible to the action of these antibiotics. Hence, the inhibition of D-*i*Glu amidation by CRISPRi and the use of β-lactams could work to produce an effective synergistic antimicrobial effect.

The amidated D-*i*Glu residue of the PG has been shown to contribute to mycobacterial evasion of the host innate immune system, through an impaired recognition and activation of NOD1[37,54,126,128]. In order to investigate this, RAW 264.7 murine macrophages infections were performed with a *gatD* knockdown mutant and the bacterial intracellular survival was assessed by determining the number of CFUs/mL. It was observed a significant decrease in the number of CFUs/mL of PLJR962:sgRNA2 *gatD*$^{-}$ mutant in the presence of ATc, at 1, 4, and 24 h post-infection, comparing to the WT strain in the presence of ATc and to the untreated mutant. Based on the previous mentioned evidences, since the D-*i*Glu amidation is deficient in this mutant, the significative changes could be explained by a higher recognition of mycobacteria by macrophages, resulting in a higher phagocytosis rate and, consequently, in a reduced capacity of intracellular survival inside the macrophages. This data supports the idea that PG D-*i*Glu amidation could be a mycobacterial strategy to avoid recognition by the innate immune system.

This work is a pioneer project for the investigation of the role of this PG modification in the important global pathogen *M. tuberculosis.* With this in mind, all *M. tuberculosis* H37Ra sgRNAs, that were initially designed, were confirmed as identical for *M. tuberculosis* H37Rv, allowing a posterior application of these experiments in *M. tuberculosis* H37Rv or in clinical isolates, including MDR and XDR strains, in BSL3 conditions. In the future, additional experiments must be performed, namely, the conclusion of the construction of *murT, gatD*, and *asnB* knockdown mutants in *M. tuberculosis*, followed by characterization of all *M. smegmatis* and *M. tuberculosis* mutants by spotting dilutions, growth curves and microscopy. Additionally, it would be of great relevance to analyse of the expression of dCas9$_{Sth1}$ and the *murT, gatD*, and *asnB* repression in all mutants by performing qRT-PCR.

To assess the significance of PG amidation in antibiotic resistance, the MICs and MBCs of β-lactams and anti-TB drugs of all mutants should be investigated, in addition to perform disk diffusion assays. The contribution of this modification to the host immune recognition and virulence should be also evaluated, namely by performing infections of human macrophages with *M. tuberculosis* mutants and with amidated vs. non-amidated PG muropeptides, followed by CFUs counting and flow cytometry, to determine the bacterial intracellular survival and cell viability. Moreover, to assess the immune response after macrophages infection, the mRNA expression levels of NOD1, NOD2, TLR1, and TLR2 should be assessed by qRT-PCR, as well as the investigation of the production of several cytokines (TNF-α, IL-1β, IL-6, IL-10, IL-12, IFN-γ) or chemokines (MCP-1, CCL3, CXCL1) by sandwich enzyme-linked immunosorbent assay (ELISA). Additionally, it would be interesting to evaluate the differences in the binding affinity between fluorescent recombinant immune receptors and amidated vs. non-amidated PG by quantitative pull-down assays and by fluorescence microscopy.

5. References

1. World Health Organization. *Global Tuberculosis Report 2020*. https://apps.who.int/iris/bitstream/handle/10665/336069/9789240013131-eng.pdf?ua=1 (2020).
2. Glaziou, P., Floyd, K. & Raviglione, M. C. Global Epidemiology of Tuberculosis. *Semin. Respir. Crit. Care Med.* **39**, 271–285 (2018).
3. Barberis, I., Bragazzi, N. L., Galluzzo, L. & Martini, M. The history of tuberculosis: From the first historical records to the isolation of Koch's bacillus. *J. Prev. Med. Hyg.* **58**, E9–E12 (2017).
4. Daniel, T. M. The history of tuberculosis. *Respir. Med.* **100**, 1862–1870 (2006).
5. Salvatore, P. P. & Zhang, Y. *Tuberculosis: Molecular Basis of Pathogenesis*. *Reference Module in Biomedical Sciences* (Elsevier Inc., 2017). doi:10.1016/b978-0-12-801238-3.95697-6.
6. World Health Organization. *Global Tuberculosis Report 2019*. http://apps.who.int/bookorders. (2019).
7. Cassidy, R. & Manski, C. F. Tuberculosis diagnosis and treatment under uncertainty. *Proc. Natl. Acad. Sci. U. S. A.* **116**, 22990–22997 (2019).
8. World Health Organization. *WHO treatment guidelines for drug-resistant tuberculosis*. https://apps.who.int/iris/bitstream/handle/10665/250125/9789241549639-eng.pdf?sequence=1 (2016).
9. World Health Organization. *WHO consolidated guidelines on drug-resistant tuberculosis treatment*.

https://apps.who.int/iris/bitstream/handle/10665/311389/9789241550529-eng.pdf?ua=1 (2019).
10. Lange, C. *et al.* Drug-resistant tuberculosis: An update on disease burden, diagnosis and treatment. *Respirology* **23**, 656–673 (2018).
11. Sotgiu, G., Centis, R., D'Ambrosio, L. & Battista Migliori, G. Tuberculosis treatment and drug regimens. *Cold Spring Harb. Perspect. Med.* **5**, (2015).
12. Comas, I. & Gagneux, S. The past and future of tuberculosis research. *PLoS Pathog.* **5**, 1–8 (2009).
13. Johansen, M. D., Herrmann, J. L. & Kremer, L. Non-tuberculous mycobacteria and the rise of Mycobacterium abscessus. *Nat. Rev. Microbiol.* (2020) doi:10.1038/s41579-020-0331-1.
14. Fedrizzi, T. *et al.* Genomic characterization of Nontuberculous Mycobacteria. *Sci. Rep.* **7**, 1–14 (2017).
15. Behr, M. A. Evolution of Mycobacterium tuberculosis. in *The new paradigm of immunity to tuberculosis* (ed. Divangahi, M.) vol. 783 81–91 (Springer New York, 2013).
16. Hayman, J. MYCOBACTERIUM ULCERANS: AN INFECTION FROM JURASSIC TIME? *Lancet* **324**, 1015–1016 (1984).
17. Gagneux, S. Ecology and evolution of Mycobacterium tuberculosis. *Nat. Rev. Microbiol.* **16**, 202–213 (2018).
18. Saviola, B. & Felton, J. Acidochromogenicity is a common characteristic in nontuberculous mycobacteria. *BMC Res. Notes* **4**, 4–8 (2011).
19. Hershkovitz, I. *et al.* Tuberculosis origin: The Neolithic scenario. *Tuberculosis* **95**, S122–S126 (2015).
20. Swenson, C., Zerbe, C. S. & Fennelly, K. Host Variability in NTM Disease: Implications for Research Needs. *Front. Microbiol.* **9**, (2018).
21. Cole, S. T. *et al.* Deciphering the biology of Mycobacterium tuberculosis from the complete genome sequence. *Nature* **396**, 190–190 (1998).
22. Zheng, H. *et al.* Genetic basis of virulence attenuation revealed by comparative genomic analysis of Mycobacterium tuberculosis strain H37Ra versus H37Rv. *PLoS One* **3**, (2008).
23. He, Z. L., Du, F. W. & Du, X. Z. The viable Mycobacterium tuberculosis H37Ra strain induces a stronger mouse macrophage response compared to the heat-inactivated H37Rv strain. *Mol. Med. Rep.* **7**, 1597–1602 (2013).
24. Brown-Elliott, B. A. & Wallace, R. J. Clinical and taxonomic status of pathogenic nonpigmented or late-pigmenting rapidly growing mycobacteria. *Clin. Microbiol. Rev.* **15**, 716–746 (2002).
25. Etienne, G. *et al.* The cell envelope structure and properties of Mycobacterium smegmatis mc2155: Is there a clue for the unique transformability of the strain? *Microbiology* **151**, 2075–2086 (2005).
26. Maitra, A. *et al.* Cell wall peptidoglycan in Mycobacterium tuberculosis: An Achilles' heel for the TB-causing pathogen. *FEMS Microbiol. Rev.* **43**, 548–575 (2019).
27. Catalão, M. J., Filipe, S. R. & Pimentel, M. Revisiting anti-tuberculosis therapeutic strategies that target the peptidoglycan structure and synthesis. *Front. Microbiol.* **10**, 1–11 (2019).
28. Crick, D. C., Chatterjee, D., Scherman, M. S. & McNeil, M. R. Structure and Biosynthesis of the Mycobacterial Cell Wall. in *Comprehensive Natural Products II* vol. 6 381–406 (Elsevier, 2010).
29. Jankute, M., Cox, J. A. G., Harrison, J. & Besra, G. S. Assembly of the Mycobacterial Cell Wall. *Annu. Rev. Microbiol.* **69**, 405–423 (2015).
30. Abrahams, K. A. & Besra, G. S. Mycobacterial cell wall biosynthesis: a multifaceted antibiotic target. *Parasitology* **145**, 116–133 (2018).
31. Morlot, C. *et al.* Structure of the essential peptidoglycan amidotransferase MurT/GatD complex from Streptococcus pneumoniae. *Nat. Commun.* **9**, 1–12 (2018).
32. Vollmer, W., Blanot, D. & De Pedro, M. A. Peptidoglycan structure and architecture. *FEMS Microbiol. Rev.* **32**, 149–167 (2008).
33. Münch, D. *et al.* Identification and in vitro analysis of the GatD/MurT enzyme-complex catalyzing lipid II amidation in Staphylococcus aureus. *PLoS Pathog.* **8**, 1–12 (2012).
34. Heijenoort, J. v. Formation of the glycan chains in the synthesis of bacterial peptidoglycan. *Glycobiology* **11**, 25R-36R (2001).
35. Munshi, T. *et al.* Characterisation of ATP-Dependent Mur Ligases Involved in the Biogenesis of Cell Wall Peptidoglycan in Mycobacterium tuberculosis. *PLoS One* **8**, 1–12 (2013).
36. Raymond, J. B., Mahapatra, S., Crick, D. C. & Pavelka, M. S. Identification of the namH gene, encoding the hydroxylase responsible for the N-glycolylation of the mycobacterial peptidoglycan. *J. Biol. Chem.* **280**, 326–333 (2005).
37. Figueiredo, T. A. *et al.* Identification of genetic determinants and enzymes involved with the amidation of glutamic acid residues in the peptidoglycan of Staphylococcus aureus. *PLoS Pathog.* **8**, (2012).
38. Dajkovic, A. *et al.* Hydrolysis of peptidoglycan is modulated by amidation of meso-diaminopimelic acid and Mg2+ in Bacillus subtilis. *Mol. Microbiol.* **104**, 972–988 (2017).
39. Mahapatra, S. *et al.* Mycobacterial lipid II is composed of a complex mixture of modified muramyl and peptide moieties linked to decaprenyl phosphate. *J. Bacteriol.* **187**, 2747–2757 (2005).

40. Mohammadi, T. *et al.* Identification of FtsW as a transporter of lipid-linked cell wall precursors across the membrane. *EMBO J.* **30**, 1425–1432 (2011).
41. Ruiz, N. Bioinformatics identification of MurJ (MviN) as the peptidoglycan lipid II flippase in Escherichia coli. *Proc. Natl. Acad. Sci. U. S. A.* **105**, 15553–15557 (2008).
42. Turapov, O. *et al.* Two Faces of CwlM, an Essential PknB Substrate, in Mycobacterium tuberculosis. *Cell Rep.* **25**, 57-67.e5 (2018).
43. Mahapatra, S., Bhakta, S., Ahamed, J. & Basu, J. Characterization of derivatives of the high-molecular-mass penicillin-binding protein (PBP) 1 of Mycobacterium leprae. *Biochem. J.* **350 Pt 1**, 75–80 (2000).
44. Bhakta, S. & Basu, J. Overexpression, purification and biochemical characterization of a class a high-molecular-mass penicillin-binding protein (PBP), PBP1* and its soluble derivative from Mycobacterium tuberculosis. *Biochem. J.* **361**, 635–639 (2002).
45. Dasgupta, A., Datta, P., Kundu, M. & Basu, J. The serine/threonine kinase PknB of Mycobacterium tuberculosis phosphorylates PBPA, a penicillin-binding protein required for cell division. *Microbiology* **152**, 493–504 (2006).
46. Patru, M. M. & Pavelka, M. S. A role for the class a penicillin-binding protein PonA2 in the survival of Mycobacterium smegmatis under conditions of nonreplication. *J. Bacteriol.* **192**, 3043–3054 (2010).
47. Kieser, K. J. *et al.* Phosphorylation of the Peptidoglycan Synthase PonA1 Governs the Rate of Polar Elongation in Mycobacteria. *PLoS Pathog.* **11**, 1–28 (2015).
48. Gupta, R. *et al.* The Mycobacterium tuberculosis protein Ldt Mt2 is a nonclassical transpeptidase required for virulence and resistance to amoxicillin. *Nat. Med.* **16**, 466–469 (2010).
49. Lavollay, M. *et al.* The peptidoglycan of stationary-phase Mycobacterium tuberculosis predominantly contains cross-links generated by L,D-transpeptidation. *J. Bacteriol.* **190**, 4360–4366 (2008).
50. Hansen, J. M. *et al.* N-glycolylated peptidoglycan contributes to the immunogenicity but not pathogenicity of mycobacterium tuberculosis. *J. Infect. Dis.* **209**, 1045–1054 (2014).
51. Sassetti, C. M., Boyd, D. H. & Rubin, E. J. Genes required for mycobacterial growth defined by high density mutagenesis. *Mol. Microbiol.* **48**, 77–84 (2003).
52. Ngadjeua, F. *et al.* Critical Impact of Peptidoglycan Precursor Amidation on the Activity of l,d-Transpeptidases from Enterococcus faecium and Mycobacterium tuberculosis. *Chem. - A Eur. J.* **24**, 5743–5747 (2018).
53. Zapun, A. *et al.* In vitro reconstitution of peptidoglycan assembly from the gram-positive pathogen streptococcus pneumoniae. *ACS Chem. Biol.* **8**, 2688–2696 (2013).
54. Wang, Q. *et al.* Synthesis of characteristic Mycobacterium peptidoglycan (PGN) fragments utilizing with chemoenzymatic preparation of meso-diaminopimelic acid (DAP), and their modulation of innate immune responses. *Org. Biomol. Chem.* **14**, 1013–1023 (2016).
55. Leisico, F. *et al.* First insights of peptidoglycan amidation in Gram-positive bacteria-The high-resolution crystal structure of Staphylococcus aureus glutamine amidotransferase GatD. *Sci. Rep.* **8**, 1–13 (2018).
56. Nöldeke, E. R. *et al.* Structural basis of cell wall peptidoglycan amidation by the GatD/MurT complex of Staphylococcus aureus. *Sci. Rep.* **8**, 1–15 (2018).
57. Dejesus, M. A. *et al.* Comprehensive essentiality analysis of the Mycobacterium tuberculosis genome via saturating transposon mutagenesis. *MBio* **8**, 1–17 (2017).
58. Liu, X. *et al.* High-throughput CRISPRi phenotyping identifies new essential genes in Streptococcus pneumoniae . *Mol. Syst. Biol.* **13**, 931 (2017).
59. Figueiredo, T. A., Ludovice, A. M. & Sobral, R. G. Contribution of peptidoglycan amidation to beta-lactam and lysozyme resistance in different genetic lineages of staphylococcus aureus. *Microb. Drug Resist.* **20**, 238–249 (2014).
60. Nakel, M., Ghuysen, J. M. & Kandler, O. Wall Peptidoglycan in Aerococcus viridans Strains 201 Evans and ATCC 11563 and in Gaffkya homari Strain ATCC 10400. *Biochemistry* **10**, 2170–2175 (1971).
61. Mir, M. *et al.* The extracytoplasmic domain of the mycobacterium tuberculosis ser/thr kinase PknB binds specific muropeptides and is required for PknB localization. *PLoS Pathog.* **7**, (2011).
62. Bui, N. K. *et al.* Isolation and analysis of cell wall components from Streptococcus pneumoniae. *Anal. Biochem.* **421**, 657–666 (2012).
63. Gonçalves, B. V. *et al.* Role of MurT C-Terminal Domain in the Amidation of Staphylococcus aureus Peptidoglycan. *Antimicrob. Agents Chemother.* **63**, 1–16 (2019).
64. Nöldeke, E. R. & Stehle, T. Unraveling the mechanism of peptidoglycan amidation by the bifunctional enzyme complex GatD/MurT: A comparative structural approach. *Int. J. Med. Microbiol.* **309**, 151334 (2019).
65. Bernard, E., Rolain, T., Courtin, P., Hols, P. & Chapot-Chartier, M. P. Identification of the amidotransferase AsnB1 as being responsible for meso-Diaminopimelic acid amidation in Lactobacillus plantarum peptidoglycan. *J. Bacteriol.* **193**, 6323–6330 (2011).
66. Larsen, T. M. *et al.* Three-dimensional structure of Escherichia coli asparagine synthetase B: A short

journey from substrate to product. *Biochemistry* **38**, 16146–16157 (1999).
67. Levefaudes, M. *et al.* Diaminopimelic acid amidation in corynebacteriales new insights into the role of ltsa in peptidoglycan modification. *J. Biol. Chem.* **290**, 13079–13094 (2015).
68. Ren, H. & Liu, J. AsnB is involved in natural resistance of Mycobacterium smegmatis to multiple drugs. *Antimicrob. Agents Chemother.* **50**, 250–255 (2006).
69. Mitani, Y., Meng, X., Kamagata, Y. & Tamura, T. Characterization of LtsA from Rhodococcus erythropolis, an Enzyme with Glutamine Amidotransferase Activity. *J. Bacteriol.* **187**, 2582–2591 (2005).
70. Van Heeke, G. & Schuster, S. M. The N-terminal cysteine of human asparagine synthetase is essential for glutamine-dependent activity. *J. Biol. Chem.* **264**, 19475–19477 (1989).
71. Hirasawa, T., Wachi, M. & Nagai, K. A mutation in the corynebacterium glutamicum ltsA gene causes susceptibility to lysozyme, temperature-sensitive growth, and L-glutamate production. *J. Bacteriol.* **182**, 2696–2701 (2000).
72. Meisner, J. *et al.* FtsEX is required for CwlO peptidoglycan hydrolase activity during cell wall elongation in Bacillus subtilis. *Mol. Microbiol.* **89**, 1069–1083 (2013).
73. Salzberg, L. I. *et al.* The WalRK (YycFG) and σI RsgI regulators cooperate to control CwlO and LytE expression in exponentially growing and stressed Bacillus subtilis cells. *Mol. Microbiol.* **87**, 180–195 (2013).
74. Ammam, F. *et al.* AsnB is responsible for peptidoglycan precursor amidation in Clostridium difficile in the presence of vancomycin. *Microbiology* (2020) doi:10.1099/mic.0.000917.
75. Birch, H. L. *et al.* Biosynthesis of mycobacterial arabinogalactan: Identification of a novel α(1→3) arabinofuranosyltransferase. *Mol. Microbiol.* **69**, 1191–1206 (2008).
76. Takayama, K. & Kilburn, J. O. Inhibition of synthesis of arabinogalactan by ethambutol in Mycobacterium smegmatis. *Antimicrob. Agents Chemother.* **33**, 1493–1499 (1989).
77. Mikusova, K., Slayden, R. A., Besra, G. S. & Brennan, P. J. Biogenesis of the mycobacterial cell wall and the site of action of ethambutol. *Antimicrob. Agents Chemother.* **39**, 2484–2489 (1995).
78. Vilchèze, C. Mycobacterial Cell Wall: A Source of Successful Targets for Old and New Drugs. *Appl. Sci.* **10**, 2278 (2020).
79. Pawar, A. *et al.* Ethambutol targets the glutamate racemase of Mycobacterium tuberculosis—an enzyme involved in peptidoglycan biosynthesis. *Appl. Microbiol. Biotechnol.* **103**, 843–851 (2019).
80. Schubert, K. *et al.* The antituberculosis drug ethambutol selectively blocks apical growth in CMN group bacteria. *MBio* **8**, 1–21 (2017).
81. Telenti, A. *et al.* The emb operon, a gene cluster of Mycobacterium tuberculosis involved in resistance to ethambutol. *Nat. Med.* **3**, 567–570 (1997).
82. Safi, H., Sayers, B., Hazbón, M. H. & Alland, D. Transfer of embB codon 306 mutations into clinical Mycobacterium tuberculosis strains alters susceptibility to ethambutol, isoniazid, and rifampin. *Antimicrob. Agents Chemother.* **52**, 2027–2034 (2008).
83. Banerjee, A. *et al.* inhA , a Gene Encoding a Target for Isoniazid and Ethionamide in Mycobacterium tuberculosis Sun Um , Theresa Wilson , Des Collins , Geoffrey de Lisle and William R . Jacobs Jr . Published by : American Association for the Advancement of Science Stable URL. *Science (80-.).* **263**, 227–230 (1994).
84. Takayama, K., Wang, L. & David, H. L. Relationship Between the Uptake of Isoniazid and Its Action on In Vivo Mycolic Acid Synthesis in Mycobacterium tuberculosis. *Antimicrob. Agents Chemother.* **2**, 438–441 (1972).
85. Wengenack, N. L. *et al.* Recombinant Mycobacterium tuberculosis KatG(S315T) Is a Competent Catalase-Peroxidase with Reduced Activity toward Isoniazid. *J. Infect. Dis.* **176**, 722–727 (1997).
86. Vilchèze, C. *et al.* Transfer of a point mutation in Mycobacterium tuberculosis inhA resolves the target of isoniazid. *Nat. Med.* **12**, 1027–1029 (2006).
87. Kandler, J. L. *et al.* Validation of Novel Mycobacterium tuberculosis Isoniazid Resistance Mutations Not Detectable by Common Molecular Tests. *Antimicrob. Agents Chemother.* **62**, 1–16 (2018).
88. Hugonnet, J.-E., Tremblay, L. W., Boshoff, H. I., Barry, C. E. & Blanchard, J. S. Meropenem-Clavulanate Is Effective Against Extensively Drug-Resistant Mycobacterium tuberculosis. *Science (80-.).* **323**, 1215–1218 (2009).
89. Rullas, J. *et al.* Combinations of β-lactam antibiotics currently in clinical trials are efficacious in a dhp-i-deficient mouse model of tuberculosis infection. *Antimicrob. Agents Chemother.* **59**, 4997–4999 (2015).
90. Goffin, C. & Ghuysen, J.-M. Multimodular Penicillin-Binding Proteins: An Enigmatic Family of Orthologs and Paralogs. *Microbiol. Mol. Biol. Rev.* **62**, 1079–1093 (1998).
91. Virudachalam, R. & Rao, V. S. R. THEORETICAL STUDIES ON β-LACTAM ANTIBIOTICS: I. Conformational Similarity of Penicillins and Cephalosporins to X-D-Alanyl-D-Alanine and Correlation of Their Structure with Activity*. *Int. J. Pept. Protein Res.* **10**, 51–59 (1977).
92. Spratt, B. G. Distinct penicillin binding proteins involved in the division, elongation, and shape of

Escherichia coli K 12. *Proc. Natl. Acad. Sci. U. S. A.* **72**, 2999–3003 (1975).
93. Wivagg, C. N., Bhattacharyya, R. P. & Hung, D. T. Mechanisms of β-lactam killing and resistance in the context of Mycobacterium tuberculosis. *J. Antibiot. (Tokyo).* **67**, 645–654 (2014).
94. Flores, A. R., Parsons, L. M. & Pavelka, M. S. Genetic analysis of the β-lactamases of Mycobacterium tuberculosis and Mycobacterium smegmatis and susceptibility to β-lactam antibiotics. *Microbiology* **151**, 521–532 (2005).
95. Gygli, S. M., Borrell, S., Trauner, A. & Gagneux, S. Antimicrobial resistance in Mycobacterium tuberculosis: Mechanistic and evolutionary perspectives. *FEMS Microbiol. Rev.* **41**, 354–373 (2017).
96. Nasiri, M. J. *et al.* New insights in to the intrinsic and acquired drug resistance mechanisms in mycobacteria. *Front. Microbiol.* **8**, (2017).
97. Brennan, P. J. The Envelope of Mycobacteria. *Annu. Rev. Biochem.* **64**, 29–63 (1995).
98. Hugonnet, J. E. & Blanchard, J. S. Irreversible inhibition of the Mycobacterium tuberculosis β-lactamase by clavulanate. *Biochemistry* **46**, 11998–12004 (2007).
99. Donald, P. R. *et al.* Early bactericidal activity of amoxicillin in combination with clavulanic acid in patients with sputum smear-positive pulmonary tuberculosis. *Scand. J. Infect. Dis.* **33**, 466–469 (2001).
100. Chambers, H. F., Kocagoz, T., Sipit, T., Turner, J. & Hopewell, P. C. Activity of Amoxicillin/Clavulanate in Patients with Tuberculosis. *Clin. Infect. Dis.* **26**, 874–877 (1998).
101. Cynamon, M. H. & Palmer, G. S. In vitro activity of amoxicillin in combination with clavulanic acid against Mycobacterium tuberculosis. *Antimicrob. Agents Chemother.* **24**, 429–431 (1983).
102. Cohen, K. A. *et al.* Paradoxical Hypersusceptibility of Drug-resistant Mycobacterium tuberculosis to β-lactam Antibiotics. *EBioMedicine* **9**, 170–179 (2016).
103. Salvo, F., De Sarro, A., Caputi, A. P. & Polimeni, G. Amoxicillin and amoxicillin plus clavulanate: A safety review. *Expert Opin. Drug Saf.* **8**, 111–118 (2009).
104. Dubée, V. *et al.* Inactivation of Mycobacterium tuberculosis L,D-transpeptidase Ldt Mt1 by carbapenems and cephalosporins. *Antimicrob. Agents Chemother.* **56**, 4189–4195 (2012).
105. Lobritz, M. A. *et al.* Antibiotic efficacy is linked to bacterial cellular respiration. *Proc. Natl. Acad. Sci. U. S. A.* **112**, 8173–8180 (2015).
106. Flores, A. R., Parsons, L. M. & Pavelka, M. S. Characterization of novel Mycobacterium tuberculosis and Mycobacterium smegmatis mutants hypersusceptible to β-lactam antibiotics. *J. Bacteriol.* **187**, 1892–1900 (2005).
107. Hammond, M. L. Ertapenem: A group 1 carbapenem with distinct antibacterial and pharmacological properties. *J. Antimicrob. Chemother.* **53**, 7–10 (2004).
108. Jaganath, D., Lamichhane, G. & Shah, M. Carbapenems against Mycobacterium tuberculosis: A review of the evidence. *Int. J. Tuberc. Lung Dis.* **20**, 1436–1447 (2016).
109. Payen, M. C. *et al.* Meropenem-clavulanate for drug-resistant tuberculosis: A follow-up of relapse-free cases. *Int. J. Tuberc. Lung Dis.* **22**, 34–39 (2018).
110. Veziris, N., Truffot, C., Mainardi, J. L. & Jarlier, V. Activity of carbapenems combined with clavulanate against murine tuberculosis. *Antimicrob. Agents Chemother.* **55**, 2597–2600 (2011).
111. England, K. *et al.* Meropenem-clavulanic acid shows activity against Mycobacterium tuberculosis in vivo. *Antimicrob. Agents Chemother.* **56**, 3384–3387 (2012).
112. Ernst, J. D. The immunological life cycle of tuberculosis. *Nat. Rev. Immunol.* **12**, 581–591 (2012).
113. de Martino, M., Lodi, L., Galli, L. & Chiappini, E. Immune Response to Mycobacterium tuberculosis: A Narrative Review. *Front. Pediatr.* **7**, 1–8 (2019).
114. Blomgran, R., Desvignes, L., Briken, V. & Ernst, J. D. Mycobacterium tuberculosis inhibits neutrophil apoptosis, leading to delayed activation of naive CD4 T cells. *Cell Host Microbe* **11**, 81–90 (2012).
115. Davis, J. M. & Ramakrishnan, L. The Role of the Granuloma in Expansion and Dissemination of Early Tuberculous Infection. *Cell* **136**, 37–49 (2009).
116. Kwan, C. & Ernst, J. D. HIV and tuberculosis: A deadly human syndemic. *Clin. Microbiol. Rev.* **24**, 351–376 (2011).
117. Harris, J. & Keane, J. How tumour necrosis factor blockers interfere with tuberculosis immunity. *Clin. Exp. Immunol.* **161**, 1–9 (2010).
118. O'Garra, A. *et al. The Immune Response in Tuberculosis*. *Annual Review of Immunology* vol. 31 (2013).
119. Jo, E. K., Yang, C. S., Choi, C. H. & Harding, C. V. Intracellular signalling cascades regulating innate immune responses to Mycobacteria: Branching out from Toll-like receptors. *Cell. Microbiol.* **9**, 1087–1098 (2007).
120. Bafica, A. *et al.* TLR9 regulates Th1 responses and cooperates with TLR2 in mediating optimal resistance to Mycobacterium tuberculosis. *J. Exp. Med.* **202**, 1715–1724 (2005).
121. Banaiee, N., Kincaid, E. Z., Buchwald, U., Jacobs, W. R. & Ernst, J. D. Potent Inhibition of Macrophage Responses to IFN-γ by Live Virulent Mycobacterium tuberculosis Is Independent of Mature Mycobacterial Lipoproteins but Dependent on TLR2 . *J. Immunol.* **176**, 3019–3027 (2006).

122. Caruso, R., Warner, N., Inohara, N. & Núñez, G. NOD1 and NOD2: Signaling, host defense, and inflammatory disease. *Immunity* **41**, 898–908 (2014).
123. Wang, Q. *et al.* Synthesis of characteristic Mycobacterium peptidoglycan (PGN) fragments utilizing with chemoenzymatic preparation of meso-diaminopimelic acid (DAP), and their modulation of innate immune responses. *Org. Biomol. Chem.* **14**, 1013–1023 (2016).
124. Coulombe, F. *et al.* Increased NOD2-mediated recognition of N-glycolyl muramyl dipeptide. *J. Exp. Med.* **206**, 1709–1716 (2009).
125. Brooks, M. N. *et al.* NOD2 controls the nature of the inflammatory response and subsequent fate of Mycobacterium tuberculosis and M. bovis BCG in human macrophages. *Cell. Microbiol.* **13**, 402–418 (2011).
126. Girardin, S. E. *et al.* Peptidoglycan Molecular Requirements Allowing Detection by Nod1 and Nod2. *J. Biol. Chem.* **278**, 41702–41708 (2003).
127. Wolfert, M. A., Roychowdhury, A. & Boons, G. J. Modification of the structure of peptidoglycan is a strategy to avoid detection by nucleotide-binding oligomerization domain protein 1. *Infect. Immun.* **75**, 706–713 (2007).
128. Roychowdhury, A., Wolfert, M. A. & Boons, G. J. Synthesis and proinflammatory properties of muramyl tripeptides containing lysine and diaminopimelic acid moieties. *ChemBioChem* **6**, 2088–2097 (2005).
129. Vijayrajratnam, S. *et al.* Bacterial peptidoglycan with amidated meso-diaminopimelic acid evades NOD1 recognition: An insight into NOD1 structure-recognition. *Biochem. J.* **473**, 4573–4592 (2016).
130. Schneider, T. *et al.* Plectasin, a Fungal Defensin, Targets the Bacterial Cell Wall Precursor Lipid II. *Science (80-.).* **328**, 1168–1172 (2010).
131. Choudhary, E., Thakur, P., Pareek, M. & Agarwal, N. Gene silencing by CRISPR interference in mycobacteria. *Nat. Commun.* **6**, 1–11 (2015).
132. Rock, J. M. *et al.* Programmable transcriptional repression in mycobacteria using an orthogonal CRISPR interference platform. *Nat. Microbiol.* **2**, 1–9 (2017).
133. Horvath, P. & Barrangou, R. CRISPR/Cas, the immune system of Bacteria and Archaea. *Science (80-.).* **327**, 167–170 (2010).
134. Barrangou, R. *et al.* CRISPR Provides Acquired Resistance Against Viruses in Prokaryotes. *Science (80-.).* **315**, 1709–1712 (2007).
135. Qi, L. S. *et al.* Repurposing CRISPR as an RNA-guided platform for sequence-specific control of gene expression. *Cell* **152**, 1173–83 (2013).
136. Makarova, K. S. *et al.* Evolution and classification of the CRISPR-Cas systems. *Nat. Rev. Microbiol.* **9**, 467–477 (2011).
137. Jansen, R., Van Embden, J. D. A., Gaastra, W. & Schouls, L. M. Identification of genes that are associated with DNA repeats in prokaryotes. *Mol. Microbiol.* **43**, 1565–1575 (2002).
138. Mojica, F. J. M., Díez-Villaseñor, C., García-Martínez, J. & Almendros, C. Short motif sequences determine the targets of the prokaryotic CRISPR defence system. *Microbiology* **155**, 733–740 (2009).
139. Deltcheva, E. *et al.* CRISPR RNA maturation by trans-encoded small RNA and host factor RNase III. *Nature* **471**, 602–607 (2011).
140. Garneau, J. E. *et al.* The CRISPR/cas bacterial immune system cleaves bacteriophage and plasmid DNA. *Nature* **468**, 67–71 (2010).
141. Jinek, M. *et al.* A programmable dual-RNA-guided DNA endonuclease in adaptive bacterial immunity. *Science (80-.).* **337**, 816–821 (2012).
142. Peters, J. M. *et al.* A Comprehensive, CRISPR-based Functional Analysis of Essential Genes in Bacteria. *Cell* **165**, 1493–1506 (2016).
143. Bikard, D. *et al.* Programmable repression and activation of bacterial gene expression using an engineered CRISPR-Cas system. *Nucleic Acids Res.* **41**, 7429–7437 (2013).
144. Singh, A. K. *et al.* Investigating essential gene function in Mycobacterium tuberculosis using an efficient CRISPR interference system. *Nucleic Acids Res.* **44**, (2016).
145. Deveau, H. *et al.* Phage response to CRISPR-encoded resistance in Streptococcus thermophilus. *J. Bacteriol.* **190**, 1390–1400 (2008).
146. Rock, J. M. *CRISPRi gene silencing in mycobacteria*. https://media.addgene.org/data/plasmids/115/115163/115163-attachment_vIKvu61hzB2c.pdf (2017).
147. Parish, T. & Roberts, D. M. *Mycobacteria Protocols*. (Humana Press, 2015). doi:10.1007/978-1-4939-2450-9.
148. Wiegand, I., Hilpert, K. & Hancock, R. E. W. *Agar and broth dilution methods to determine the minimal inhibitory concentration (MIC) of antimicrobial substances*. *Nature Protocols* vol. 3 (2008).
149. Gama, B. Restoring Drug Resistant Mycobacteria Susceptibility to β -lactam Antibiotics. (Universidade Nova de Lisboa, 2019).
150. Bettencourt, P., Pires, D., Carmo, N. & Anes, E. *Application of Confocal Microscopy for Quantification*

of Intracellular Mycobacteria in Macrophages. Microscopy: Science, Technology, Applications and Education vol. 1 http://www.formatex.info/microscopy4/614-621.pdf%0Ahttps://www.researchgate.net/publication/258654237_Application_of_Confocal_Microscopy_for_Quantification_of_Intracellular_Mycobacteria_in_Macrophages (2010).
151. Taciak, B. *et al.* Evaluation of phenotypic and functional stability of RAW 264.7 cell line through serial passages. *PLoS One* **13**, 1–13 (2018).
152. Pires, D. *et al.* Esters of pyrazinoic acid are active against pyrazinamide-resistant strains of Mycobacterium tuberculosis and other naturally resistant mycobacteria in vitro and ex vivo within macrophages. *Antimicrob. Agents Chemother.* **59**, 7693–7699 (2015).
153. Schön, T. *et al.* Mycobacterium tuberculosis drug-resistance testing: challenges, recent developments and perspectives. *Clin. Microbiol. Infect.* **23**, 154–160 (2017).
154. Li, X., Zhang, L. & Nikaido, H. Efflux pump-mediated intrinsic drug resistance in Mycobacterium smegmatis. *Antimicrob. Agents Chemother.* **48**, 2415–23 (2004).
155. Ambler, R. P. *et al.* A standard numbering scheme for the class A β-lactamases. *Biochem. J.* **276**, 269–270 (1991).
156. Viswanathan, G., Yadav, S. & Raghunand, T. R. Identification of mycobacterial genes involved in antibiotic sensitivity: Implications for the treatment of tuberculosis with β-lactam-containing regimens. *Antimicrob. Agents Chemother.* **61**, 1–6 (2017).
157. Nguyen, T. V. *et al.* The Discovery of 2-Aminobenzimidazoles That Sensitize Mycobacterium smegmatis and M. tuberculosis to β-Lactam Antibiotics in a Pattern Distinct from β-Lactamase Inhibitors. *Angew. Chemie - Int. Ed.* **56**, 3940–3944 (2017).
158. Brackett, S. M. *et al.* Meridianin D analogues possess antibiofilm activity against Mycobacterium smegmatis . *RSC Med. Chem.* **11**, 92–97 (2020).
159. Voladri, R. K. R. *et al.* Recombinant expression and characterization of the major β-lactamase of Mycobacterium tuberculosis. *Antimicrob. Agents Chemother.* **42**, 1375–1381 (1998).
160. Basu, D., Narayankumar, D. V., Van Beeumen, J. & Basu, J. Characterization of a beta-lactamase from Mycobacterium smegmatis SN2. *IUBMB Life* **43**, 557–562 (1997).
161. Solapure, S. *et al.* In vitro and in vivo efficacy of β-lactams against replicating and slowly growing/nonreplicating mycobacterium tuberculosis. *Antimicrob. Agents Chemother.* **57**, 2506–2510 (2013).
162. Veziris, N., Truffot, C., Mainardi, J. & Jarlier, V. Activity of Carbapenems Combined with Clavulanate against Murine Tuberculosis □. **55**, 2597–2600 (2011).
163. Alcaide, F., Pfyffer, G. E. & Telenti, A. Role of embB in natural and acquired resistance to ethambutol in mycobacteria. *Antimicrob. Agents Chemother.* **41**, 2270–2273 (1997).
164. Agrawal, P., Miryala, S. & Varshney, U. Use of Mycobacterium smegmatis deficient in ADP-ribosyltransferase as surrogate for Mycobacterium tuberculosis in drug testing and mutation analysis. *PLoS One* **10**, 1–13 (2015).
165. Wolff, K. A. *et al.* Protein kinase G is required for intrinsic antibiotic resistance in mycobacteria. *Antimicrob. Agents Chemother.* **53**, 3515–3519 (2009).
166. Yamori, S., Ichiyama, S., Shimokata, K. & Tsukamura, M. Bacteriostatic and Bactericidal Activity of Antituberculosis Drugs against Mycobacterium tuberculosis, Mycobacterium avium-Mycobacterium intracellulare Complex and Mycobacterium kansasii in Different Growth Phases. *Microbiol. Immunol.* **36**, 361–368 (1992).
167. Anes, E. *et al.* Dynamic life and death interactions between mycobacterium smegmatis and J774 macrophages. *Cell. Microbiol.* **8**, 939–960 (2006).

6. Annexes

Supplementary information is available via the Open Science Framework in the following link: https://osf.io/mc86e/?view_only=1b646136c3f948fd8e1e4a3bd810975f

A

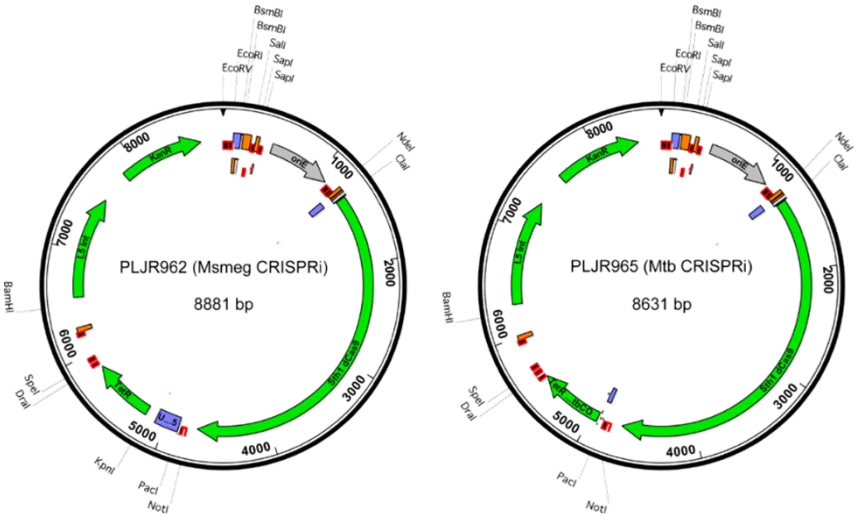

B

PAM	Fold repression	SD
5'-NNAGAAG-3'	216.7	10.0
5'-NNAGAAT-3'	216.2	10.4
5'-NNAGAAA-3'	158.1	22.8
5'-NNGGAAG-3'	145.2	5.3
5'-NNAGAAC-3'	120.5	7.9
5'-NNGGAAA-3'	110.5	26.4
5'-NNAGCAT-3'	84.6	5.2
5'-NNAGGAG-3'	82.2	9.2
5'-NNAGGAT-3'	64.7	8.7
5'-NNAGCAA-3'	53.4	9.9
5'-NNGGAAC-3'	51.5	6.2
5'-NNGGAAT-3'	47.3	3.3
5'-NNAGCAG-3'	42.2	7.0
5'-NNAGGAA-3'	38.5	5.2
5'-NNAGGAC-3'	25.5	0.8
5'-NNGGGAG-3'	24.7	1.9
5'-NNGGGAT-3'	24.2	3.4
5'-NNGGGAA-3'	12.3	0.8
5'-NNAGCAC-3'	11.9	1.2
5'-NNGGGAC-3'	7.9	1.0
5'-NNGGCAT-3'	6.7	0.9
5'-NNGGCAG-3'	4.0	0.3
5'-NNGGCAA-3'	3.3	0.3
5'-NNGGCAC-3'	2.7	0.3
ctrl sgRNA	1.3	0.1

Figure 6.1 – **The CRISPRi-dCas9$_{Sth1}$ system optimized by Rock *et al.* in mycobacteria.** (A) CRISPRi backbone plasmids for *M. smegmatis* (PLJR962, left) and *M. tuberculosis* (PLJR965, right) with indication of enzymatic restriction sites. bp, base pair; dCas9, deficient Cas9 protein; KanR, kanamycin resistance cassette; L5 int, single copy L5-inegrative backbone with the integrase gene and an *attP* site; OriE, *E. coli* derived pBR3222 origin of replication; Sth1 dCas9, dCas9 from *S. thermophilus*. (B) Different PAM position variants for dCas9$_{Sth1}$. The 15 PAMs (PAM1-15) that were described as able to cause a >25-fold repression and that were used in this project are indicated by a blue rectangle. PAM, proto-spacer adjacent motif; SD, standard deviation; sgRNA, single guide RNA. Adapted from Rock *et al.* (2017).

Table 6.1 – qRT-PCR primers for assessment of CRISPRi-mediated gene repression. The mRNA expression levels were evaluated and the housekeeping gene *dnaK* was used as reference.

Target gene in *M. smegmatis* mc^{2}155	Forward and Reverse Primers (5'-3')	Size (bp)	Tm (^{o}C)	% GC	Product size
dnaK	CGACGAACTTCTCCGTCTGG	20	58	57	156
	CAAGATCCAGGAAGGCTCCG	20	58	57	
gatD	GCGACGGTTTCGACGGTG	18	59	66	167
	AGGCGCTCAGAACGCAAAC	19	59	59	
murT	AATCGACCACCACCAGGAT	19	60	52	212
	CGACAGATTGAGCAGAACGA	20	60	50	
MSMEG_6275	GAAGCTGTAGTCGAACCCCG	20	60	60	159
	CTCAACCCTGGTGTCGATCC	20	60	60	
MSMEG_6278	TTGAACACCCCGACGATCAC	20	60	55	153
	CGATGTCCTCGACTTCGCA	19	60	58	

Table 6.2 – ***murT* sgRNA oligonucleotides designed for *M. smegmatis* mc^{2}155 and *M. tuberculosis* H37Ra.** The sgRNAs were decreasingly ordered by PAM strength.

	Oligos name	PAM (5'-3')	Forward and Reverse Primers (5'-3')	Size (bp)	Gene location 5'-3' (bp)
***M. smegmatis* mc^{2}155**	sgRNA1	CGAGAAG	GGGAGCCGCGACCACCTGCACACC	24	1061
			AAACGGTGTGCAGGTGGTCGCGGC		
	sgRNA2	GCAGAAC	GGGAGCTGATCACGCGACAGATTGA	25	406
			AAACTCAATCTGTCGCGTGATCAGC		
	sgRNA3	TCAGCAT	GGGAGTGCGGCGCGCCCACGGACGG	25	28
			AAACCCGTCCGTGGGCGCGCCGCAC		
	sgRNA4	GCAGGAT	GGGAACCTCGACGTGCCCGGGTGG	24	1175
			AAACCCACCCGGGCACGTCGAGGT		
	sgRNA5	GCAGGAA	GGGAATGACAGCCGCCGGTTCAGTT	25	1222
			AAACAACTGAACCGGCGGCTGTCAT		
	sgRNA6	TGAGCAG	GGGAGAGCTGATCACGCGACAGAT	24	408
			AAACATCTGTCGCGTGATCAGCTC		
	sgRNA7	CCAGCAG	GGGAGCCAGCCGGCCGGGTTCTTGG	25	922
			AAACCCAAGAACCCGGCCGGCTGGC		
	sgRNA8	CAGGAAC	GGGAGACAGCCGCCGGTTCAGTTG	24	1220
			AAACCAACTGAACCGGCGGCTGTC		
	sgRNA9	GCAGGAC	GGGAGCGGCCCTGGCCGAGCTGCC	24	153
			AAACGGCAGCTCGGCCAGGGCCGC		
***M. tuberculosis* H37Ra**	sgRNA1	GCAGGAT	AAACGCCAACTCGGGATGGGCCGGC	25	154
			GGGAGCCGGCCCATCCCGAGTTGGC		
	sgRNA2	GCAGGAT	AAACTGGCCAAAAACCCGGCCGGC	24	927
			GGGAGCCGGCCGGGTTTTTGGCCA		
	sgRNA3	TGAGCAA	AAACACCTCTCCCGAGACCAGCTGGAC	27	411
			GGGAGTCCAGCTGGTCTCGGGAGAGGT		
	sgRNA4	CAGGAAC	AAACCAGCTGCAACGAGCATTGGC	24	1229
			GGGAGCCAATGCTCGTTGCAGCTG		
	sgRNA5	CCAGCAG	AAACCCAAAAACCCGGCCGGCTGGC	25	931

			GGGAGCCAGCCGGCCGGGTTTTTGG		
	sgRNA6	GCAGGAA	AAACAGCTGCAACGAGCATTGGCGC	25	1231
			GGGAGCGCCAATGCTCGTTGCAGCT		
	sgRNA7	CCAGGAC	AAACTTGTGGGACGTGCGCTTCGAGC	26	1042
			GGGAGCTCGAAGCGCACGTCCCACAA		

Table 6.3 – ***gatD*** **sgRNA oligonucleotides designed for *M. smegmatis* mc^{2}155 and *M. tuberculosis* H37Ra.** The sgRNAs were decreasingly ordered by PAM strength.

	Oligos name	**PAM (5'-3')**	**Forward and Reverse Primers (5'-3')**	**Size (bp)**	**Gene location 5'-3' (bp)**
***M. smegmatis* mc^{2}155**	sgRNA1	CGAGAAG	AAACGTTCCGACGCACGTCCGCTC	24	498
			GGGAGAGCGGACGTGCGTCGGAAC		
	sgRNA2	CGGGAAG	AAACAGGTCGAACGTTTGCGTTCT	24	690
			GGGAAGAACGCAAACGTTCGACCT		
	sgRNA3	TCAGAAC	AAACGCGCCTCGCCGCGCCGCGGC	24	712
			GGGAGCCGCGGCGCGGCGAGGCGC		
	sgRNA4	CGAGGAT	AAACCGATCTGCGCGGCCATCCAGGT	26	299
			GGGAACCTGGATGGCCGCGCAGATCG		
	sgRNA5	TCGGAAC	AAACCGCACGTCCGCTCGGCGCGGT	25	506
			GGGAACCGCGCCGAGCGGACGTGCG		
	sgRNA6	CGAGCAG	AAACACGCCACCACCTCTCCGCAGGAGGC	29	383
			GGGAGCCTCCTGCGGAGAGGTGGTGGCGT		
	sgRNA7	AGAGCAG	AAACCCCGCGTGGTCGGCGATCTGC	25	652
			GGGAGCAGATCGCCGACCACGCGGG		
***M. tuberculosis* H37Ra**	sgRNA1	CCAGCAA	AAACATGTGACCACGTCACCGCAGGAT	27	366
			GGGAATCCTGCGGTGACGTGGTCACAT		
	sgRNA2	CCAGCAA	AAACCCGGTTTGACCCAACCCTTGAC	26	428
			GGGAGTCAAGGGTTGGGTCAAACCGG		
	sgRNA3	GCAGCAG	AAACTGCGCGGCATCGCCGCCGAGAT	26	110
			GGGAATCTCGGCGGCGATGCCGCGCA		
	sgRNA4	GCAGCAG	AAACGCGGCATCGCCGCCGAGATC	24	111
			GGGAGATCTCGGCGGCGATGCCGC		
	sgRNA5	GCAGCAG	AAACTGAGCAAGGTGGTTGGTGAGC	25	634
			GGGAGCTCACCAACCACCTTGCTCA		
	sgRNA6	TCAGCAG	AAACGCAAGGTGGTTGGTGAGCTGGC	26	638
			GGGAGCCAGCTCACCAACCACCTTGC		
	sgRNA7	GCAGCAG	AAACGCCGCGAACGGCTATCCGCGC	25	691
			GGGAGCGCGGATAGCCGTTCGCGGC		
	sgRNA8	CGAGGAC	AAACGGCCCGGAACGTCGCCCTTGGGC	27	486
			GGGAGCCCAAGGGCGACGTTCCGGGCC		

Table 6.4 - *asnB* sgRNA oligonucleotides designed for *M. smegmatis* mc^{2}155 and *M. tuberculosis* H37Ra. The sgRNAs were decreasingly ordered by PAM strength.

	Oligos name	PAM (5'-3')	Forward and Reverse Primers (5'-3')	Size (bp)	Gene location 5'-3' (bp)
***M. smegmatis* mc^{2}155**	sgRNA1	CCAGAAG	AAACTCTTCAACGGCGAGATCTAC GGGAGTAGATCTCGCCGTTGAAGA	24	300
	sgRNA2	ACAGAAC	AAACGCGCGTGACCCGTTCGGCAT GGGAATGCCGAACGGGTCACGCGC	24	497
	sgRNA3	GAAGAAC	AAACATCGCGCGCGAGGCCCGCAAGC GGGAGCTTGCGGGCCTCGCGCGCGAT	26	1144
	sgRNA4	CAAGCAG	AAACCCCTGGTGACCGACCCGTCC GGGAGGACGGGTCGGTCACCAGGG	24	36
	sgRNA5	ACAGCAG	AAACCCCTGGCCGACCGCCTGGGC GGGAGCCCAGGCGGTCGGCCAGGG	24	585
	sgRNA6	GCAGCAG	AAACACCGCGGTTCGCTGACGCTC GGGAGAGCGTCAGCGAACCGCGGT	24	1338
	sgRNA7	CGAGGAC	AAACGGTTCAACCGGCTGTCGATC GGGAGATCGACAGCCGGTTGAACC	24	210
***M. tuberculosis* H37Ra**	sgRNA1	CGAGAAC	AAACCCGCAGCCGGTGCTATCCCAGT GGGAACTGGGATAGCACCGGCTGCGG	26	-212

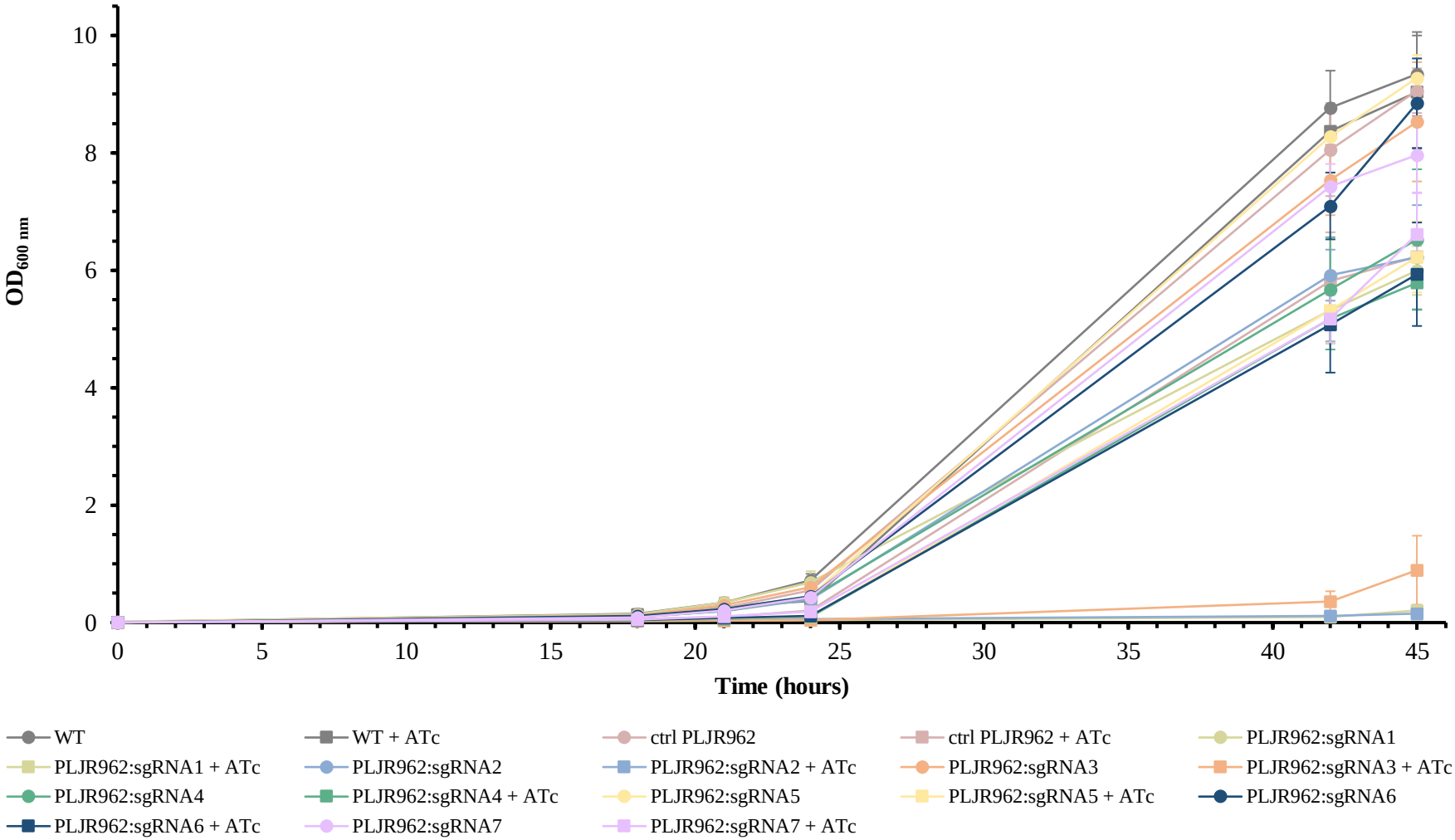

Figure 6.2 – **Growth curves of *M. smegmatis* mc²155 WT, ctrl PLJR962, and *gatD*⁻ mutants (PLJR962:sgRNA1 to 7) in the presence (■) and absence (●) of ATc.** The sgRNAs are decreasingly ordered by PAM strength. *M. smegmatis* mc²155 WT and ctrl PLJR962 were used as controls. The ctrl PLJR962 mutant is a non-targeting control harbouring an empty vector. The cultures were grown from mid- to late-log phase, washed and diluted to a theoretical $OD_{600\ nm}$ of 0.001 (t = 0 h). The 100 ng/mL ATc addition was made at 0 and 24 h. The growth profile of cultures was followed by $OD_{600\ nm}$ measurement at 0, 18, 21, 24, 42, and 45 h. The data represent the mean ± SEM of three independent experiments.

Table 6.5 – **Medians of MICs and MBCs of eight different antibiotics for *M. smegmatis* mc²155 (WT), ctrl PLJR962, and *gatD*⁻ mutants (PLJR962:sgRNA1 to 7) in the presence and absence of 100 ng/mL ATc.** A bacteriostatic effect or undetermined MBCs are highlighted in grey and all other cases correspond to an antibiotic bactericidal effect. Based on EUCAST non-species related PK-PD breakpoints for β-lactams and critical concentrations for ethambutol and isoniazid, the MIC values were coloured with blue (susceptible), green (intermediate), and orange (resistant). *M. smegmatis* mc²155 WT and ctrl PLJR962 were used as controls. The ctrl PLJR962 mutant is a non-targeting control harbouring an empty vector. The sgRNAs of mutants are decreasingly ordered by PAM strength. The data corresponds to three independent experiments. Amoxicillin (AMX); cefotaxime (CEF); meropenem (MER); clavulanate 2.5 µg/mL (+ Clav); ethambutol (EMB); isoniazid (INH).

µg/mL		- ATc									+ ATc								
		WT	**ctrl PLJR962**	**sgRNA1**	**sgRNA2**	**sgRNA3**	**sgRNA4**	**sgRNA5**	**sgRNA6**	**sgRNA7**	**WT**	**ctrl PLJR962**	**sgRNA1**	**sgRNA2**	**sgRNA3**	**sgRNA4**	**sgRNA5**	**sgRNA6**	**sgRNA7**
AMX	MIC	64	64	64	64	64	128	64	64	128	128	128	64	32	128	64	128	64	64
	MBC	64	256	128	128	64	128	64	>128	128	128	128	64	>128	128	256	128	128	128
AMX + Clav	MIC	8	8	8	8	8	8	8	4	8	8	8	2	4	8	4	8	4	8
	MBC	16	16	8	8	16	8	16	16	8	16	16	8	>8	8	>8	8	4	8
CEF	MIC	>256	>256	>256	256	>256	>256	256	256	256	>256	128	16	32	32	64	256	32	64
	MBC	>256	>256	>256	>256	>256	>256	>256	>256	256	>256	>256	>32	32	64	256	>256	128	256
CEF + Clav	MIC	256	64	128	128	128	128	128	32	128	64	>256	8	16	16	16	64	16	64
	MBC	>256	>256	>256	>256	>256	>256	>256	>128	>256	256	>256	32	>64	16	64	64	>32	>64
MER	MIC	4	4	4	4	4	4	4	4	4	4	4	1	2	2	2	4	2	4
	MBC	4	8	>8	8	8	4	4	8	4	4	>8	1	4	2	>4	8	2	4
MER + Clav	MIC	4	4	4	4	4	4	2	4	2	4	4	1	2	2	2	4	2	2
	MBC	4	8	4	4	8	4	4	4	8	4	8	2	2	2	>4	4	2	4
EMB	MIC	1	0.5	0.5	0.5	1	0.5	0.5	0.5	0.5	1	0.5	1	0.5	0.5	0.5	1	0.5	1
	MBC	4	>2	>2	>2	>4	>2	>2	2	>2	4	2	>2	2	2	>2	4	1	2
INH	MIC	16	16	32	16	16	32	16	16	16	32	16	8	8	8	16	16	16	16
	MBC	64	64	>64	32	>64	32	>32	16	16	64	32	32	16	16	32	32	16	64